AN ABSTRACT OF THE THESIS OF

I-Ming Shih for the degree of Doctor of Philosophy in Civil Engineering presented on June 10, 1998. Title: Stochastic Analysis of Complex Nonlinear System Response under Narrowband Excitations.

Abstract approved: _____

Solomon C.S. Yim

Response behavior of a nonlinear structural system subject to environmental loadings is investigated in this study. The system contains a nonlinear restoring force due to large geometric displacement. The external excitation is modeled as a narrowband stochastic process possessing dynamic characteristics of typical environmental loadings.

A semi-analytical method is developed to predict the stochastic nonlinear response behavior under narrowband excitations in both the primary and the subharmonic resonance regions. Preservation of deterministic response characteristics under the narrowband random field is assumed. The stochastic system response induced by variations in the narrowband excitations is considered as a sequence of successive transient states.

Due to the system nonlinearity, under a combination of excitation conditions, several response attraction domains may co-exist. Presence of co-existence of attraction domains and variations in the excitation amplitude often induce complex response inter-domain transitions. The response characteristics are found to be attraction domain dependent. Among different response attraction domains, their corresponding response amplitude domains overlap. In addition, within an individual attraction domain, response amplitude domains corresponding

to different excitation amplitudes also overlap. Overlapping of response amplitude domains and the time-dependent variations in the excitation parameters induce response intra-domain transitions.

Stationary Markovian assumption is employed to characterize the stochastic behavior of the response amplitude process and the excitation parameter processes. Based on the stochastic excitation properties and the deterministic response characteristics, governing equations of the response amplitude probability inter- and intra-domain transitions are formulated. Numerical techniques and an iteration procedure are employed to evaluate the stationary response amplitude probability distribution.

The proposed semi-analytical method is validated by extensive numerical simulations. The capability of the method is demonstrated by good agreements among the predicted response amplitude distributions and the simulation results in both the primary and the subharmonic resonance regions. Variations in the stochastic response behavior under varying excitation bandwidth and variance are also predicted accurately. Repeated occurrences of various subharmonic responses observed in the numerical simulations are taken into account in the proposed analysis. Comparisons of prediction results with those obtained by existing analytical methods and simulation histograms show that a significant improvement in the prediction accuracy is achieved.

STOCHASTIC ANALYSIS OF COMPLEX NONLINEAR SYSTEM RESPONSE UNDER NARROWBAND EXCITATIONS

by

I-Ming Shih

A THESIS

submitted to

Oregon State University

in partial fulfillment of
the requirements for the
degree of

Doctor of Philosophy

Presented June 10, 1998
Commencement June 1999

Doctor of Philosophy thesis of I-Ming Shih presented on June 10, 1998

APPROVED:

Redacted for Privacy

Major Professor, representing Civil Engineering

Redacted for Privacy

Chair of Department of Civil, Construction, and Environmental Engineering

Redacted for Privacy

Dean of Graduate School

I understand that my thesis will become part of the permanent collection of Oregon State University libraries. My signature below authorizes release of my thesis to any reader upon request.

Redacted for Privacy

I-Ming Shih, Author

TABLE OF CONTENTS

TABLE OF CONTENTS (continued)

TABLE OF CONTENTS (continued)

LIST OF FIGURES

LIST OF FIGURES (continued)

LIST OF FIGURES (continued)

LIST OF FIGURES (continued)

LIST OF FIGURES (continued)

LIST OF TABLES

LIST OF APPENDICES

LIST OF SYMBOLS

$x(t)$	system response displacement.
c_s	system damping coefficient.
a_1	coefficient of system linear restoring force.
a_3	coefficient of system cubic nonlinear restoring force.
$f(t)$	external excitation.
$A(t)$	excitation (amplitude) envelop process.
$\phi(t)$	excitation phase angle process.
$A^{(1)}$, $A^{(2)}$	excitation amplitudes of two consecutive cycles.
$\phi^{(1)}$, $\phi^{(2)}$	excitation phase angles of two consecutive cycles.
Φ	excitation phase angle difference = $\phi^{(2)} - \phi^{(1)}$.
ω	excitation angular frequency.
ω_f	peak (or central) angular frequency of narrow-band excitation.
$S_{ff}(\omega)$	spectral density function of excitation.
γ	bandwidth parameter of narrow-band excitation.
σ_f^2	variance of excitation.
$R(t)$	response (amplitude) envelop process.
$R^{(1)}$, $R^{(2)}$	response amplitudes corresponding to the excitation cycles with amplitude $A^{(1)}$ and $A^{(2)}$, respectively.
D_d	response attraction domain "d".
D_d^R	response amplitude domain associated with D_d.
D_d^A	excitation amplitude domain associated with D_d.
$(D_d^R)_A$	response amplitude domain corresponding to an excitation amplitude $A \in D_d^A$ in D_d^R.
$(D_d^R)_A^{(1,2)}$	$(D_d^R)_A$ in two consecutive excitation cycles.
p	probability density function (continuous form) or probability (discrete form)
$\hat{p}$, $\hat{y}$	probability distribution vectors.
$\tilde{p}$	approximate distribution vector.
K	response inter-domain probability transition matrix

STOCHASTIC ANALYSIS OF COMPLEX NONLINEAR SYSTEM RESPONSE UNDER NARROWBAND EXCITATIONS

1. INTRODUCTION

1.1 Background

In the analysis of response of engineering systems to environmental loads, the excitation forces can often be classified as narrowband stochastic processes. For mechanical, ocean and structural engineering systems, the environmental loads include wind, wave, current and earth excitations (Rice, 1954; Stratonovich, 1963; Lin, 1967; Nigam, 1983; Dean and Dalrymple, 1984; Roberts and Spanos, 1990; Ochi, 1990; Newland, 1993; Soong and Grigoriu, 1993; Lutes and Sarkani, 1997). Dynamic system responses behavior under narrowband stochastic excitations have been studied for decades (Rice, 1954; Lyon, *et al*, 1961; Dimentberg, 1971; Richard and Anand, 1983; Davies and Liu, 1990; Koliopulos and Bishop, 1993). To date, the stochastic behavior of linear systems is well understood by using the frequency domain (spectral analysis) techniques (Crandall and Mark, 1963; Lin, 1967; Nigam, 1983; Roberts and Spanos, 1990; Newland, 1993; Soong and Grigoriu, 1993; Lutes and Sarkani, 1997). However, relatively little understanding on the stochastic behavior of nonlinear systems subject to narrowband excitations has been achieved because of the complexity of the system response characteristics.

The complex response behavior of a nonlinear mechanical or structural system under deterministic excitations includes the response amplitude jump phenomenon, subharmonic response, superharmonic response and even chaotic response (Nayfeh and Mook, 1979;

Burton and Rahman, 1986; Guckenheimer and Holmes, 1986; Thompson and Stewart, 1986; Jordan and Smith, 1987; Wiggins, 1990). To investigate these complex responses, semi-analytical methods and numerical techniques (Gottlieb and Yim, 1992; Yim and Lin, 1991) are required in general. For a practical physical system, its dynamic behavior is often significantly affected by the randomness in the environmental excitations (which is not taken into account under deterministic analysis). As a result, to fully characterize the response behavior of a practical engineering system, stochastic analysis techniques are needed (Lin and Yim, 1995 and 1997).

In recent years, Richard and Anand (1983), Davies and Nandlall (1986) and Roberts and Spanos (1990) used the equivalent linearization method to study the response of nonlinear systems subject to Gaussian narrowband excitations. In their studies, the jump phenomenon in the system response, similar to that under deterministic excitations, was observed in both the analytical solution and the simulations when the dominant excitation frequency is close to one of the (linear) resonance frequencies of the system.

An application of multiple time scale perturbation method in the study of nonlinear oscillators subject to narrowband random excitation was presented by Rajan and Davies (1988) and Francescutto (1990). In their work, an analytical expression of the response statistics evolution was obtained. In addition, the existence of nonlinear superharmonic and subharmonic responses under narrowband excitations was studied. They concluded that the existence of subharmonic response is a short term system behavior at the beginning of the response process. Once the system exits from the subharmonic response domain due to variations in the excitation, subharmonic response would not be observed in the rest of the process.

Roberts and Spanos (1986) and Davies and Liu (1990) approximated the excitation and the response as Markov processes and pointed out a general rule of applying the stochastic averaging method in analyzing the stochastic system response under narrowband excitations. By solving the associated Fokker-Planck equation relating the excitation envelope and the response envelope, an approximate probability density function of the response envelope process was obtained.

Alternatively, a quasi-harmonic method was introduced by Koliopulos and Bishop (1993). Under the assumption that both the excitation and response processes are narrowband, the quasi-harmonic analysis leads to the formulation of a probability density function of the response envelope. However, the excitation bandwidth effect on the response behavior is not taken into account by this method. Thus, the applicability of this method is limited to the cases with an extremely small excitation bandwidth, although the validity of this method can be determined by an extra parameter which indicates the occurrence and persistence of the response amplitude jump phenomenon. Again, the jump phenomenon of the nonlinear system response under a narrowband random excitation was confirmed in their study through an approximate analytical solution and numerical simulations.

Note that, in these previous studies, the analytical methods developed were based on deterministic techniques. In order to obtain analytical expressions of the solutions, the system responses are assumed implicitly to be close to certain deterministic steady states. However, in actuality, due to the random nature of stochastic processes, the excitation amplitude and phase angle vary with time. As a result, the system response may not stay close to the steady state in general, unless the randomness in the excitation is small. In other words, the system response should be considered as in a transient state, and nearly steady-state behavior should

be a special case under small randomness of the excitation. Moreover, current technology in predicting nonlinear stochastic response behavior is still limited to the case when the system is in a primary resonance region. For complex nonlinear response behavior including subharmonic and superharmonic responses under narrowband excitations, analytical predictions are not yet available.

1.2 Objectives and Scope

The main goal of this study is to develop a semi-analytical method capable of more accurately characterizing and predicting detailed stochastic nonlinear response behavior under narrowband excitations. The method will be extended to analyze the nonlinear response behavior of the system in the subharmonic resonance regions as well as the primary resonance region. Predictions of the response amplitude probability distribution will be presented as part of the results of the analysis of the stochastic response behavior.

To achieve these objectives, firstly, structural system modeling and descriptions of general properties of narrowband random processes will be presented in *Chapter 2*. Secondly, to gain further understanding of the system response behavior than that obtained and employed by previous studies (i.e., steady-state response behavior in the primary resonance region), the deterministic transient-state and inter-domain-transition-state response behavior characteristics will be investigated in depth in *Chapter 3*. Especially, the studies will be focused on both the primary and the subharmonic resonance response behavior. Then, in *Chapter 4*, a semi-analytical procedure to analyze the stochastic response behavior under narrowband excitations will be developed based on the stochastic properties of the excitation processes described in Chapter 2 and the deterministic system response characteristics gained

in Chapter 3. In addition, the analysis of the stochastic response behavior will be extended to the subharmonic resonance region. The detailed incorporation of the knowledge gained in Chapter 2 and Chapter 3 into the development of the semi-analytical procedure is presented through a flow chart in *Appendix A*.

In *Chapter 5*, to verify the methodology proposed, extensive long duration narrowband simulations will be conducted and employed to thoroughly investigate the complex nonlinear response behavior, especially in the existence of the subharmonic responses, and the influence of varying excitation bandwidth and variance on the response behavior. In addition, to demonstrate the capability and to assess the accuracy of the method proposed, predictions of the response amplitude probability distribution in both the primary and the subharmonic resonance regions will be compared against results from two existing analytical (stochastic averaging and quasi-harmonic) methods and simulations. Finally, several issues for future research will be addressed in *Chapter 6*.

2. SYSTEM AND EXCITATION MODELS

2.1 Structural System Description

In this study, a class of single degree-of-freedom structural systems with a nonlinear restoring force is examined. Damping force is assumed to be linear or can be linearized using standard equivalent linearization techniques (Roberts and Spanos, 1990; Lin and Yim, 1995). This class of nonlinear structural systems include moored floating platforms (Gottlieb and Yim, 1992) articulated offshore loading towers (Choi and Lou, 1991; Gottlieb, Yim and Hudspeth, 1992) and roll motion of vessels (Hsieh, Shaw and Troesch, 1993; Lin and Yim, 1995). For simplicity of modeling and to facilitate the interpretation of the complex nonlinear stochastic response results, a simple nonlinear oscillator of the Duffing type is selected to represent the structural system. The selection of the Duffing system enables us to take advantage of its well understood nonlinear behavior (Nayfeh and Mook, 1979; Jordan and Smith, 1987) and its wide variety of applications in mechanical, ocean and structural engineering (Gottlieb and Yim, 1992). Dynamic response behavior of a multi-point mooring system subject to ocean wave (shown in Fig.2.1), for example, is governed by the following equation,

$$\ddot{x} + F_D(\dot{x}) + F_R(x) = F(x,\dot{x},\ddot{x},t) \tag{2.1}$$

where, x is the surge motion of the moored buoy; $F_D(\dot{x})$ and $F_R(x)$ are the structural damping force and restoring force, respectively; $F(x, \dot{x}, \ddot{x}, t)$ is a time dependent external force. The structural restoring force, $F_R(x)$, is modeled as (Gottlieb and Yim, 1992)

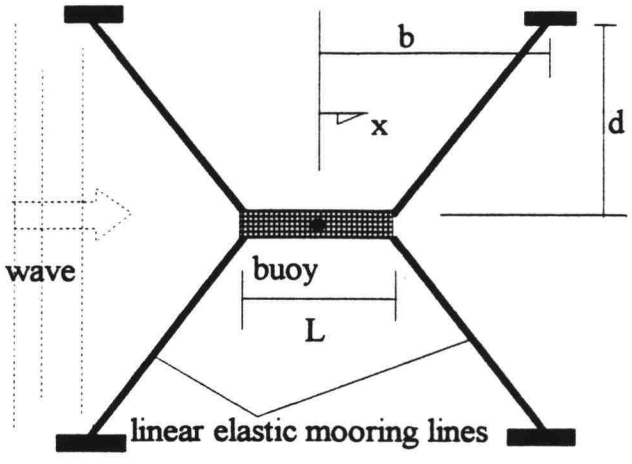

Figure 2.1 Multi-point mooring system subject to ocean wave.

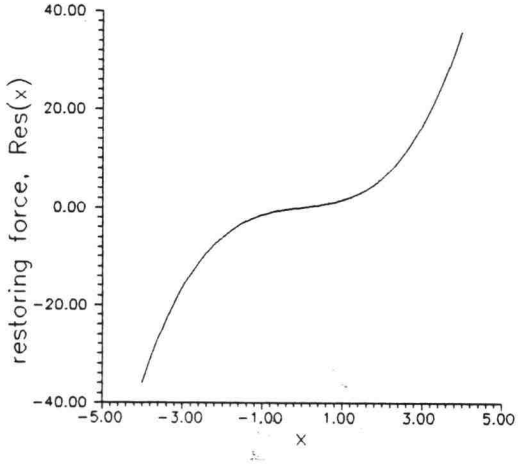

Figure 2.2 Nonlinear restoring force of the mooring system shown in Fig.2.1.

$$F_R(x) = k\left\{4x + L_c\left[(2b - L)\frac{L_1 - L_2}{L_1 L_2} - 2x\frac{L_1 + L_2}{L_1 L_2}\right]\right\} \tag{2.2}$$

where

$$L_{1,2} = \left[d^2 + \left(\frac{L}{2}\right)^2 + (b \pm x)^2 - L(b \pm x)\right]^{1/2}$$

and k is the elastic force coefficient and L_c is the initial pre-tensioned length of the mooring line; L, b and d are shown in Fig.2.2. Note that the upper sign refers to L_1 and the lower sign to L_2. Although the mooring lines are linear elastic, Eq.(2.2) reveals the geometric nonlinearity of the mooring system as shown in Fig.2.2. Gottlieb and Yim (1992) show that this nonlinearity in the structural system can be approximated by an odd order polynomial representation. If only the first and the third order terms are retained, the equation of motion expressed in Eq.(2.1) becomes a Duffing type nonlinear system.

The governing equation of motion of a general Duffing oscillator is expressed as

$$\ddot{x} + c_S\dot{x} + a_1 x + a_3 x^3 = f(t) \tag{2.3}$$

where, the constant c_S is the damping coefficient, and a_1 and a_3 are the linear and nonlinear stiffness coefficients of system, respectively. The system is subjected to an external excitation f(t). The elastic restoring force represented by the cubic polynomial is the only source of nonlinearity in the system. Due to the nonlinear system stiffness, various interesting phenomena can be observed in the response behavior.

2.2 Deterministic Excitation Model

When the external excitation, f(t), is deterministic, the response of the representative system described in Eq.(2.3) will also be deterministic. For periodic forcing such as those generated by monochromatic waves, the excitation parameters are all time independent and f(t) can be expressed as

$$f(t) = A\cos(\omega t + \phi) \tag{2.4}$$

Where, A, ω and ϕ are referred to as the forcing amplitude, frequency and phase angle, respectively. Behavior of the system considered in Eq.(2.3) subject to harmonic excitation defined in Eq.(2.4) has been studied extensively (Nayfeh and Mook, 1979; Jordan and Smith, 1987). Results in the literature show interesting phenomena, such as response jumping between distinct amplitude levels, complex transient behavior from initial conditions to steady state responses including resonance, subharmonic, superharmonic and even chaotic responses (Thompson and Stewart, 1987; Gottlieb and Yim, 1992). It should be noted that the sinusoidal wave form of the excitation expressed in Eq.(2.4) remains unchanged in various system behavior and the occurrence of these interesting phenomena depends on the system parameters and the initial physical states of the system (i.e., displacement and velocity at time $t = 0$).

2.3 Stochastic Excitation Model

2.3.1 Excitation Process Description

If the external excitation, f(t), is a stochastic process, the parameters (A, ω, ϕ) then become time dependent random variables instead of constants and their behavior may vary significantly depending on the spectral bandwidth of the process. For a stochastic process with spectral energy concentrated locally around certain frequency, the stochastic process is called narrowband. The frequency domain and time domain descriptions of narrowband processes are presented in this section.

Frequency Domain Definition: The term "narrowband" originated from the fact that the spectral density function of the process is sharply concentrated in a neighborhood containing the peak frequency ω_f (Ochi, 1990). The spectral intensity is negligibly small everywhere except within a narrow frequency band, $\omega_f - \Delta\omega/2 \leq \omega \leq \omega_f + \Delta\omega/2$, where $\Delta\omega << \omega_f$ (Stratonovich, 1963).

A process with its spectral density function described above can be obtained by passing a white noise process through a specially designed linear filter. In fact, a narrowband process can be modeled as the output process of a lightly damped linear (oscillator) system with a white noise process as the excitation (Stratonovich, 1963). This linear system can be expressed in the form of a stochastic differential equation as

$$\ddot{f} + \gamma\dot{f} + \omega_f^2 f = \gamma^{1/2}\omega_f W_0 \qquad (2.5)$$

where the damping coefficient γ serves as a bandwidth parameter (Ochi, 1990). The natural frequency of the linear system ω_f is the peak frequency of the output process f(t) and W_0 is a stationary Gaussian white noise process with zero mean and spectral intensity S_0. The spectral density function of the system output takes the form

$$S_{ff}(\omega) = \frac{\gamma \omega_f^2 S_0}{(\omega_f^2 - \omega^2)^2 + (\gamma\omega)^2}, \qquad -\infty < \omega < \infty \tag{2.6}$$

For γ being small, the spectral intensity $S_{ff}(\omega)$ is small everywhere except in the neighborhood of the peak frequency ω_f. Conversion from the two sided spectrum expressed in Eq.(2.6) to a one sided spectrum, which is more convenient for the purpose of practical use, can be achieved by doubling the spectral intensity everywhere except at $\omega = 0$. Eq.(2.6) can be employed in the time domain simulation of a stochastic process (Shinozuka, 1971). In addition, the variance, σ_f^2, of the stochastic process, f(t), can be obtained as the area under the spectral density function expressed in Eq.(2.6) and is equal to πS_0.

Time Domain Definition: In the time domain, realizations of a stationary narrowband random process are close to sinusoidal oscillations of a fixed frequency ω_f for time interval equal to a large number of oscillation cycles (Stratonovich, 1963). In addition, the amplitude and phase of the process vary slowly and randomly while the frequency retains a constant value (Ochi, 1990). The phase plane of a narrowband process has a spiral line moving slowly inward and outward in a random fashion. A more quantitative time-domain description of the narrowband process will be presented in the next section.

2.3.2 Envelope and Phase Representation

The envelope and phase processes associated with a given random process is a useful concept in the theory of random vibration (Langley, 1986). Behavior of a narrowband stochastic process can be characterized by a suitably defined slowly varying envelope and phase processes.

Physically, for a narrowband stochastic process f(t), the envelope process is a smooth curve joining the peaks of f(t). Associated with the envelope process is a phase process such that f(t) can be represented as a cosine function having time varying amplitude governed by the envelope process, and time varying frequency governed by the phase process (Langley, 1986). That is,

$$f(t) = A(t)\cos[\omega_f t + \phi(t)] \tag{2.7}$$

where, A(t) and $\phi(t)$ are the envelope and the phase processes, respectively (see detail definitions in Appendix B).

By assuming the narrowband random process f(t) to be Gaussian with zero-mean and variance σ_f^2, the joint probability density function of the envelope A(t) and the phase $\phi(t)$ processes reads (Ochi, 1990; see also Appendix B)

$$p(A,\phi) = \frac{A}{2\pi\sigma_f^2}\exp\left[-\frac{A^2}{2\sigma_f^2}\right], \qquad 0 \le A < \infty, \quad 0 \le \phi \le 2\pi \tag{2.8}$$

where, the time parameter, t, is neglected for simplicity without loss of generality. The marginal probability density function of A(t) can be obtained as

$$p(A) = \int_0^{2\pi} p(A,\phi)\, d\phi = \frac{A}{\sigma_f^2} \exp\left[-\frac{A^2}{2\sigma_f^2}\right], \qquad 0 \le A < \infty \tag{2.9}$$

which is a Rayleigh distribution with parameter $2\sigma_f^2$. The uniformly distributed marginal probability density function of the phase process is obtained as

$$p(\phi) = \int_0^{\infty} p(A,\phi)\, dA = \frac{1}{2\pi}, \qquad 0 \le \phi \le 2\pi \tag{2.10}$$

The joint probability density function $p(A, \phi)$ being the product of the individual marginal density functions, $p(A)$ and $p(\phi)$, shows that the envelope and the phase processes are statistically independent. Note that the probability density functions of the envelope and the phase processes are independent of the bandwidth of the narrowband process.

2.3.3 Narrowband Process Simulation

A stationary narrowband stochastic process can be represented as (Shinozuka, 1970),

$$f'(t) = \left(\frac{2\sigma_f^2}{N}\right)^{1/2} \sum_{n=1}^{N} \cos(\omega_n t + \phi_n) \tag{2.11}$$

where, $f'(t)$ is the approximate narrowband process; σ_f^2 is the variance of the target process $f(t)$; the ω_n's are independent random variables identically distributed with the density function $g(\omega)$ equal to the normalized spectral density function of $f(t)$ (i.e., $g(\omega)$ =

$S_{ff}(\omega)/(\pi S_0)$, and $S_{ff}(\omega)$ is obtained from Eq.(2.6)); the ϕ_n's are independent random variables identically and uniformly distributed with density $1/(2\pi)$ between 0 and 2π. Note that the ω_n's and ϕ_n's are statistically independent. In addition, when dealing with temporal averages, the ω_n's and ϕ_n's are not considered as random variables but as sample values of these random variables.

The value of N employed in Eq.(2.11) plays an important role in the accuracy and the efficiency of the simulation. Extensive studies have shown that the value of N equal to 400 will provide computational efficiency with reasonable accuracy (Shinozuka and Deodatis, 1991).

2.4 Typical Nonlinear Responses

For the nonlinear system considered, interesting response behavior, including harmonic response oscillating at different amplitudes under identical excitation, subharmonic response and a large variation in the response amplitude under a small variation in the excitation amplitude, is demonstrated in this section.

2.4.1 Harmonic responses

Harmonic responses with a large and a small amplitude are shown in Figs.2.3b and 2.3c, respectively. These two responses are of the same structural system with different initial states (displacement and velocity at time $t = 0$) under an identical excitation shown in Fig.2.3a. For time greater than 160 sec., each of the system responses is practically in a stable state, (i.e., maximum response displacement over one cycle is close to constant). The

(a)

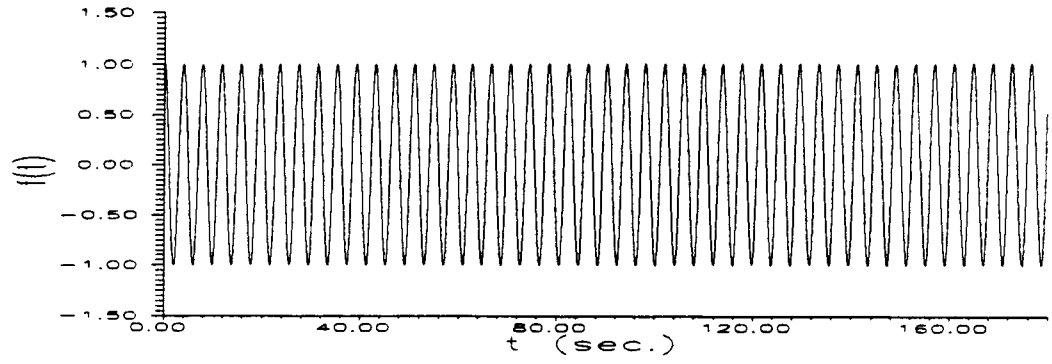

(b)

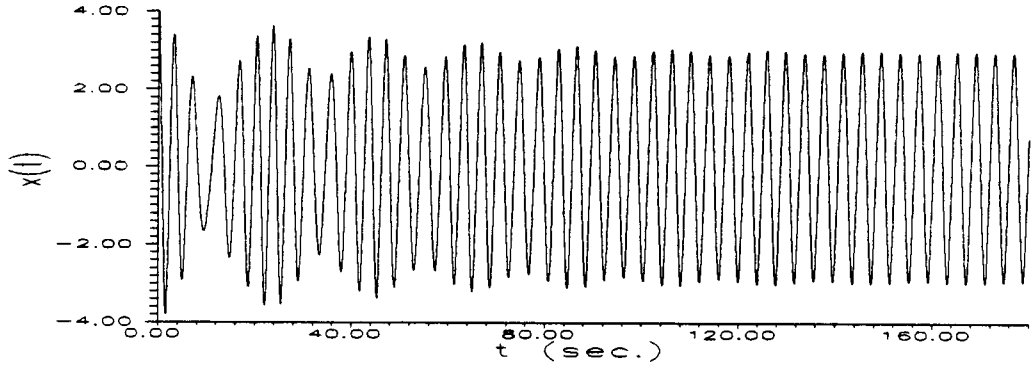

(c)

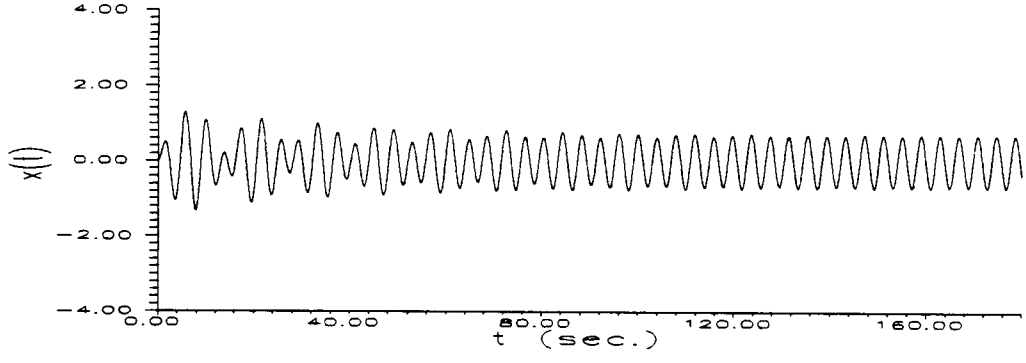

Figure 2.3 Time series of (a) excitation, (b) large amplitude harmonic response, and (c) small amplitude harmonic response.

maximum response displacement is called the response amplitude. When the system response is in a steady state, the response amplitude will be constant. Transition of the system response from the initial states to steady state is called a transient state. During the transient state, the response amplitude varies with time as show in Figs.2.3b and 2.3c after the time t = 0 and before the system reaches steady state.

2.4.2 Subharmonic Responses

Figs.2.4b and 2.4c show two subharmonic responses of the same structural system with different initial conditions under an identical excitation shown in Fig.2.4a. In the time series shown in Fig.2.4b, the oscillation period of the system response is equal to twice the excitation period. This type of system response is called a 1/2 subharmonic response. However, in Fig.2.4c, the system response is observed to oscillate at period equal to three times of the excitation period and is called a 1/3 subharmonic response. Thus, under an identical excitation, the system response may exhibit entirely different behavior depending on the initial condition specified.

2.4.3 Response amplitude jump phenomena

For a nonlinear system, a small amount of variation in the excitation amplitude may induce changes in the response characteristics, e.g., from a large amplitude harmonic response to a small amplitude harmonic response, from a subharmonic response to a harmonic response and even, for the subharmonic responses, from a particular order (1/2) to another order (1/3). Variations in the steady-state response amplitudes associated with these changes in the response characteristics are commonly obvious and often referred to as the response

(a)

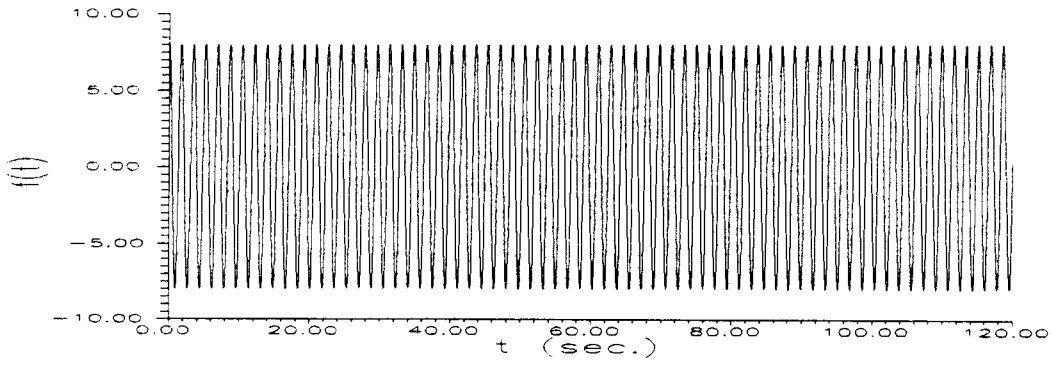

(b)

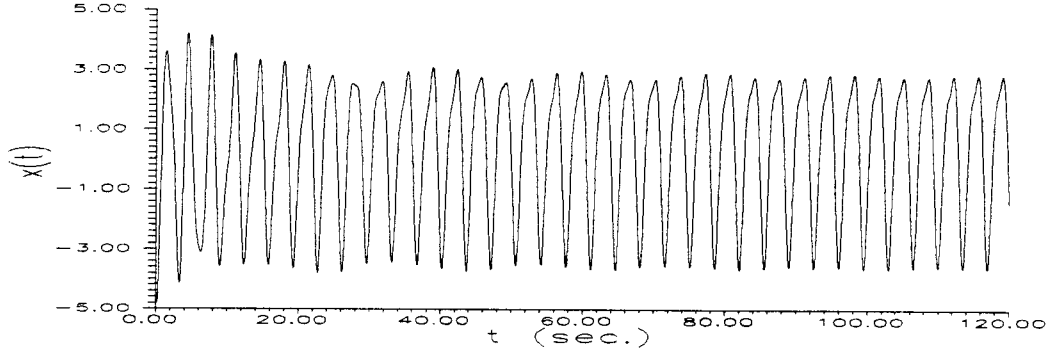

(c)

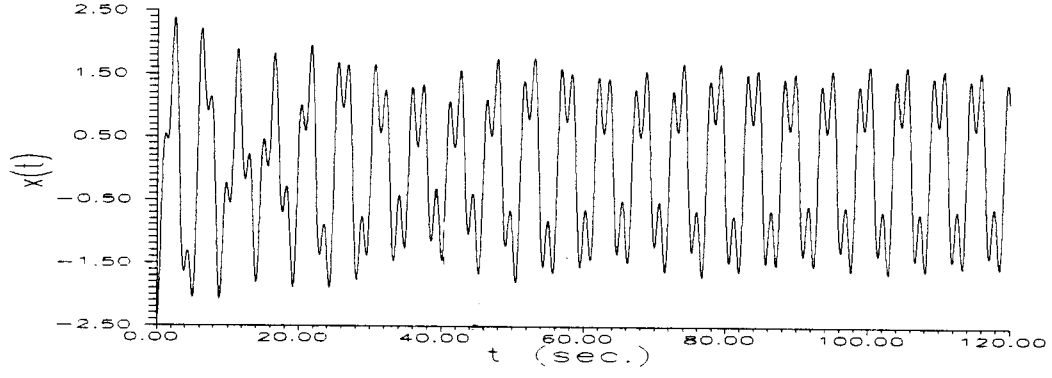

Figure 2.4 Time series of (a) excitation (b) 1/2 subharmonic response (c) 1/3 subharmonic response.

amplitude jump phenomena. Several typical examples are shown in Figs.2.5-10. Fig.2.5 shows a small excitation amplitude increase induces a rapidly increasing transient response amplitude and the system response is eventually changed from a small amplitude harmonic response to a large amplitude harmonic response. The amplitude jump phenomenon from a large amplitude harmonic response to a small amplitude harmonic response is shown in Fig.2.6. The changes of the response characteristics, due to small excitation amplitude changes, from a 1/2 subharmonic response to a small amplitude harmonic response, and from a 1/2 subharmonic response to a 1/3 subharmonic response are shown in Fig.2.7 and Fig.2.8, respectively. In addition, the 1/3 subharmonic responses in Figs.2.9 and 2.10 are observed to evolve to small amplitude harmonic responses when the magnitude of the excitation amplitude increases and decreases slightly, respectively.

(a)

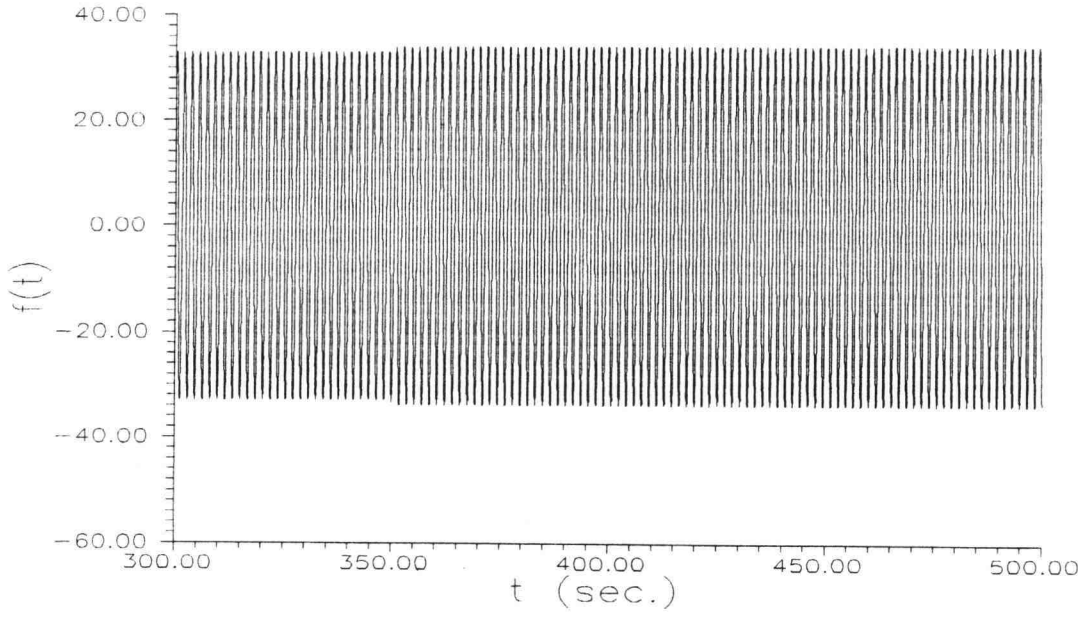

(b)

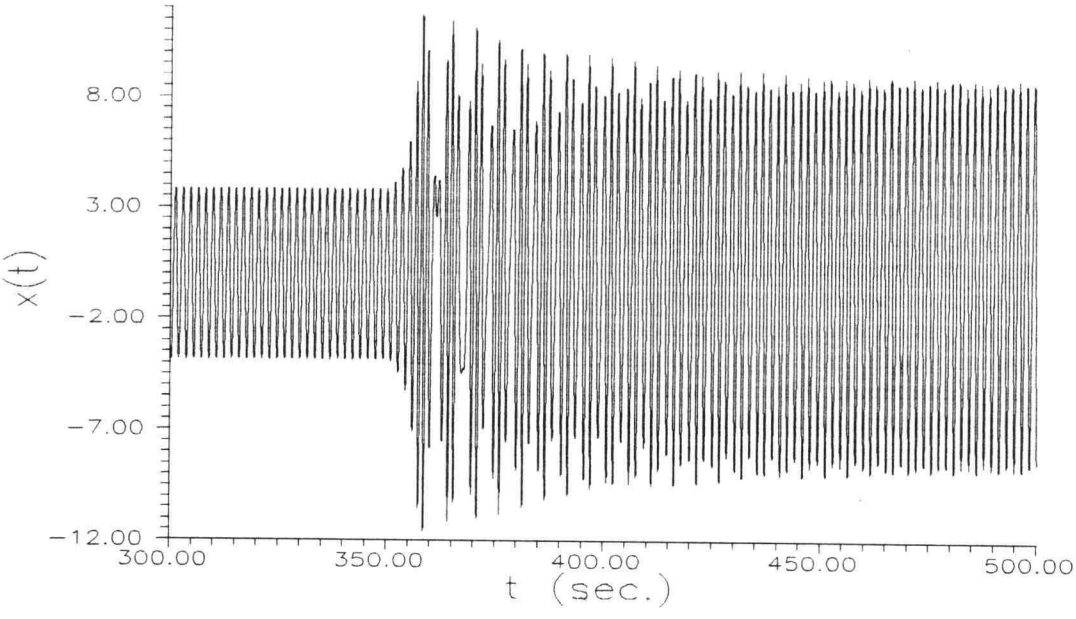

Figure 2.5 Response amplitude jump phenomenon: small amplitude harmonic domain to large amplitude harmonic domain. (a) excitation and (b) response time series.

(a)

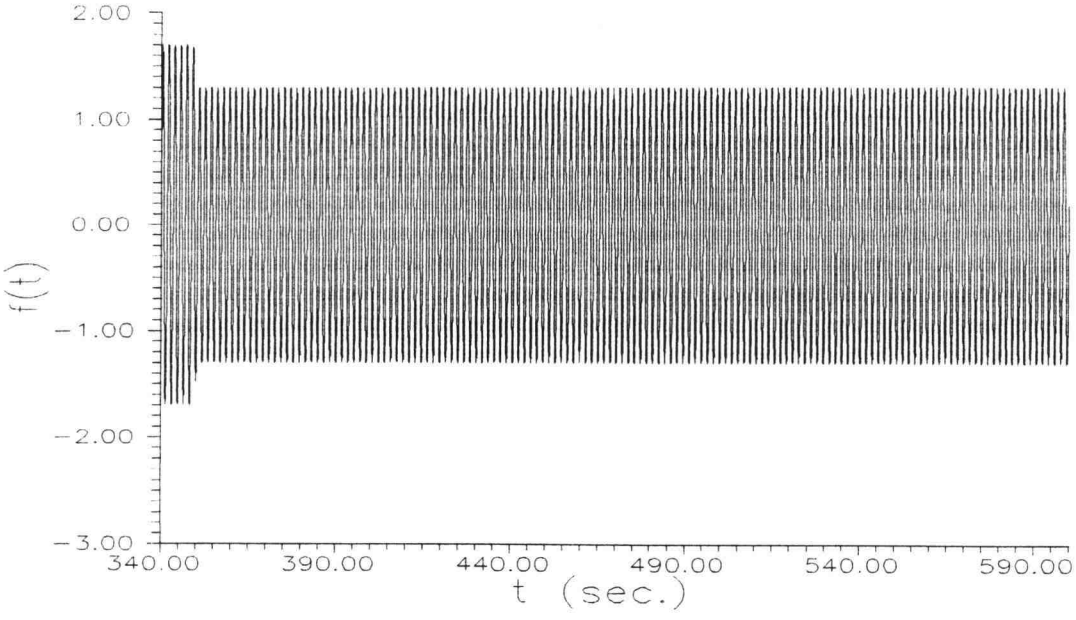

(b)

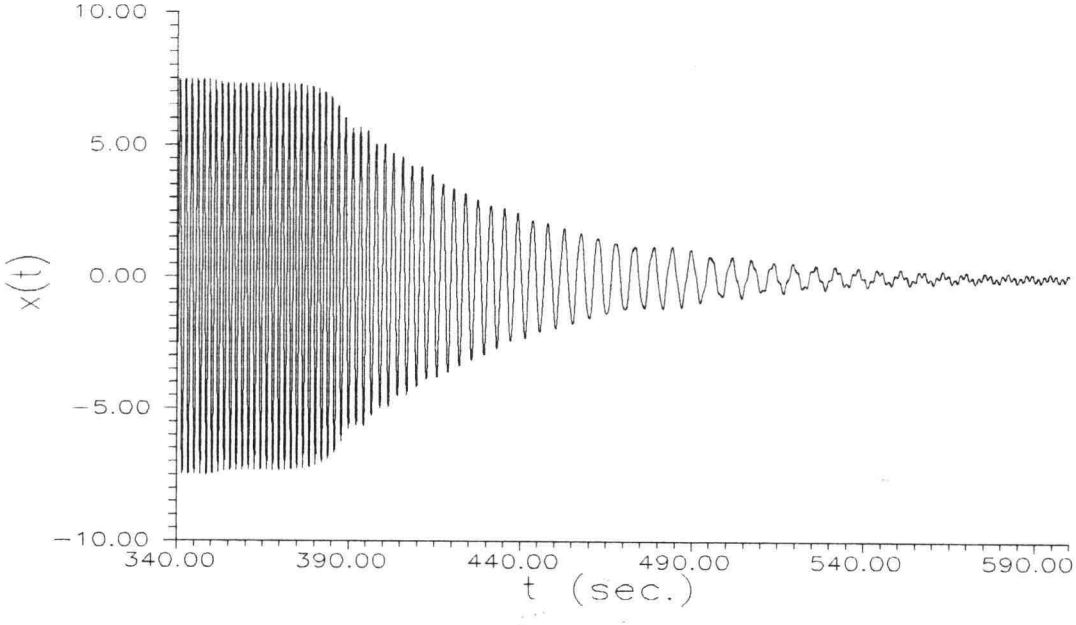

Figure 2.6 Response amplitude jump phenomenon: large amplitude harmonic domain to small amplitude harmonic domain. (a) excitation and (b) response time series.

(a)

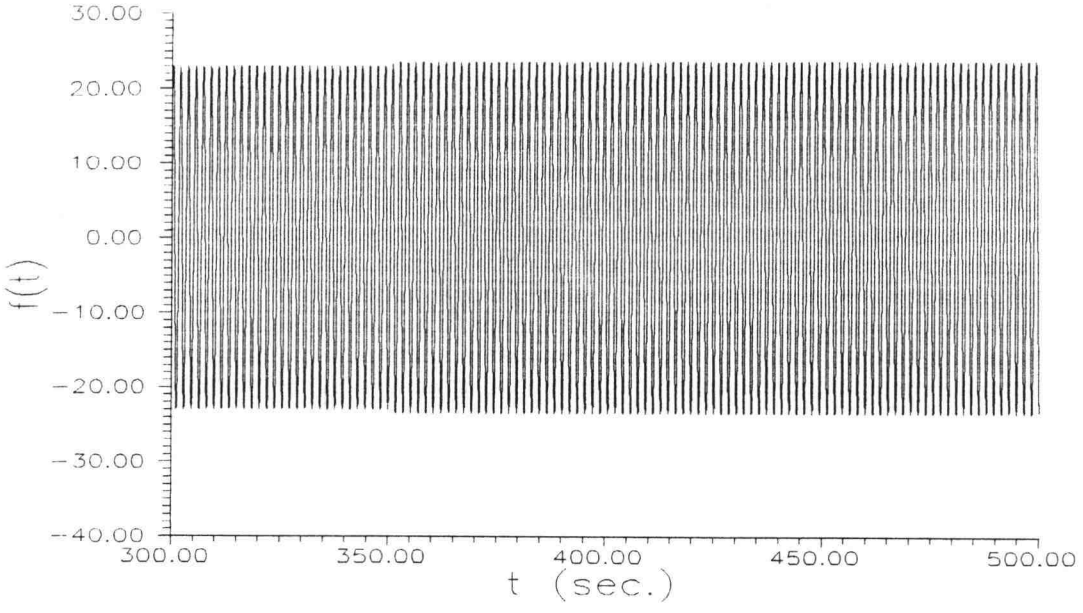

(b)

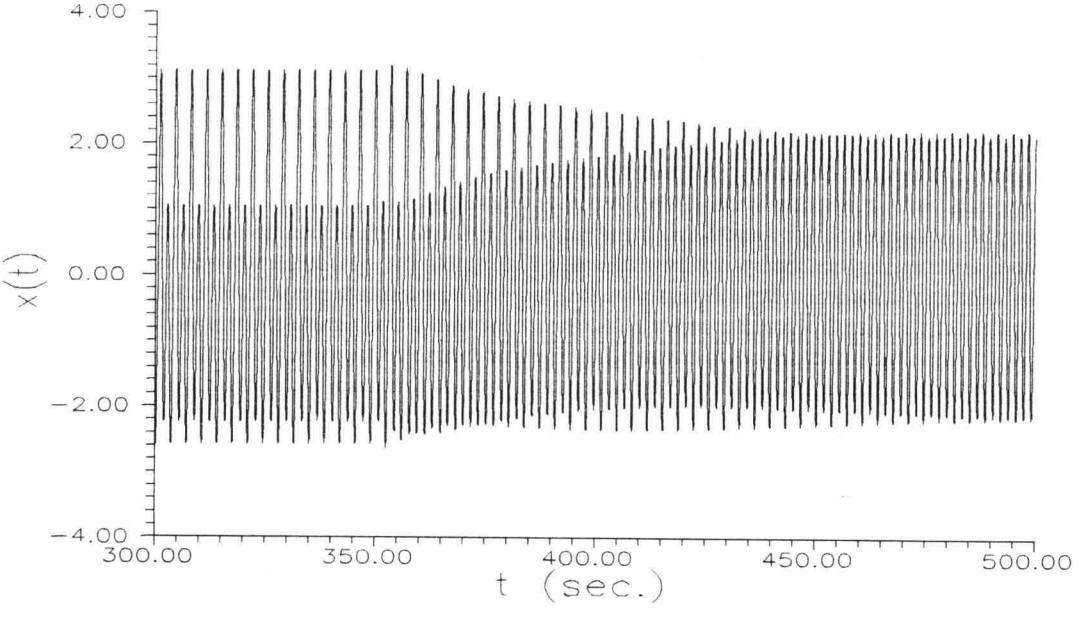

Figure 2.7 Response amplitude jump phenomenon: 1/2 subharmonic domain to small amplitude harmonic domain. (a) excitation and (b) response time series.

(a)

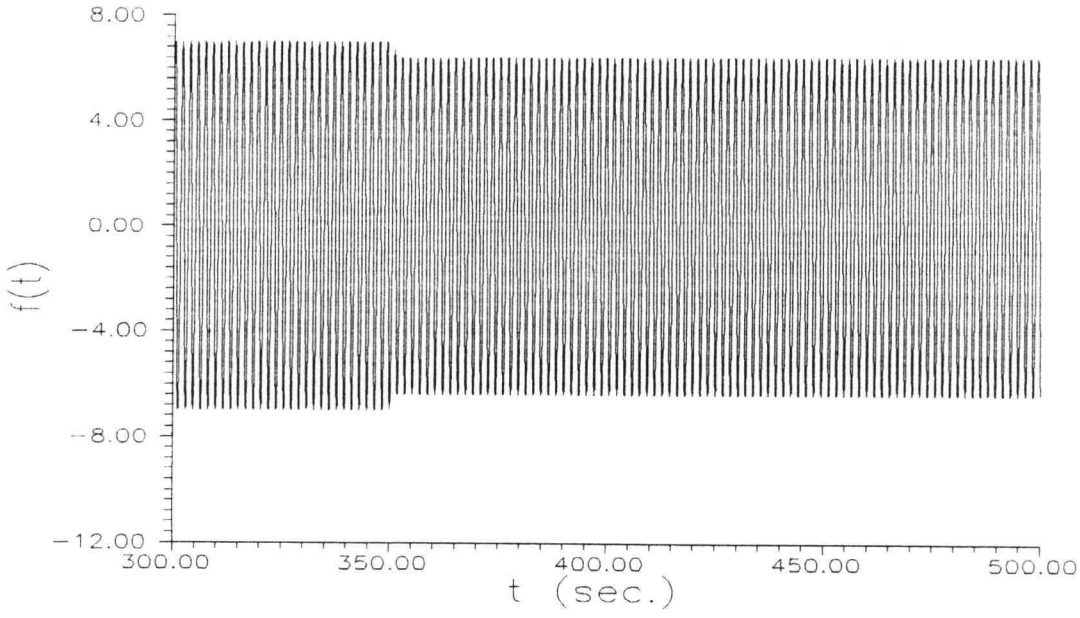

(b)

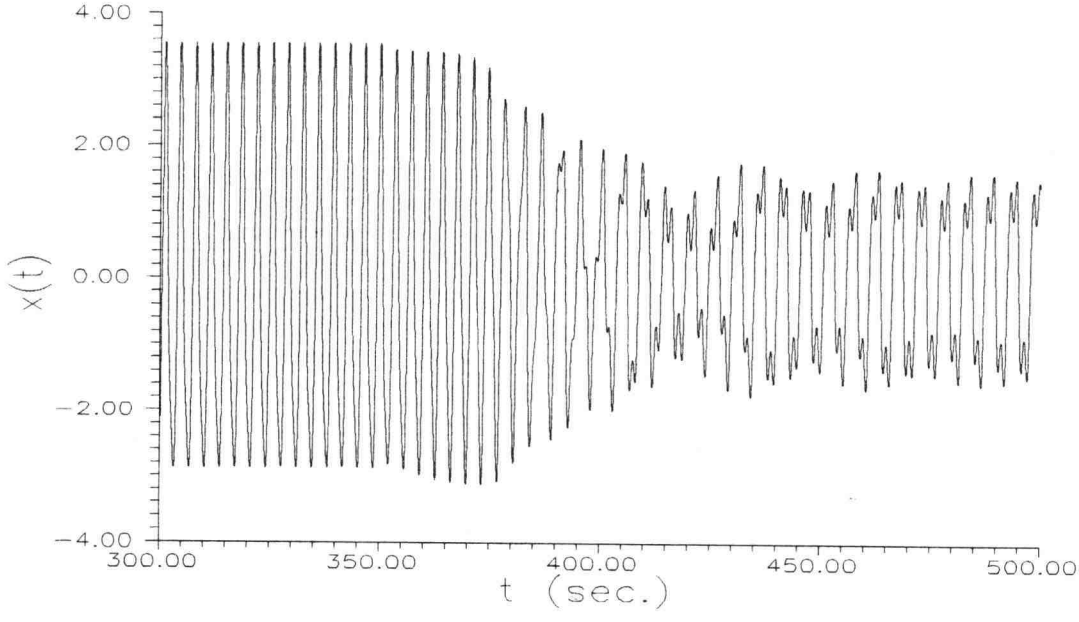

Figure 2.8 Response amplitude jump phenomenon: 1/2 subharmonic domain to 1/3 subharmonic domain. (a) excitation and (b) response time series.

(a)

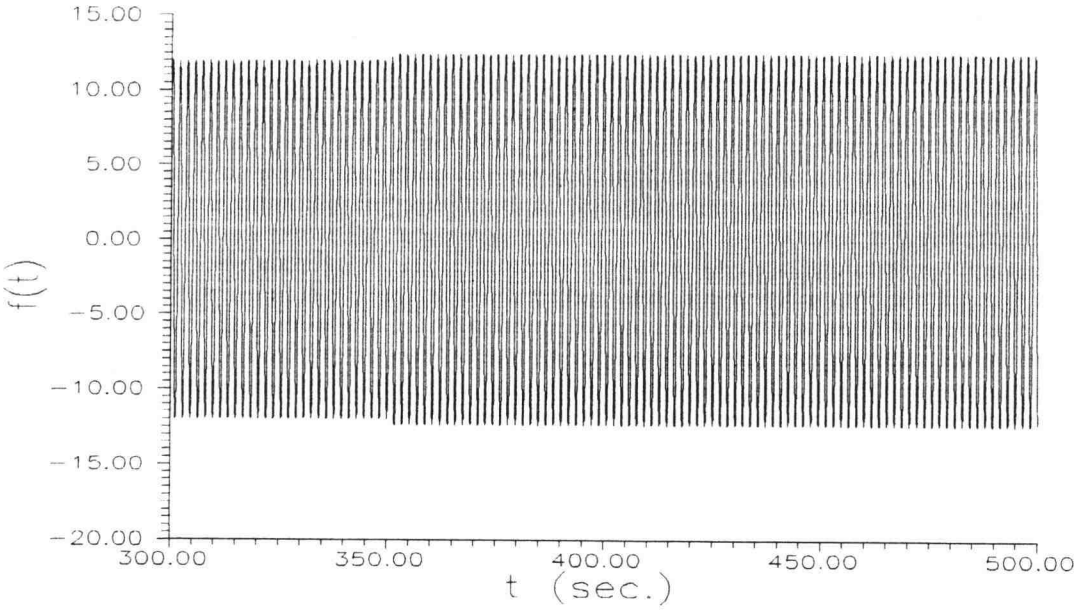

(b)

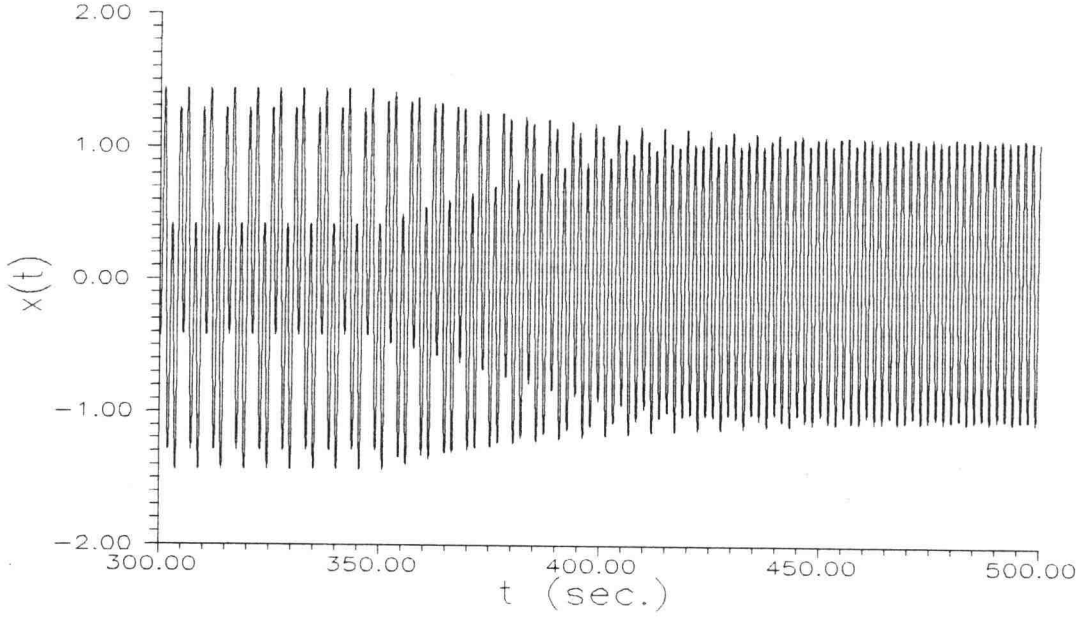

Figure 2.9 Response amplitude jump phenomenon: 1/3 subharmonic domain to small amplitude harmonic domain. (a) excitation and (b) response time series.

(a)

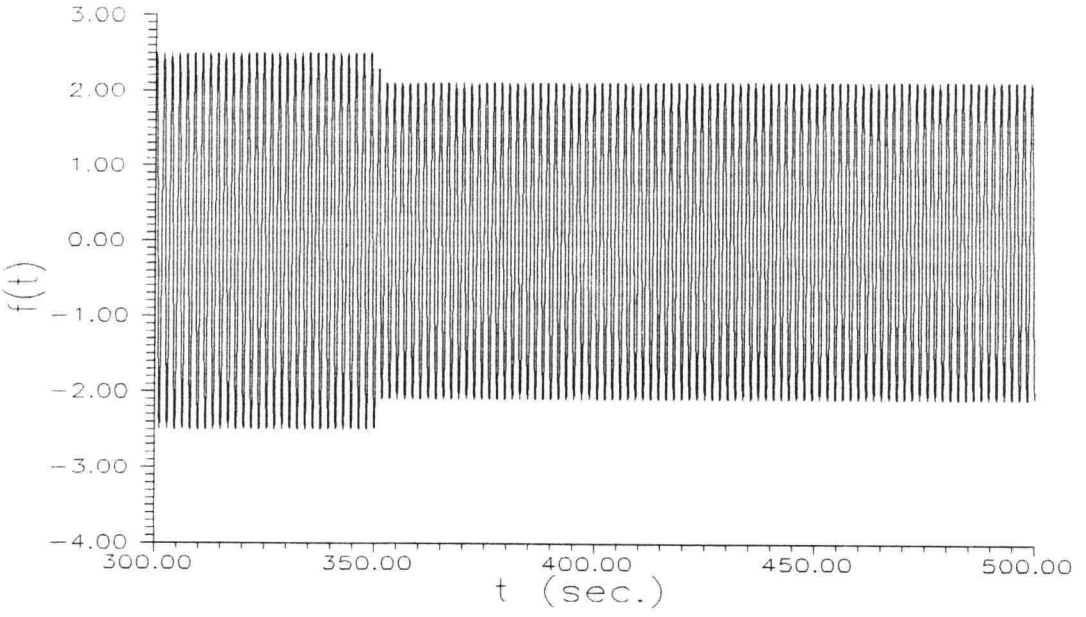

(b)

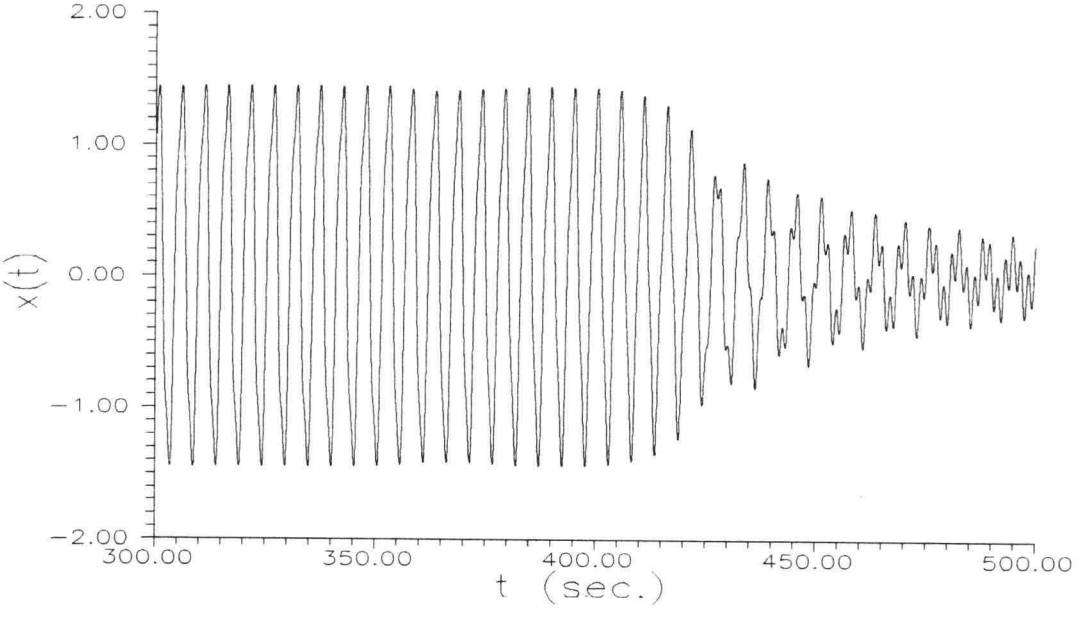

Figure 2.10 Response amplitude jump phenomenon: 1/3 subharmonic domain to small amplitude harmonic domain. (a) excitation and (b) response time series.

3. DETERMINISTIC NONLINEAR SYSTEM RESPONSE BEHAVIOR

Qualitative response characteristics of the Duffing type nonlinear system considered (Eq.(2.3)) under deterministic harmonic excitation (Eq.(2.4)) are investigated. The investigation is performed through an examination of the amplitude response curves, the response attraction domains and the first-return maps associated with the system responses (Nayfeh and Mook, 1979; Thompson and Stewart, 1986; Jordan and Smith, 1987; Drazin, 1992). The relationship between the system response and the associated first-return map is interpreted from a system total energy evolution point of view. The derived system response characteristics will be employed to facilitate numerical evaluations of the response behavior under narrowband excitations in Chapters 4 and 5. Note that in this chapter, the excitation parameters considered are the excitation amplitude A and the excitation phase angle ϕ only. The excitation frequency ω is considered as a constant, unless noted otherwise.

3.1 Attraction Domains Co-existence and Initial Condition Dependency

A major difference in the response characteristics between a linear system and a nonlinear system is the dependence of the steady-state response on the system initial (displacement x(0), and velocity dx/dt(0)) conditions. For a linear damped system, the steady-state response behavior is independent of initial conditions and is uniquely determined by the excitation parameters only (Clough and Penzien, 1993). However, for a nonlinear system, under identical excitation parameters, the steady-state response, as demonstrated in Section 2.4 (Figs.2.3-4), may exhibit totally different behavior depending on the initial conditions specified.

In a phase plane (x, dx/dt), the set of phase points corresponding to all initial conditions leading the system to the same steady-state response forms a domain of attraction. The corresponding steady-state response is called the "attractor" of that domain. For a linear system, for all given initial conditions, the dynamic responses will converge the unique steady-state response. Hence, only a single attractor exists, and the corresponding domain covers the entire phase plane. For a nonlinear system, different initial conditions may yield different steady-state responses. Hence, a number of "co-existing" attractors may result with the union of their corresponding (non-overlapping) attraction domains covering the phase plane. Note that the presence of co-existing domains implies the dependence of response behavior on initial conditions. However, it does not necessarily imply the existence of different types of response behavior (to be defined in the following).

3.1.1 Co-Existing Attraction Domains in Primary Resonance Region

A system is said to be in primary (or harmonic) resonance when the response frequency is equal to the excitation frequency, which is close to the linear natural frequency (i.e. $\sqrt{a_1}$) of the system (Nayfeh and Mook, 1979). Approximate steady-state solutions of the (harmonic) response obtained by the harmonic balance method (Jordan and Smith, 1987) are shown as (see Appendix B.1)

$$\left[\left(a_1-\omega^2+\frac{3}{4}a_3R^2\right)^2+c_S^2\omega^2\right]R^2=A^2 \qquad (3.1)$$

where, A, ω and ϕ are the excitation amplitude, frequency and phase angle, respectively; a_1, a_3 and c_S are defined in Eq.(2.1); and R is the steady-state response amplitude. It has been

shown that, in certain excitation parameter region(s), there exist two response amplitudes corresponding to the solutions of Eq.(3.1), but only one response amplitude exists for other regions (Nayfeh and Mook, 1979; Jordan and Smith, 1987).

Solution curves of the steady-state response amplitude as a function of the excitation amplitude with a fixed excitation frequency are called the amplitude response curves (Nayfeh and Mook, 1979). The amplitude response curves obtained by solving Eq.(3.1) is shown in Fig.3.1. Small amplitude responses exist only when the excitation amplitude is less than A_{2U} (right vertical line in the figure) and, thus, A_{2U} serves as the upper boundary of the small amplitude domain. Similarly, the left vertical line in the figure, A_{1L}, serves as the lower boundary of the large amplitude domain of the amplitude response curves. Between A_{1L} and A_{2U}, overlapping of the two domains indicates the co-existence of two primary resonance response attractors. Convergence of the system response to the large or the small amplitude attractor depends on initial conditions (Jordan and Smith, 1987). To clearly demonstrate the system response initial condition dependency and thus, the co-existing attraction domain phenomenon, the two attraction domains (shaded area) corresponding to an excitation amplitude (A = 0.8) in the overlapping area are shown in Fig.3.2. For convenience of notations, the large amplitude and small amplitude attraction domains are denoted as D_L and D_S, respectively, for physical reasons. These domain will also be called D_1 and D_2, respectively, for convenience of probability computations in later sections. The intervals of the excitation amplitudes in which D_L (or D_1) and D_S (or D_2) exist are denoted as D_1^A and D_2^A, respectively. That is, $D_1^A = [A_{1L}, \infty)$ and $D_2^A = (0, A_{2U}]$, as shown in Fig.3.1. Overlapping of D_1^A and D_2^A is observed. Note that, in attraction domains D_1 and D_2, their corresponding steady-state response amplitudes form domains of response amplitude D_1^R and

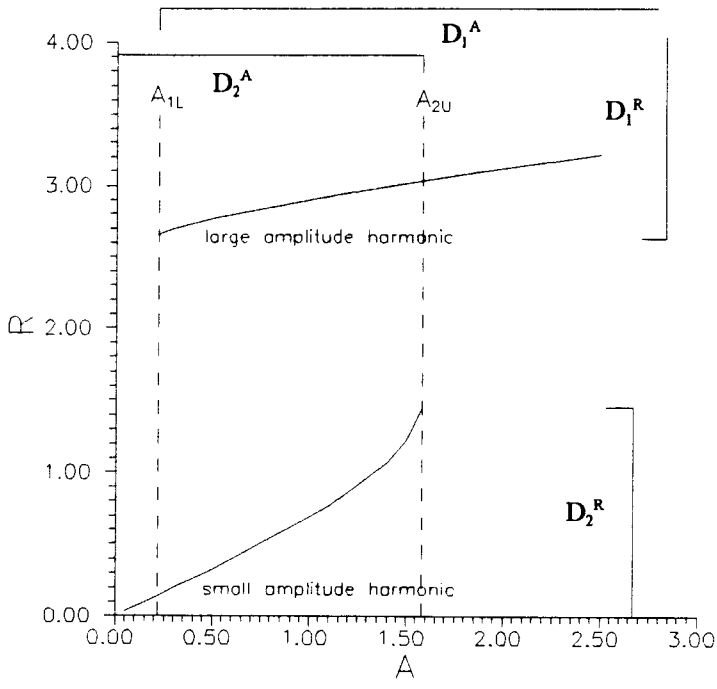

Figure 3.1 Amplitude response curves of the system in the primary resonance region. $\{c_S = 0.05, a_1 = 1, a_3 = 0.3, \omega = 1.6, \phi = 0\}$.

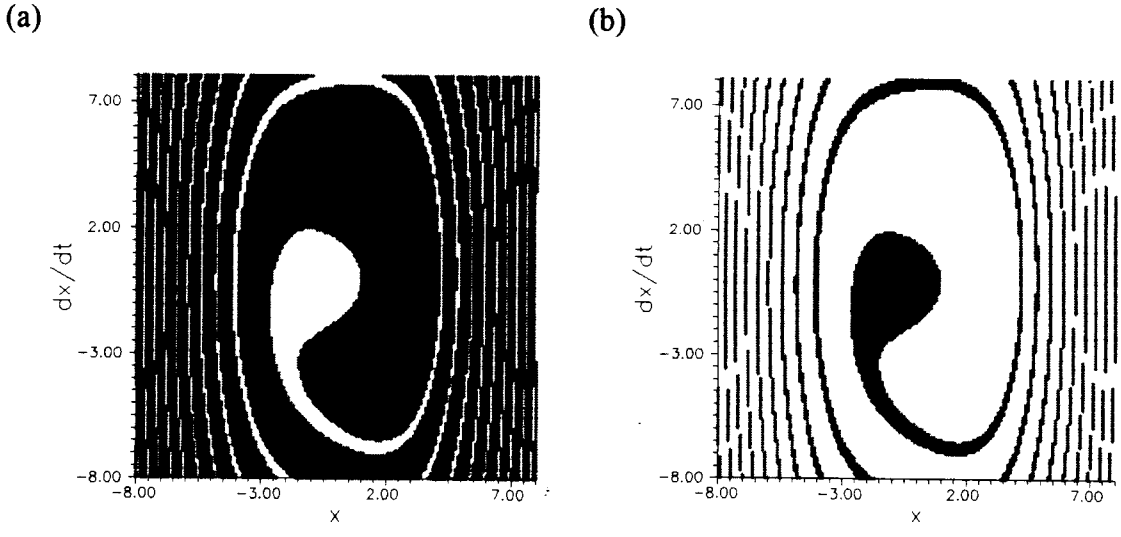

Figure 3.2 Attraction domain (shaded area) of: (a) large amplitude harmonic response, D_1 and (b) small amplitude harmonic response, D_2. $\{c_S = 0.05, a_1 = 1, a_3 = 0.3, \omega_f = 1.6, \phi = 0, A = 0.8\}$.

D_2^R, respectively, as shown in Fig.3.1. In addition, within D_d (d =1, 2), D_d^R and D_d^A is related by a one-to-one mapping characterized by the amplitude response curve associated with D_d considered. No overlapping of response amplitude domains is observed when the system responses are in their respective steady states.

3.1.2 Co-Existing Attraction Domains in Subharmonic Resonance Region

When the excitation frequency is close to an integer multiple of the system linear natural frequency, the system is said to be in subharmonic resonance (Jordan and Smith, 1987). Typical subharmonic responses of orders 1/2 and 1/3 are shown in Figs.2.4(b) and 2.4(c), respectively. Previous investigations show that, when the excitation frequency ω is close to three times the system linear natural frequency $\sqrt{a_1}$, five attraction domains co-exist (Thompson and Stewart, 1986). These attraction domains include two harmonic (large and small amplitude), two 1/2 subharmonic, and one 1/3 subharmonic responses. It is found that the two co-existing 1/2 subharmonic response attractors are of the same steady-state amplitude but with different biases in the time series. Thus, they are considered as being parts of the same attraction domain (i.e., they belong to the same attractor) henceforth in this study. For convenience of notations, the 1/2 and 1/3 subharmonic attraction domains are denoted as $D_{1/2}$ and $D_{1/3}$, respectively. Also, these domain will be called D_3 and D_4, respectively, for convenience of probability computations in later sections.

Amplitude response curves of the system in the subharmonic resonance region are shown in Fig.(3.3). Due to the complexity of solving approximate steady-state response amplitudes in these attraction domains (see Appendix B.2), these curves are obtained by direct integration of Eq.(2.1) for simplicity. In the figure, the vertical dashed lines indicate

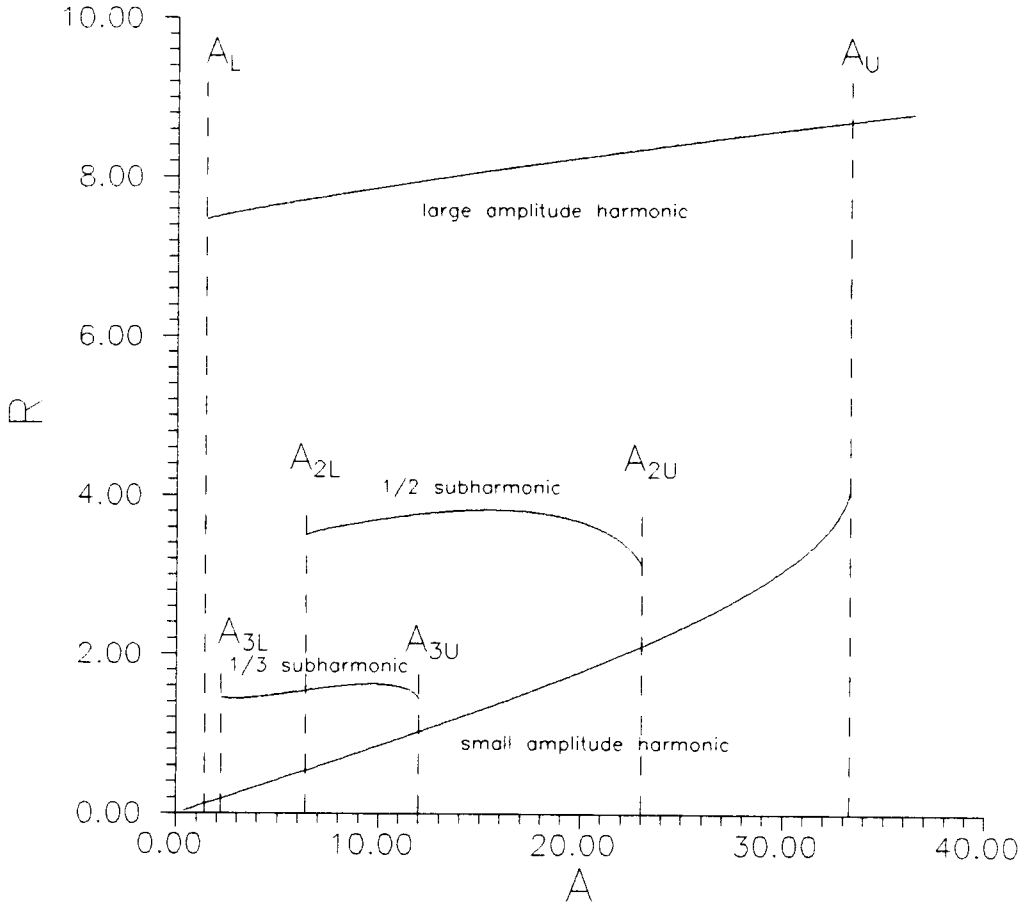

Figure 3.3 Amplitude response curves of the system in the subharmonic resonance region. $\{\omega_f = 3.6$, the rest parameters are the same as in Fig.3.1$\}$

intervals of excitation amplitudes where different types of system response, or attraction domain D_d, exist. That is, $D_1^A = [A_{1L}, \infty)$, $D_2^A = (0, A_{2U}]$, $D_3^A = [A_{3L}, A_{3U}]$ and $D_4^A = [A_{4L}, A_{4U}]$, as shown in Fig.3.3. Overlapping of these domains are observed. In the region where the D_d^A (d = 1,2,3,4) overlap, such as $[A_{3L}, A_{4U}]$, different response attraction domains co-exist and the occurrence of a particular system response depends on initial conditions (Jordan and Smith, 1987). To demonstrate the system response initial condition dependency (in this case, the co-existing domain phenomenon in the subharmonic resonance region), the four attraction domains, D_d (d =1,2,3,4), corresponding to an excitation amplitude (A = 9) in the region of $[A_{3L}, A_{4U}]$ are shown in Fig.3.4. Note that, in each domain D_d (d =1,2,3,4), the steady-state response amplitudes also form a response amplitude domain D_d^R, as shown in Fig.3.3. However, only the amplitude response curves associated with D_1 and D_2 characterize a one-to-one relationship between the steady-state response amplitude domain $D_{(1,2)}^R$ and the excitation amplitude domain $D_{(1,2)}^A$. In addition, unlike the case in the primary resonance region, response amplitude domains overlapping is observed among D_d^R (d =2,3,4). That is, a single response amplitude may belong to more than one attraction domains and thus, may correspond to different excitation amplitudes.

3.2 Response Behavior within Attraction Domains

3.2.1 System Total Energy and First-Return Map

In each attraction domain, D_d, the system response behavior can be characterized by the system total energy evolution which can also be described in the first-return map associated with the response. The system total energy, TE, is defined as the sum of the potential energy, PE (a function of the response displacement), and the kinetic energy, KE

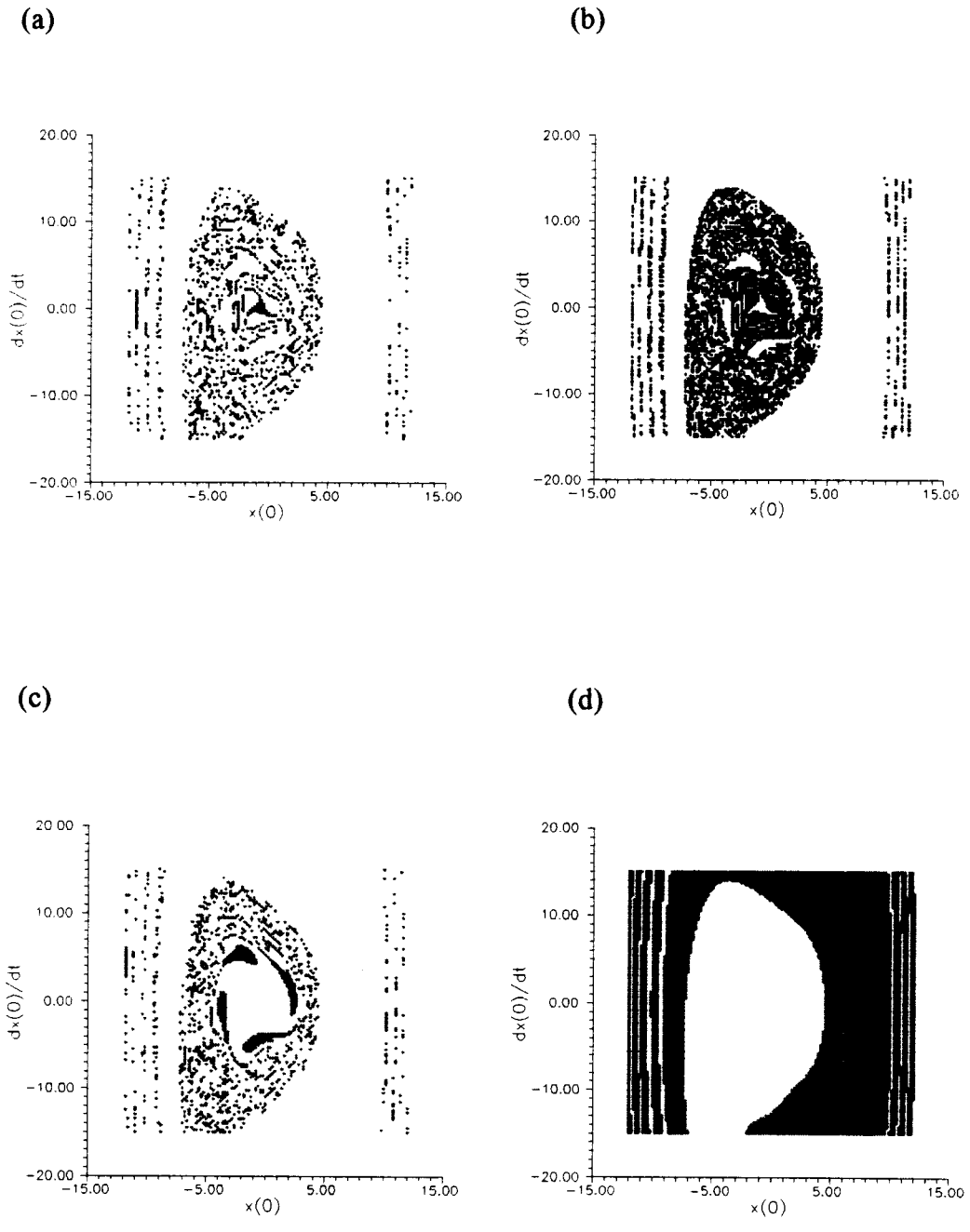

Figure 3.4 Attraction domain (shaded area) of: (a) small amplitude harmonic response, D_2, (b) 1/3 subharmonic response, D_4, (c) 1/2 subharmonic response, D_3, and (d) large amplitude harmonic response, D_1. $\{c_S = 0.05, a_1 = 1, a_3 = 0.3, \omega = 3.6, \phi = 0, A = 9\}$.

(a function of the response velocity). Thus, the system total energy can be expressed as

$$TE = PE + KE = \frac{1}{2}a_1 x^2 + \frac{1}{4}a_3 x^4 + \frac{1}{2}\dot{x}^2 \tag{3.2}$$

Variation of the system total energy over a time interval Δt, denoted by $\Delta TE(\Delta t)$, depends on the interaction between the system response and the excitation, and can be expressed as

$$\Delta TE(\Delta t) = \int_0^{\Delta t} f(t)\,dx - \int_0^{\Delta t} c_s \dot{x}(t)\,dx \tag{3.3}$$

The first-return map (Drazin, 1992) is also referred to as the Poincaré map (Thompson and Stewart, 1986; Jordan and Smith, 1987; Hagedorn, 1988). The map is obtained by sampling points along the response phase trajectory at a constant time interval equal to the excitation period T and plotting these points on a phase plane (x, dx/dt). The sample points are called the first-return points which represent the system phase status (x(nT), dx(nT)/dt) when the excitation completes one cycle. Variations of the first-return points are described by a first-return path.

A fixed point on the first return map is one that the sample points repeatedly visit infinitely often. Finite fixed points in the first-return map indicate that periodic (subharmonic) solution of the system response is obtained (Jordan and Smith, 1987). In other words, the system is in a steady state because the response phase status over one response cycle remains constant. On the other hand, when the system is transient, the response phase status varies over every cycle and the system is said to be in a transient state. Thus, during a transient

state, the sampled first-return points also vary. Variations in the first-return points are described by a first-return path which converges to the fixed point(s).

Note that, from Eqs.(3.2 and 3), variations in the system total energy associated with two consecutive first-return points represent the variations in the system total energy over one excitation cycle, or equivalently, $\Delta TE(T=2\pi/\omega)$. As a result, variations in $\Delta TE(T)$ is also indicated by the first-return path.

3.2.2 Response Characteristics

In what follows, response characteristics of the system in each attraction domain is revealed by a domain dependent repeated pattern of the first-return pont variations. In addition, the characteristics can also be discerned by the relationship between the system response and the system total energy evolution. The system response corresponding to the first-return points in a complete pattern is said to be in a group and the number of first-return points in a pattern is referred to the group size.

(1) Large amplitude harmonic domain: The phase trajectory of a large amplitude harmonic response is shown in Fig.3.5a. A first-return map corresponding to the rectangular region is shown in Fig3.5b. As the first-return points varying along the spiraling first-return path, a repeated pattern corresponding to a size-5 response group is observed (see point 0, 5, 10 ..., or points 1, 6, 11, ..., in Fig.3.5b). In the system total energy evolution (Fig.3.5c), it is also observed that $\Delta TE(T)$ has a variation cycle of group size 5 which coincides with the variation cycle of the first-return point (Fig.3.5b). Thus, the behavior of the system response within a group determines the system total energy variation cycle and vice versa. In addition, a comparison of the response time series (Fig.3.5d) with the system total energy evolution

(a)

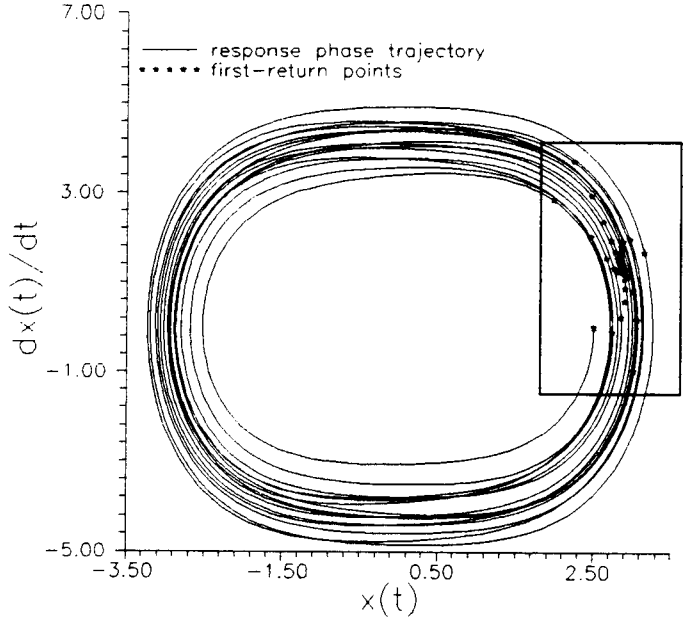

(b)

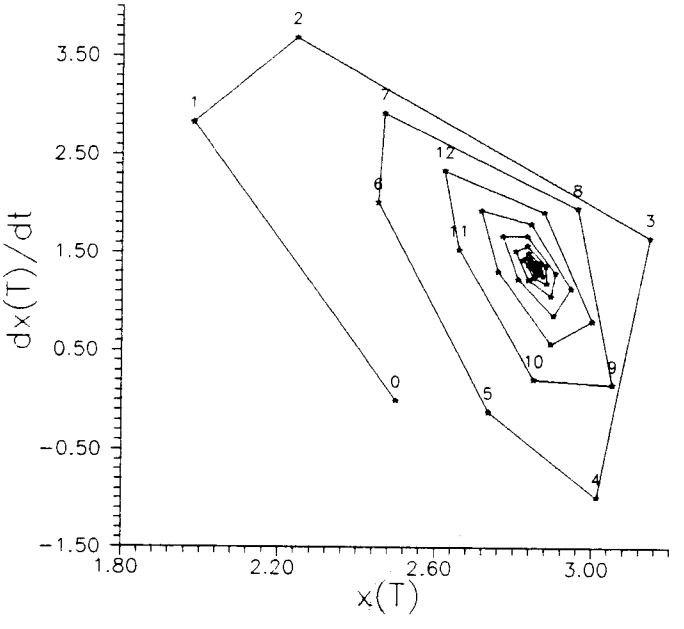

Figure 3.5 System response in the large amplitude harmonic attraction domain. (a) response phase trajectory. (b) first-return map.

(c)

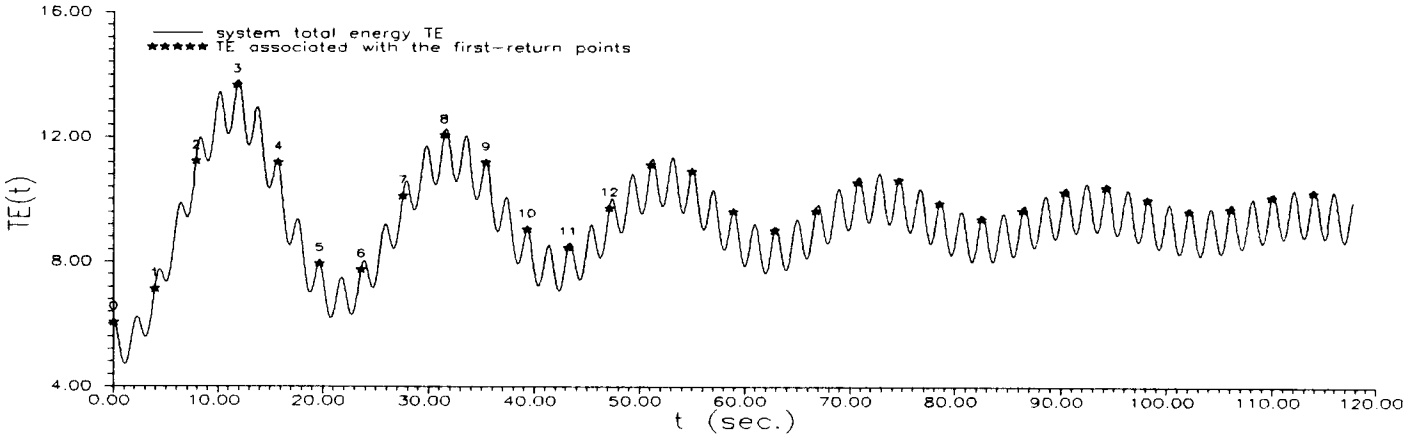

(d)

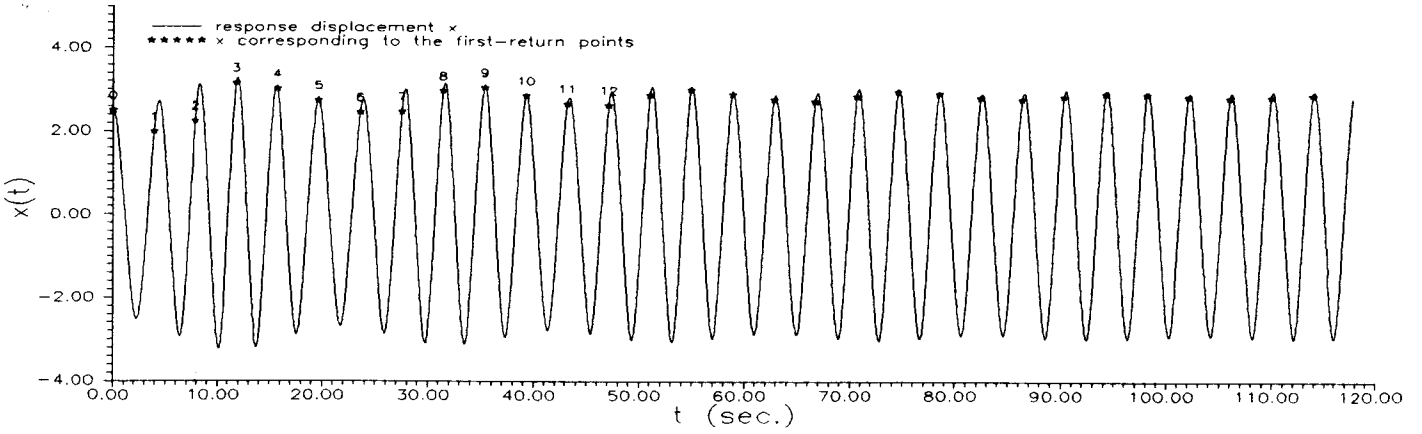

Figure 3.5 Continued. (c) system total energy evolution. (d) response displacement time series. {c_s =0.05, a_1 = 1, a_3 = 0.3, ω = 1.6, T = 3.93, ϕ = 0, A = 1, (x(0), dx/dt(0)) = (2.5, 0)}.

show that the response local extrema always coincide with the system total energy local maxima.

(2) Small amplitude harmonic domain: The phase trajectory of a small amplitude harmonic response is shown in Fig.3.6a. A first-return map corresponding to the rectangular region is shown in Fig3.6b. A repeated pattern of the first-return point variations corresponding to a response group size 3 is observed. By examining the system total energy evolution (Fig.3.6c), a system total energy variation cycle of period 3 is also observed within the response group. A comparison of the response time series (Fig.3.6d) with the system total energy evolution shows that the response local extrema are associated with the system total energy local minima.

(3) 1/2 subharmonic domain: The phase trajectory of a 1/2 subharmonic response is shown in Fig.3.7a. A first-return map corresponding to the two rectangular regions is shown in Fig3.7b. Due to the tangling of the first-return path, only a small portion of the path is shown (dashed line). The first-return points are observed to jump consistently and consecutively between two branches (solid lines). Thus, a complete pattern of the first-return point variations consists of only two points, corresponding to a response group size 2. Within the response group, the system total energy variation completes a cycle as shown in the system total energy evolution (Fig.3.7c). In the response time series shown in Fig.3.7d, the response local extrema are observed to coincide with the system total energy local minima.

(4) 1/3 subharmonic domain: The phase trajectory of a 1/3 subharmonic response is shown in Fig.3.8a. A first-return map corresponding to the three rectangular regions is shown in Fig3.8b. For clear demonstration of the trend in the variations of the first-return points, only part of the first-return path is shown in Fig.3.8b (dashed line). The first-return points

(a)

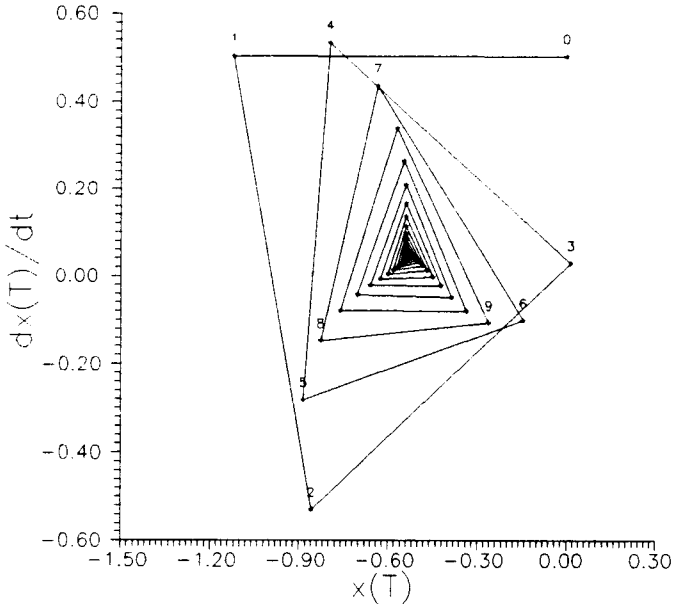

(b)

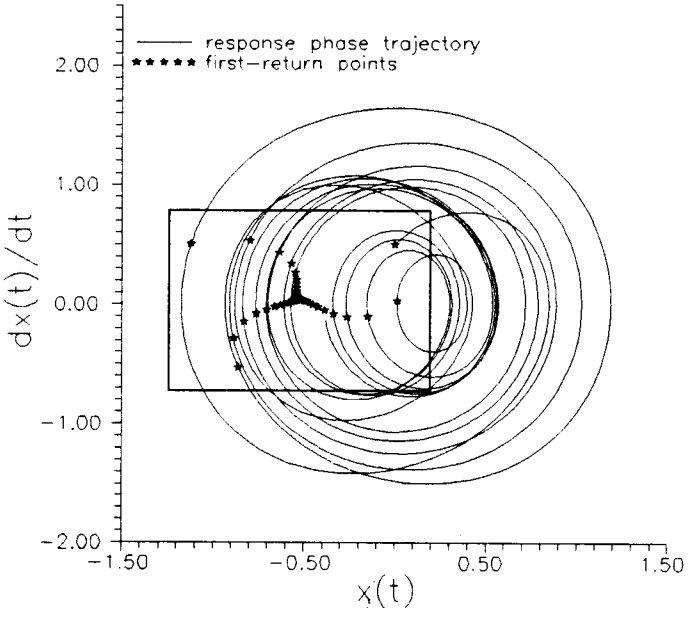

Figure 3.6 System response in the small amplitude harmonic attraction domain. (a) response phase trajectory. (b) first-return map.

(c)

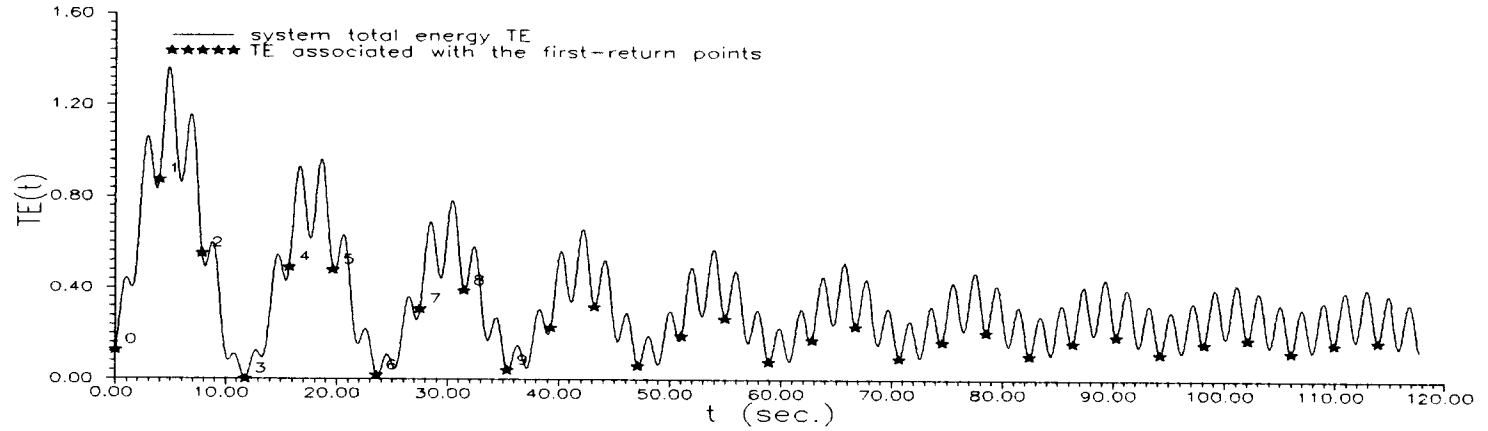

(d)

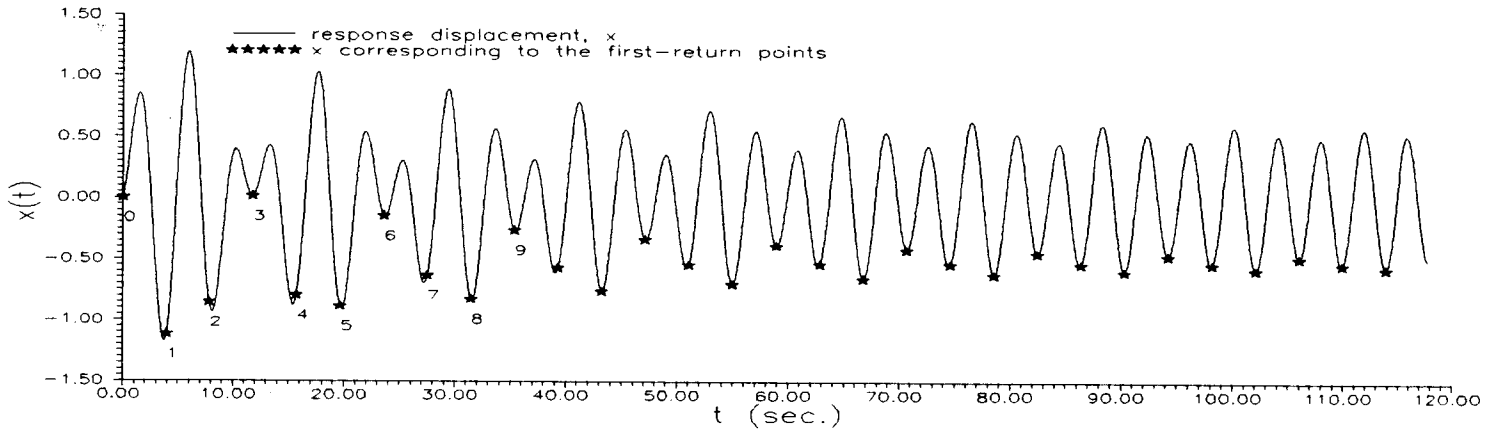

Figure 3.6 Continued. (c) system total energy evolution. (d) response displacement time series. $\{c_s = 0.05, a_1 = 1, a_3 = 0.3, \omega = 1.6, T = 3.93, \phi = 0, A = 0.8, (x(0), dx/dt(0)) = (0, 0.5)\}$.

(a)

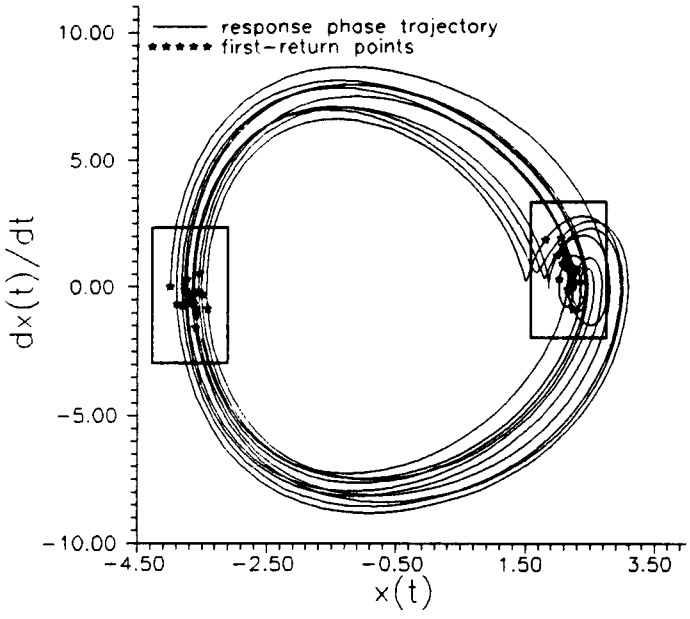

(b)

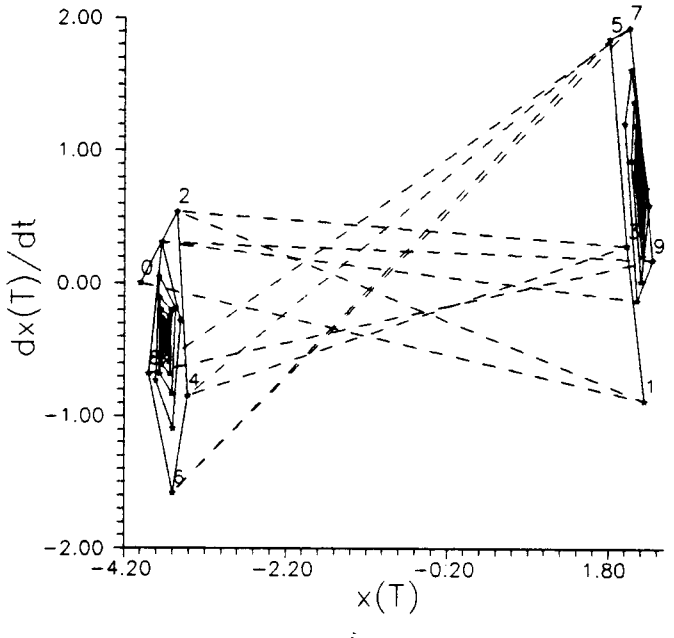

Figure 3.7 System response in the 1/2 subharmonic attraction domain. (a) response phase trajectory. (b) first-return map.

(c)

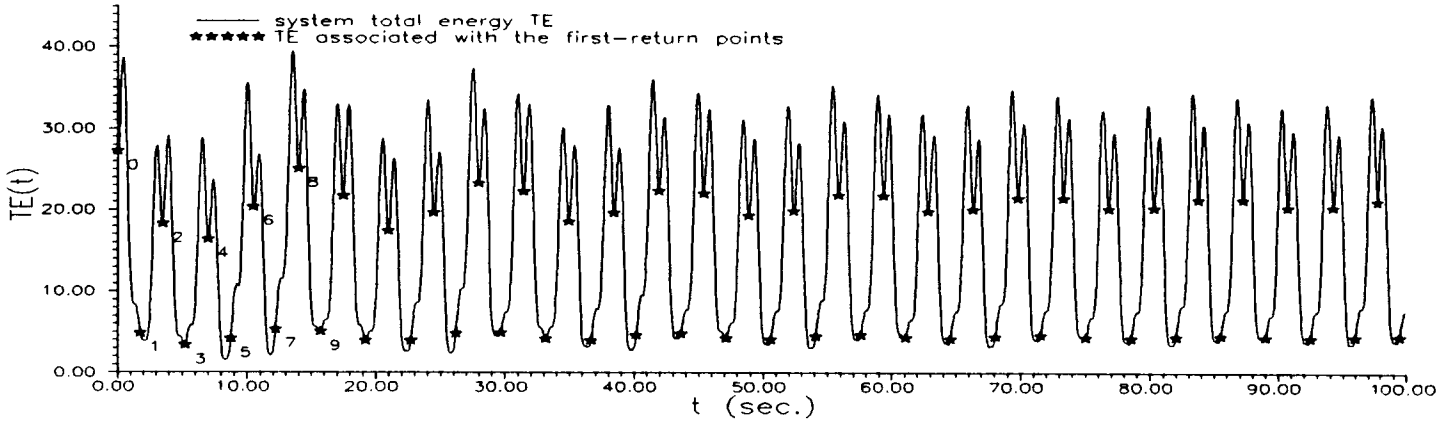

(d)

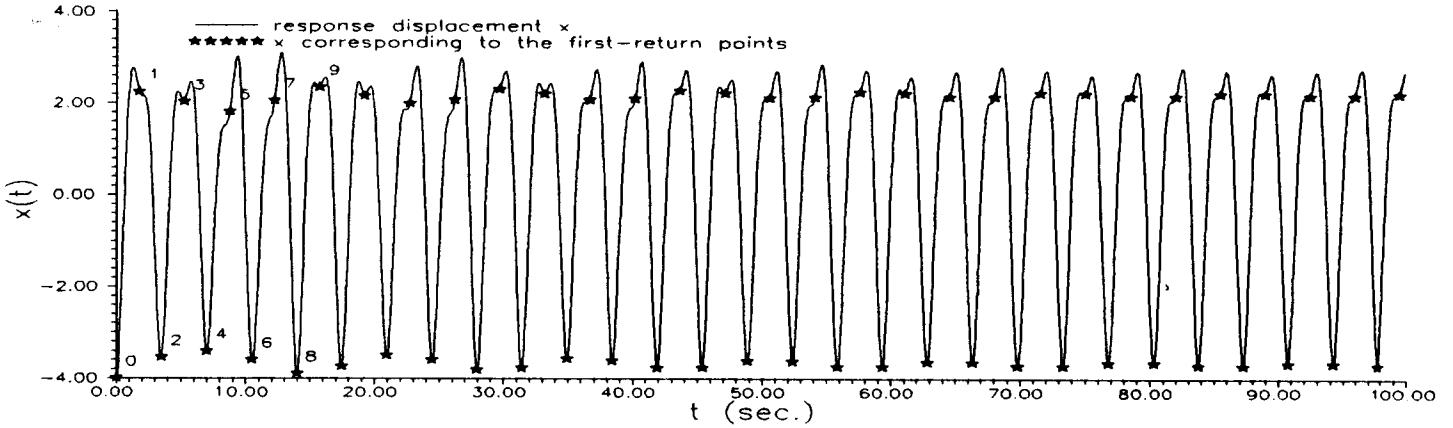

Figure 3.7 Continued. (c) system total energy evolution. (d) response displacement time series. {$c_S = 0.05$, $a_1 = 1$, $a_3 = 0.3$, $\omega = 3.6$, $T = 1.75$, $\phi = 0$, $A = 10$, $(x(0), dx/dt(0)) = (-4, 0)$}.

(a)

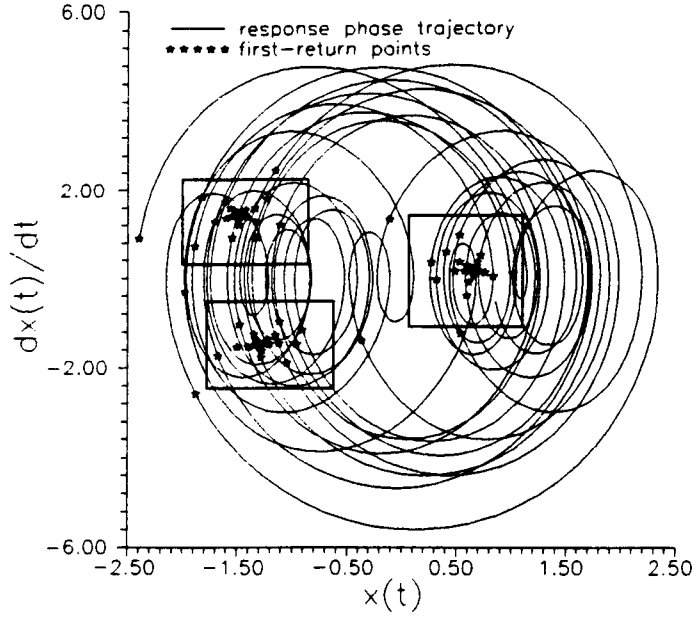

(b)

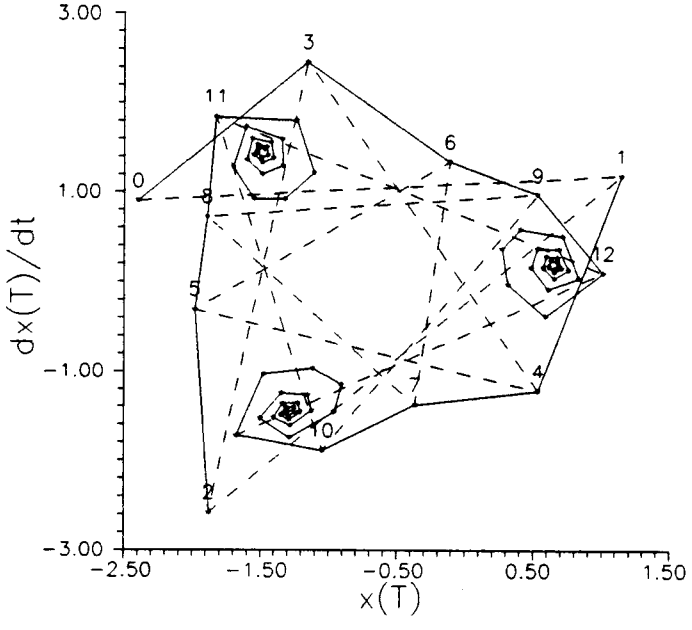

Figure 3.8 System response in the 1/3 subharmonic attraction domain. (a) response phase trajectory. (b) first-return map.

(c)

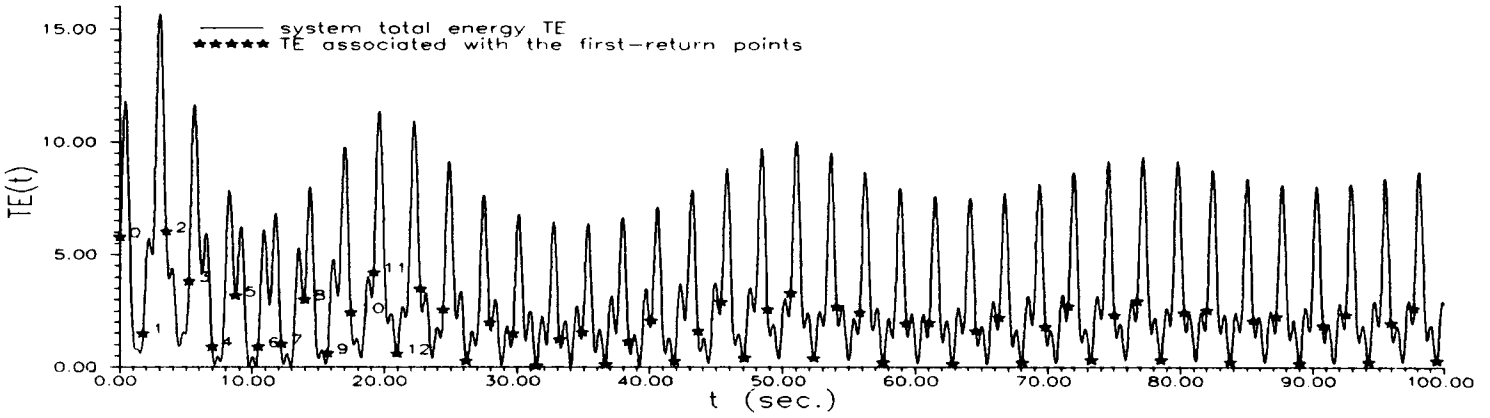

(d)

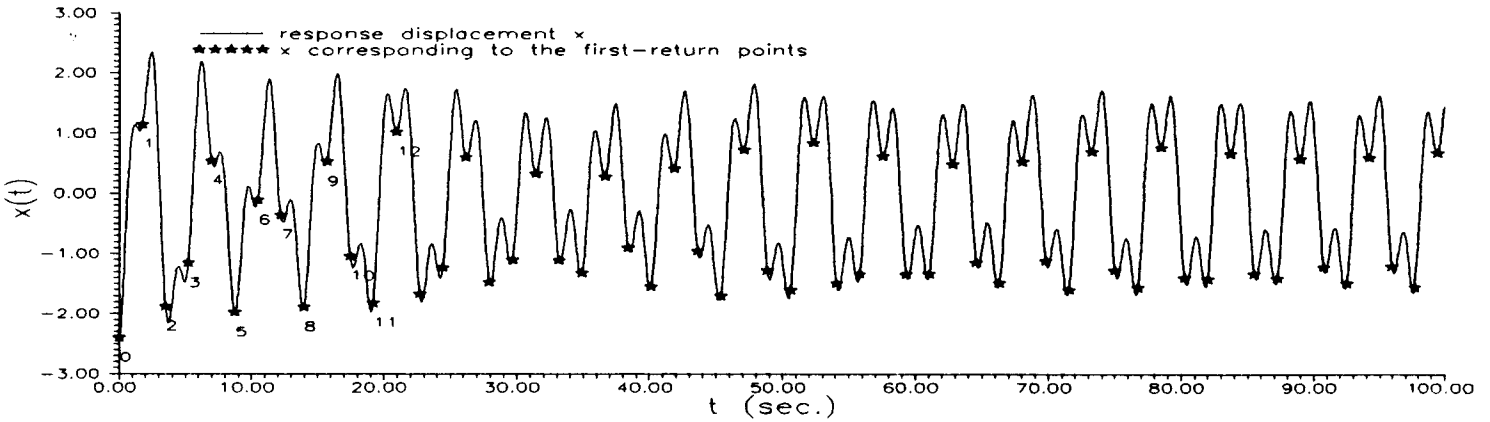

Figure 3.8 Continued. (c) system total energy evolution. (d) response displacement time series. {$c_S = 0.05$, $a_1 = 1$, $a_3 = 0.3$, $\omega = 3.6$, $T = 1.75$, $\phi = 0$, $A = 8$, $(x(0), dx/dt(0)) = (-2.4, 0.9)$}.

jump consistently and consecutively among three branches (solid lines) to form a complete pattern which corresponds to the response group size 3. The system total energy variation completes a cycle within a response group (period 3T) as shown in the system total energy evolution (Fig.3.8c). The response local extrema is also observed to coincide with the system total energy local minima as shown in the response time series (Fig.3.8d). Note that the system total energy variation cycle is the same for both the small amplitude harmonic domain and the 1/3 subharmonic domain. However, the first-return path in the small amplitude harmonic domain converges to one fixed points, whereas that of the 1/3 subharmonic domain converges to 3 fixed point. This information enables us to discern the two types of responses.

3.2.3 Response Amplitude Domain Overlapping

When the system is in a transient state, the response amplitudes vary continuously even under constant excitation parameters. In other words, the response amplitude domain $(D_d^R)_j$ corresponding to an excitation amplitude A_j in D_d^A consists no long a single value (the steady-state amplitude). Thus, the one-to-one relationships described in Section 3.1 between $D_{(1,2)}^R$ and $D_{(1,2)}^A$ does not hold in this case. As a result, when the system is in a transient state, overlapping of response amplitude domains occurs not only among different attraction domains (i.e., D_d^R (d =1,2,3,4)), but also, within an attraction domain, among different excitation amplitudes (i.e., $(D_d^R)_j$ (d = 1,2,3,4; $A_j \in D_d^A$)), as shown in Fig.3.9.

3.3 Response Inter-Domain Transitions

When the excitation amplitude varies out of the attraction domain boundaries defined in the amplitude response curves (Section 3.1), the system response may be attracted to a

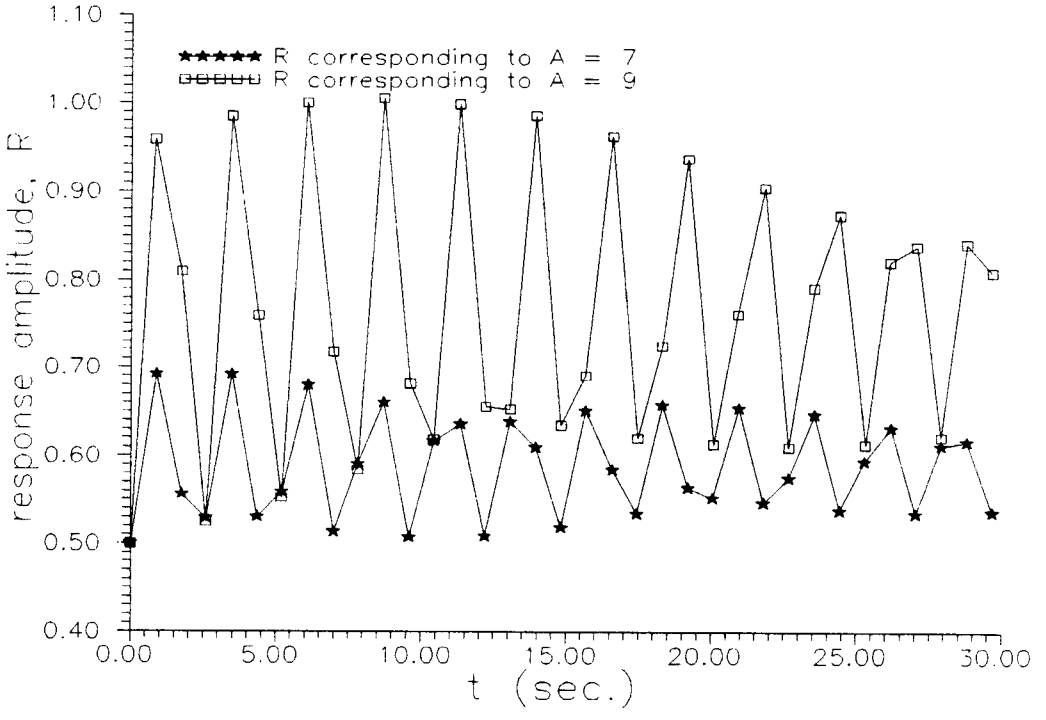

Figure 3.9 Response amplitude domain overlapping in the small amplitude harmonic response attraction domain. $\{c_S = 0.05, a_1 = 1, a_3 = 0.3, \omega = 3.6, \phi = 0, (x(0), dx/dt(0)) = (-0.5, 0.1)\}$.

competing attraction domain and a response inter-domain transition occurs. The attraction domain which the system settles to during the transition is referred to as the destination domain. In addition, the transition generally induces a large and obvious amplitude variation and is often referred to as the jump phenomenon. Note that, during the inter-domain transition, the system response is in a transient state which is often much more complex than that within an individual attraction domain due to the large number of possible destination domains.

In the primary resonance region, two attraction domains are possible and thus, an exit of the system response from one of them leads the system into another one (see Fig.3.1). In the subharmonic resonance region, when the excitation amplitude exits from the small amplitude domain by crossing A_{2U} (see Fig.3.3), the system response goes to the large amplitude harmonic domain because it is the only existing domain for $A > A_{2U}$. Similarly, an exit of the system response from the large amplitude harmonic domain by varying the excitation amplitude across A_{1L} will induce the response amplitude to jump to the small amplitude harmonic domain. This is because the small amplitude harmonic domain is the only existing one for $A < A_{1L}$.

When the response inter-domain transition occurs at a domain boundary where multiple possible destination domains exist (A_{3U}, A_{3L}, A_{4U}, and A_{4L}) the energy level of the system in the transient state can be employed to determine the destination domain the system response will settle to. The system energy level can be represented by the system mean energy which is defined as the averaged system total energy over one excitation cycle. Fig.3.10 shows the relationship between the system total energy and the system mean energy. When the system response has a higher (lower) total energy local maxima, the system mean

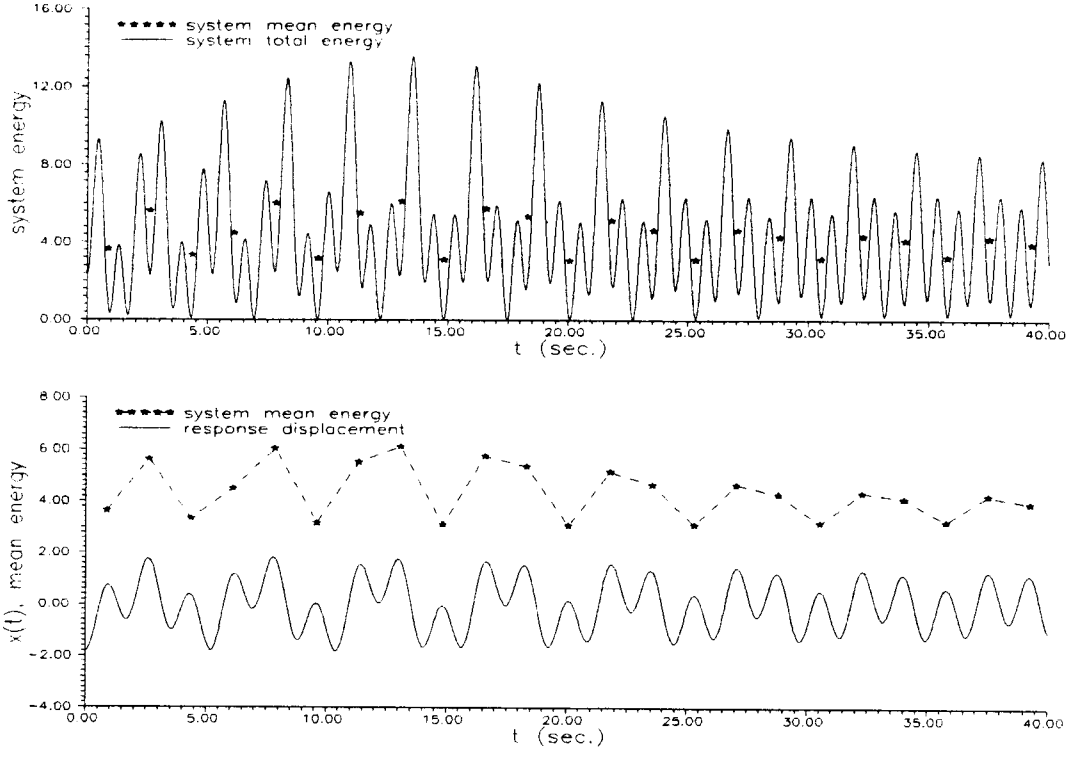

Figure 3.10 System response in the small amplitude harmonic domain. (top) relationship between transient-state system total energy and mean energy over one excitation cycle. (bottom) relationship between response displacement and mean energy. $\{c_S = 0.05, a_1 = 1, a_3 = 0.3, \omega = 3.6, \phi = 0, A = 12$ (x(0), dx/dt(0)) = (-1.8, 0)$\}$.

energy is also higher (lower). In addition, when the system response has a higher mean energy, the response also has a larger amplitude as shown in Fig.3.10.

(1) 1/2 subharmonic domain upper bound A_{3U} At the 1/2 subharmonic domain upper bound A_{3U}, the possible destination domains are the large and the small amplitude harmonic domains (see Figs.3.3 and 11). When the excitation amplitude increases from $A < A_{3U}$ ($A = 23$, in this case, see Figs.3.11a) to $A > A_{3U}$ ($A = 24$, see Figs.3.11b), the 1/2 subharmonic domain evolves into either the small or the large amplitude harmonic domains. To determine the destination domain, the relationship among the system mean energy of a typical responses in the 1/2 subharmonic, the large and the small harmonic domains at $A = A_{3U}$ shown in Figs.3.12a and 3.12b is examined. Note that for time t greater than 100 sec., the 1/2 subharmonic response is close to steady state. The system mean energy of a typical response in the small amplitude harmonic domain is observed to be less than that in the typical (almost) steady-state 1/2 subharmonic response as shown in Fig.3.12a. On the other hand, Fig.3.12b shows that the system mean energy (of a typical response) in the large amplitude harmonic domain is greater than that of the steady-state 1/2 subharmonic response. Thus, when the transient-state system mean energy is greater than the steady-state 1/2 subharmonic response mean energy at $A = A_{3U}$, the large amplitude harmonic domain may likely be the destination of the inter-domain transition. Conversely, if the transient-state system mean energy is lower than the steady-state 1/2 subharmonic response mean energy at $A = A_{3U}$, the system response will likely go to the small amplitude harmonic domain.

(2) 1/2 subharmonic domain lower bound A_{3L} At the 1/2 subharmonic domain lower bound A_{3L}, the possible destination domains are the large and the small amplitude harmonic domains, and the 1/3 subharmonic domain (see Figs.3.3 and 13). However, a jump from a

(a)

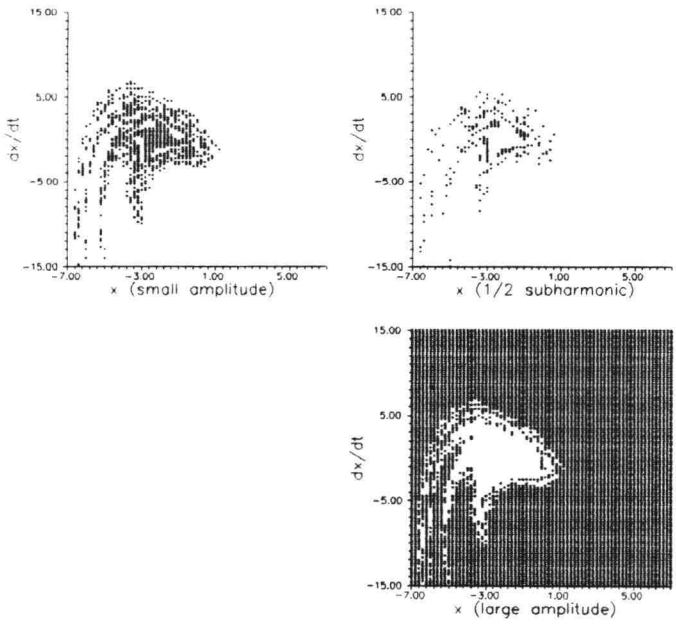

(b)

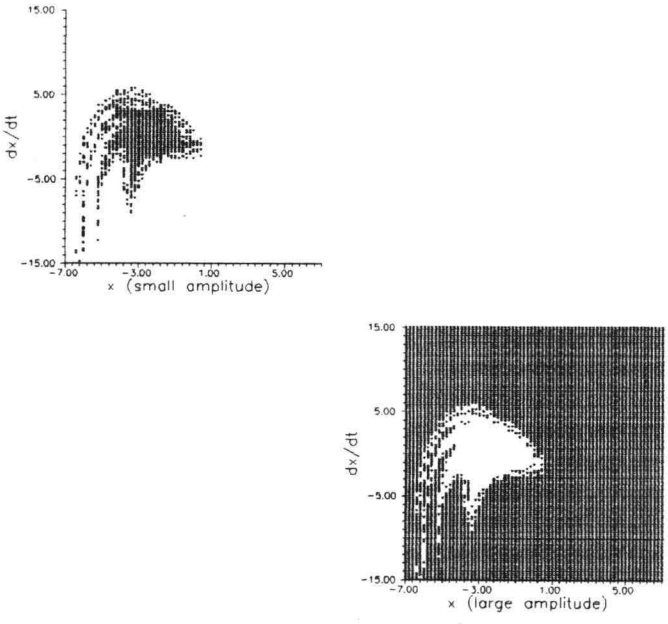

Figure 3.11 System response attraction domains (shaded areas) of (a) excitation amplitude A = 23, and (b) A = 24. $\{c_S = 0.05, a_1 = 1, a_3 = 0.3, \omega = 3.6, \phi = 0\}$.

(a)

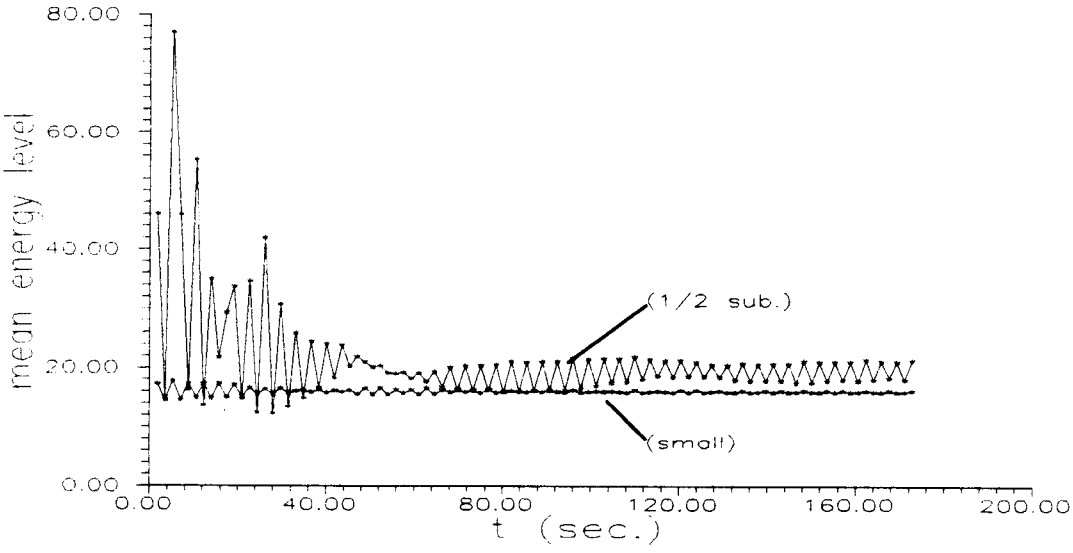

(b)

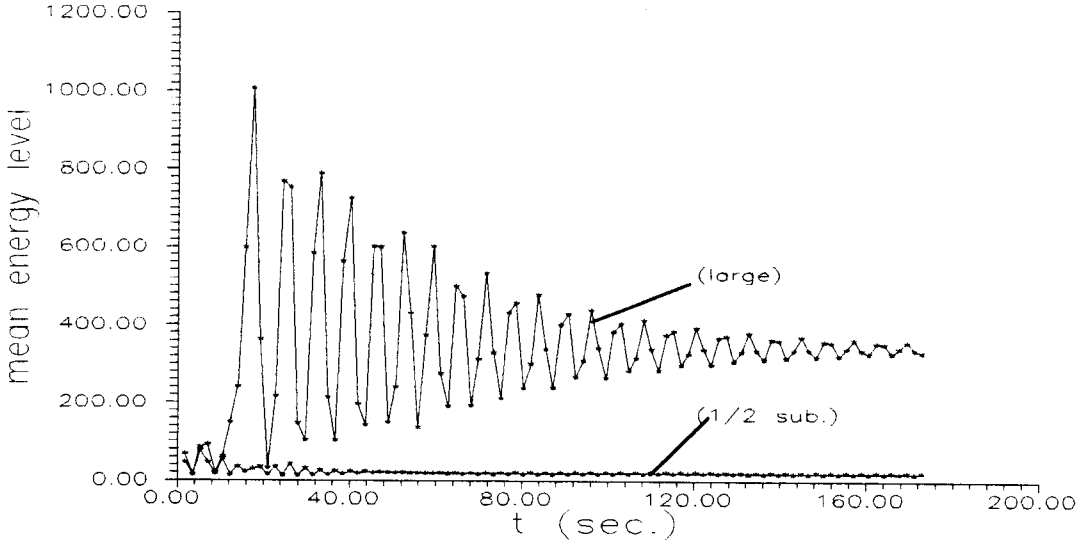

Figure 3.12 Mean energy level of the system response. (a) small amplitude harmonic and 1/2 subharmonic domains. (b) large amplitude harmonic and 1/2 subharmonic domains. $\{c_s = 0.05, a_1 = 1, a_3 = 0.3, \omega = 3.6, \phi = 0, A = 23\}$, (x(0), dx/dt(0)) = {(-2, 0.5) (small amplitude harmonic response), (-4.5, 0.5) (1/2 subharmonic response), (-5, 0.5) (large amplitude harmonic response)}.

(a)

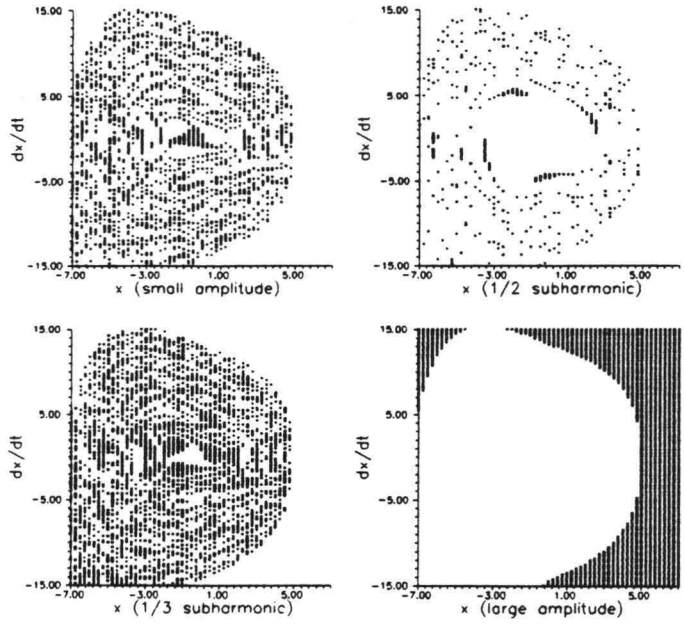

(b)

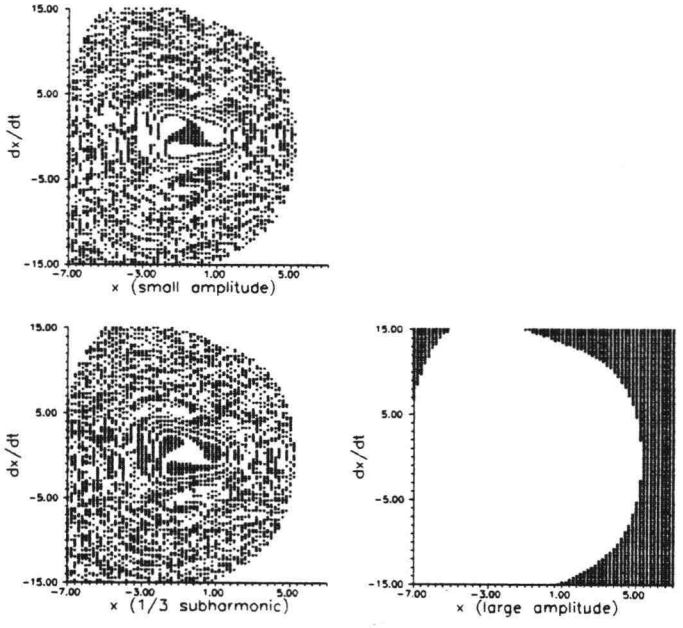

Figure 3.13 System response attraction domains (shaded areas) of (a) excitation amplitude A = 7, and (b) A = 6. $\{c_s = 0.05, a_1 = 1, a_3 = 0.3, \omega = 3.6, \phi = 0\}$.

1/2 subharmonic response domain to the large amplitude resonance response domain is highly unlikely due to the decreasing excitation amplitude (hence input energy). Thus, during the inter-domain transition, the system response may transition to either the small amplitude harmonic or the 1/3 subharmonic domain (see Figs.3.3) when the excitation amplitude varies from $A > A_{3L}$ ($A = 7$ in this case) to $A < A_{3L}$ ($A = 6$). Fig.3.14 shows that the system mean energy of a typical response in the 1/2 subharmonic domain is higher than those corresponding to the 1/3 subharmonic domain, which in turn is higher than those in the small amplitude harmonic domain. Therefore, it is assumed that, after the response exits from the 1/2 subharmonic domain, it will first visit the 1/3 subharmonic domain before it can visit the small amplitude harmonic domain.

(3) 1/3 subharmonic domain upper bound A_{4U} At 1/3 subharmonic domain upper bound A_{3U}, the possible destination domains are the large and the small amplitude harmonic domains and the 1/2 subharmonic domain (see Figs.3.3 and 15). Although the excitation amplitude is increasing (hence higher energy input), a jump from a 1/3 subharmonic response to a large amplitude resonance response is highly unlikely due to the large gap between the two energy levels and the presence of the 1/2 subharmonic domain in between. Thus, during the inter-domain transition, the system response may transition to either the small amplitude harmonic or the 1/2 subharmonic domain (see Figs.3.3) when the excitation amplitude varies from $A < A_{4U}$ ($A = 12$ in this case) to $A > A_{4U}$ ($A = 13$). It is noted in Fig.3.16 that the system mean energy of the 1/2 subharmonic response is higher than but close to that of the (almost) steady-state 1/3 subharmonic response for time t greater 100 sec. In the meantime, the system mean energy of the small amplitude harmonic response is observed to be in between those of (almost) steady-state 1/3 subharmonic response. Thus, the system response

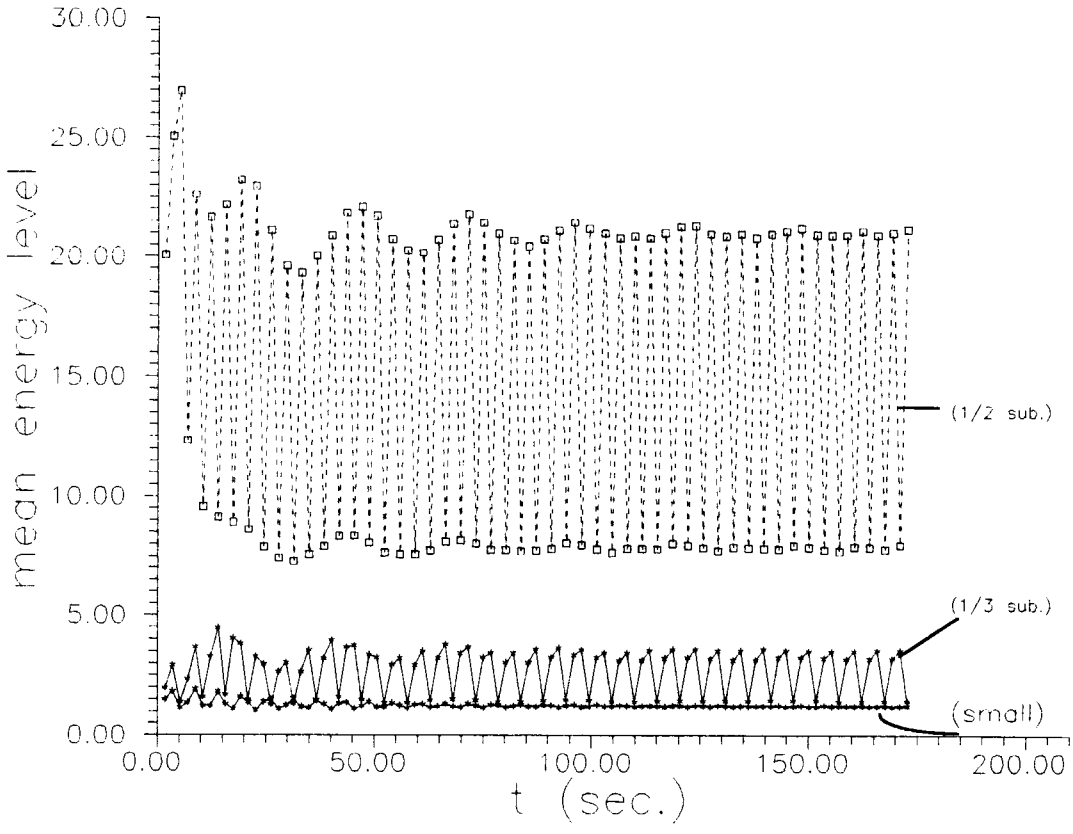

Figure 3.14 Mean energy level of the system response in the small amplitude harmonic domain and the 1/2 and 1/3 subharmonic domains. $\{c_S = 0.05, a_1 = 1, a_3 = 0.3, \omega = 3.6, \phi = 0, A = 7\}$, (x(0), dx/dt(0)) = {(-1, 0.5) (small amplitude harmonic response), (-3.75, 4.75) (1/2 subharmonic response), (-1.4, 0.75) (1/3 subharmonic response)}.

(a)

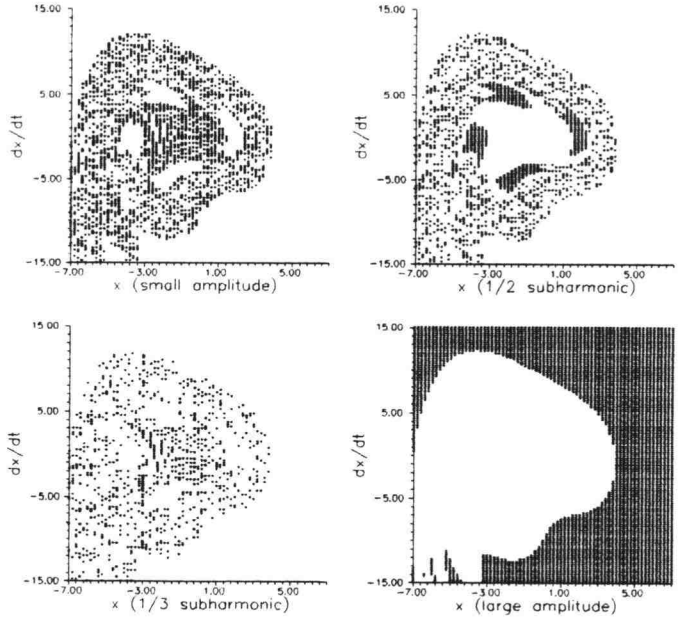

(b)

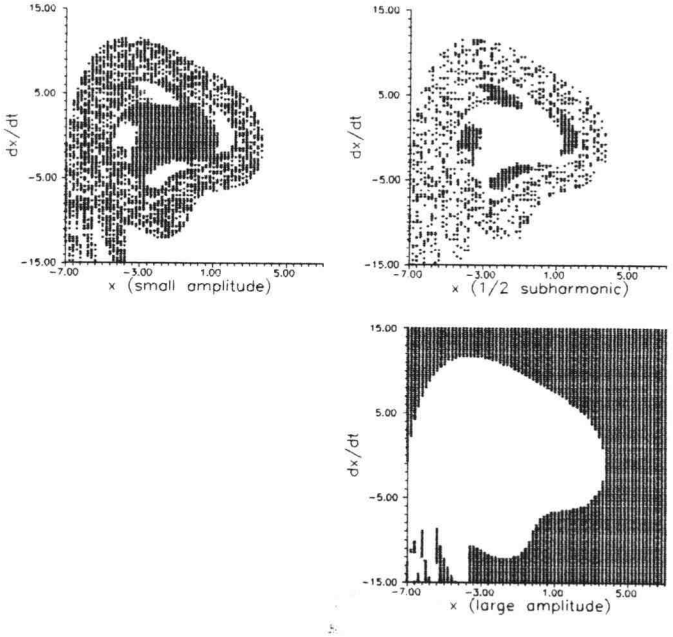

Figure 3.15 System response attraction domains (shaded areas) of (a) excitation amplitude A = 12, and (b) A = 13. $\{c_S = 0.05, a_1 = 1, a_3 = 0.3, \omega = 3.6, \phi = 0\}$.

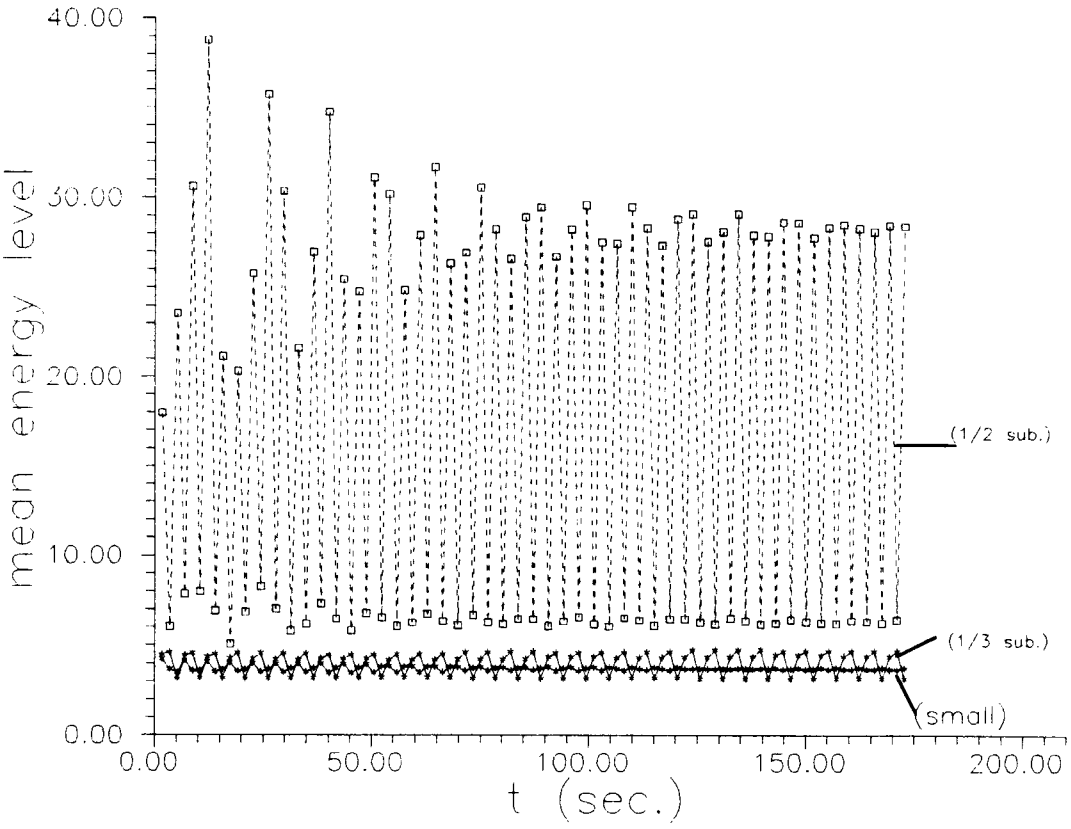

Figure 3.16 Mean energy level of the system responses in the small amplitude harmonic domain and the 1/2 and 1/3 subharmonic domains. $\{c_S = 0.05, a_1 = 1, a_3 = 0.3, \omega = 3.6, \phi = 0, A = 12\}$. (x(0), dx/dt(0)) = {(-1, 0.5) (small amplitude harmonic response), (-1.4, 3.75) (1/2 subharmonic response), (-1.4, 0.75) (1/3 subharmonic response)}.

will more likely go to the 1/2 subharmonic domain during the inter-domain transition at A = A_{4U} if the transient-state system mean energy is greater than the steady-state 1/3 subharmonic response mean energy at A = A_{4U}. Otherwise, the small amplitude harmonic domain will become the destination of the inter-domain transition.

(4) 1/3 subharmonic domain lower bound A_{4L} At the 1/3 subharmonic domain lower bound A_{4L}, the possible destination domains are the large and the small amplitude harmonic domains (see Figs.3.3 and 17). However, as explained in (2), a jump from a 1/3 subharmonic response domain to the large amplitude resonance response domain is highly unlikely due to the decreasing excitation amplitude (hence input energy). Thus, during the inter-domain transition, the system response will likely transition to the small amplitude harmonic domain (see Figs.3.3) when the excitation amplitude varies from A > A_{4L} (A = 3 in this case) to A < A_{4L} (A = 3).

(a)

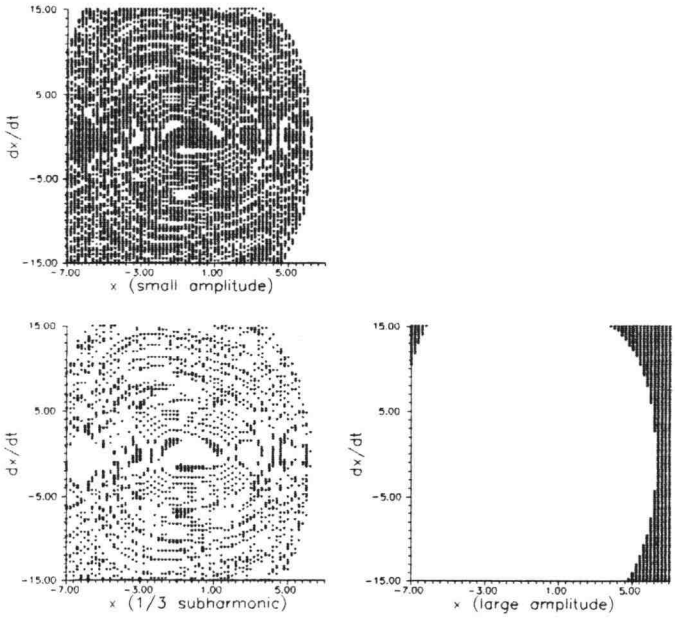

(b)

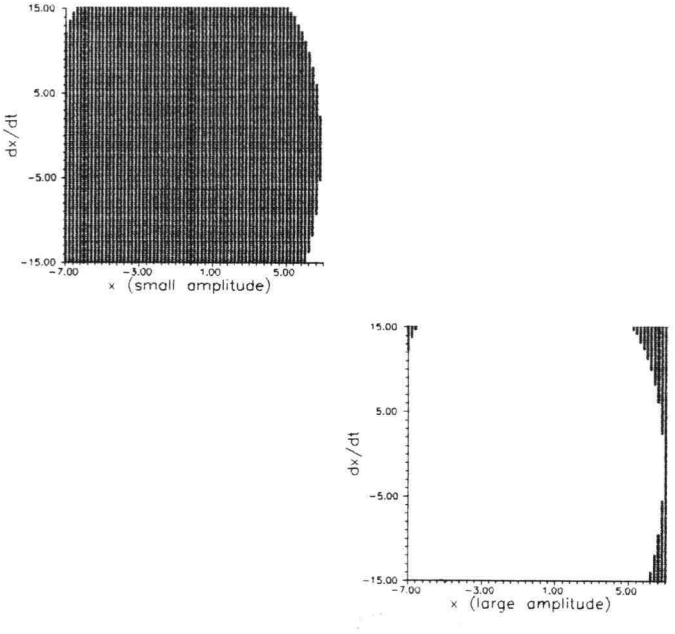

Figure 3.17 System response attraction domains (shaded areas) of (a) excitation amplitude A = 3, and (b) A = 2. $\{c_S = 0.05, a_1 = 1, a_3 = 0.3, \omega = 3.6, \phi = 0\}$.

4. STOCHASTIC SYSTEM ANALYSIS METHODOLOGY

The dynamic response behavior of the nonlinear system (Eq.2.3) under narrowband stochastic excitations, f(t) (Eq.2.7), is investigated in this chapter. Here the focus is on deriving a probability distribution of the response amplitude (or maximum excursion) over a single excitation cycle. Due to successive variations in the excitation parameters (amplitude and phase angle) as described in Section 2.3, the system response undergoes successive transitions (or transient states) accordingly. To predict the system behavior under such excitations, a semi-analytical procedure is proposed in this study. The procedure is developed based on the stochastic properties of the narrowband process (Chapter 2) and the response characteristics of the nonlinear system discussed in detail in Chapter 3.

4.1 Assumptions

For the narrowband excitation process, f(t), described in Eq.(2.7), the oscillating frequency is assumed to be constant and equal to the peak frequency ω_f of the spectrum shown in Eq.(2.6). The effect of excitation frequency variations on the response behavior is taken into account through the consideration of the excitation phase angle variations (Rice, 1954; Stratonovich, 1963; Langley, 1986).

For the response process, it is assumed that the prominent deterministic system response behavior described in Chapter 3, including co-existing attraction domains, inter-domain transitions and the domain-dependent characteristics, are preserved in the narrowband random excitation environment. Specifically, response inter-domain transitions occur only

when the excitation amplitude crosses domain boundaries prescribed in the amplitude response curves (Figs.3.1 and 3). Also, in the successive transient states, initial conditions of each transient response are assumed to be uniformly distributed over the phase trajectory of the previous response cycle.

From a stochastic point of view, the probability transitions of the excitation amplitude and phase angle processes and the response amplitude process are assumed to be ergodic Markov processes.

4.2 Excitation and Response Amplitude Probability Descriptions

4.2.1 Bandwidth Parameter and Its Influence on Response Behavior

The degree of randomness in a narrowband stochastic excitation is characterized by the bandwidth. For a finite bandwidth excitation, the randomness is characterized by the bandwidth parameter which controls the gradual variations in the excitation parameters, i.e., amplitude and phase angle. In the limit the excitation bandwidth approaches zero, randomness vanishes and the excitation becomes purely deterministic sinusoidal oscillations. In this case, the excitation parameters are constant and the corresponding steady-state response can be fully predicted as described in Chapter 3.

Suppose that the parameters of a deterministic excitation are constant over a long duration, and then change values abruptly (only once) and remain constant afterwards for a long duration. The corresponding system response will first be in a stead-state with amplitude and phase angle corresponding to the first steady-state excitation, and then undergoes a transient state (after the abrupt excitation parameter change) in the following few response

cycles. Finally, the system response will converge to a steady state corresponding to the final constant excitation parameters.

If the excitation parameters vary gradually but continuously as in the finite-bandwidth narrowband case, as a first approximation, the system response may be assumed to undergo successive transient states, with constant excitation parameters within each response cycle.

In a transient state, the system response behavior depends on the instantaneous values of the excitation and response parameters as well as the variations in the excitation parameters. Thus, the response behavior will also depend on the excitation bandwidth within an attraction domain, which controls the instantaneous values and variations in the excitation parameters. In addition, the response inter-domain transition (Section 3.3) depends on the excitation amplitude variations and thus, the excitation bandwidth. Therefore, to investigate the response behavior under narrowband excitations, the stochastic behavior of the variations in the excitation parameters needs to be characterized first. Then, by the Markovian assumption of both the excitation amplitude and the response amplitude processes, a governing equation of the response amplitude probability transition can be formulated.

4.2.2 Stochastic Behavior of Excitation Parameters

Recall that a narrowband excitation f(t) is close to sinusoidal oscillations at the peak frequency (Ochi, 1990). In addition, an associated envelope process is a smooth curve joining the peaks or the local maxima of f(t), which are the amplitudes of the sinusoidal oscillations (Langley, 1986). Thus, the amplitude process can be approximated by the envelope process. To investigate the stochastic behavior of the amplitude and the phase processes, a four dimensional joint probability density function of the random variables representing the

excitation amplitudes and phase angles corresponding to consecutive excitation cycles, i.e., $A^{(1)}$, $A^{(2)}$, $\phi^{(1)}$ and $\phi^{(2)}$, can be obtained as (Ochi, 1990)

$$p(A^{(1)},\phi^{(1)},A^{(2)},\phi^{(2)})$$

$$= \frac{A^{(1)}A^{(2)}}{4\pi^2\sqrt{|\Sigma|}} \exp\left\{\frac{-1}{2\sqrt{|\Sigma|}}\left\{\sigma_f^2\left[(A^{(1)})^2+(A^{(2)})^2\right]-2A^{(1)}A^{(2)}\left[\rho\cos(\phi^{(2)}-\phi^{(1)})+\lambda\sin(\phi^{(2)}-\phi^{(1)})\right]\right\}\right\}$$

$$0 \le A^{(1)}, A^{(2)} < \infty \qquad 0 \le \phi^{(1)}, \phi^{(2)} \le 2\pi \tag{4.1}$$

where,

$$\rho = \int_0^\infty S_{ff}(\omega)\cos[(\omega-\omega_f)T]\,d\omega$$

$$\lambda = \int_0^\infty S_{ff}(\omega)\sin[(\omega-\omega_f)T]\,d\omega \tag{4.2}$$

$$\sqrt{|\Sigma|} = \sigma_f^4 - \rho^2 - \lambda^2$$

and, superscripts (1) and (2) indicate that the quantities are in the current and the next excitation cycles, respectively; $S_{ff}(\omega)$ is the one-sided spectral density function of f(t), and can be obtained from Eq.(2.4); ω_f and σ_f^2 are the excitation peak frequency and variance, respectively, and T is the excitation period equal to $2\pi/\omega_f$. Note that the excitation bandwidth dependency of Eq.(4.1) is embedded in Eq.(4.2). If a random variable Φ is introduced to represent the phase angle difference $\phi^{(2)} - \phi^{(1)}$, the joint probability density function of $A^{(1)}$, $A^{(2)}$ and Φ can be obtained from Eq.(4.2) by the transformation of the random variables (Ochi, 1990)

$$p(A^{(1)}, A^{(2)}, \Phi)$$

$$= \frac{A^{(1)}A^{(2)}}{2\pi\sqrt{|\Sigma|}} \exp\left\{\frac{-1}{2\sqrt{|\Sigma|}}\left\{\sigma_f^2\left[(A^{(1)})^2+(A^{(2)})^2\right]-2A_j^{(1)}A_i^{(2)}\left[\rho\cos(\Phi)+\lambda\sin(\Phi)\right]\right\}\right\} \tag{4.3}$$

$$-2\pi \le \Phi \le 2\pi$$

In addition, the joint probability density function of the amplitude $A^{(1)}$ and $A^{(2)}$ can be obtained by integrating Eq.(4.1) with respect to $\phi^{(1)}$ and $\phi^{(2)}$ and expressed as

$$p(A^{(1)},A^{(2)}) = \frac{A^{(1)}A^{(2)}}{\sqrt{|\Sigma|}} \exp\left\{\frac{-1}{2\sqrt{|\Sigma|}}\sigma_f^2\left[(A^{(1)})^2+(A^{(2)})^2\right]\right\} I_0\left(\frac{A^{(1)}A^{(2)}}{\sqrt{|\Sigma|}}\sqrt{\rho^2+\lambda^2}\right) \tag{4.4}$$

where, I_0 is the modified Bessel function of order zero. The excitation bandwidth dependency of Eq.(4.1) is transferred to Eqs.(4.3-4).

Under the Markovian assumption, the stochastic behavior of the excitation amplitude process is characterized by a probability transition (or propagation) density function represented by the Markov state density function (Gillespie, 1992) as

$$p(A^{(2)}|A^{(1)}) = \frac{p(A^{(1)},A^{(2)})}{p(A^{(1)})} \tag{4.5}$$

where, $p(A^{(1)})$ is a Rayleigh-distributed marginal density function of $p(A^{(1)}, A^{(2)})$. It can also be realized that Eq.(4.5) is a conditional probability density function. Thus, if the probability density function of $A^{(1)}$ is known, the probability density function of $A^{(2)}$ can be obtained as

$$p(A^{(2)}) = \int_0^\infty p(A^{(2)}|A^{(1)})\,p(A^{(1)})\,dA^{(1)} \tag{4.6}$$

4.2.3 Response Amplitude Probability Description

For the response amplitude process, the Markovian assumption also enables a probability transition density function to characterize the stochastic behavior. The response amplitude probability transition is governed by

$$p(R^{(2)}) = \int_0^\infty p(R^{(2)}|R^{(1)})\,p(R^{(1)})\,dR^{(1)} \tag{4.7}$$

where, $p(R^{(2)}|\,R^{(1)})$ is the response amplitude probability transition (or conditional) density function; $R^{(1)}$ and $R^{(2)}$ are random variables representing the response amplitudes corresponding to the excitation cycles associated with $A^{(1)}$ and $A^{(2)}$, respectively, and $p(R^{(1)})$ and $p(R^{(2)})$ are their corresponding probability distributions. Note that, for a stationary response process, the amplitude probability distribution p(R) is time invariant. In other words, the response amplitude probability distributions $p(R^{(1)})$ and $p(R^{(2)})$ in Eq.(4.6) are identical.

As pointed out previously, the system response undergoes successive transient states when the excitation is a narrowband stochastic process. When the system response is in a transient state, the response amplitude domains D_d^R corresponding to different co-existing response attraction domains D_d may overlap, as depicted in Section 3.2.3. In addition, within an individual attraction domain, D_d, response amplitude domains $(D_d^R)_A$ corresponding to different excitation amplitudes A belonging to the same excitation amplitude domain D_d^A

associated with the attraction domain may overlap also. However, from probabilistic and physical points of view, occurrence of a response amplitude R being in the domains, D_d^R, corresponding to different attraction domains, D_d, are mutually exclusive events. Moreover, within an individual attraction domain D_d, occurrences of R being in the response amplitude domains, $(D_d^R)_A$, corresponding to different excitation amplitudes are also mutually exclusive events. Note that there exist finite number of co-existing attraction domains, D_d and thus, D_d^R and D_d^A. Therefore, according to the Bayes formula, the response amplitude probability distribution can be expressed as (Ochi, 1990)

$$p(R^{(z)}) = \sum_{d=1}^{n} p(R^{(z)} | D_d^R) p(D_d^R), \qquad z = 1, 2 \tag{4.8}$$

where, $p(D_d^R)$ is the probability that the system response amplitude is in the domain D_d^R, which is equivalent to the probability that the system response is in the attraction domain D_d, and $\{p(R^{(z)} \mid D_d^R), z = 1, 2\}$ are the conditional probability distributions of the response amplitudes given that the system responses are in the attraction domain, D_d. In addition, within an attraction domain, the response amplitude probability distribution can also be expressed as

$$p(R^{(z)} | D_d^R) = \int p\left(R^{(z)} | (D_d^R)_A\right) p\left((D_d^R)_A\right) d(D_d^R)_A, \qquad z = 1, 2 \tag{4.9}$$

where, $\{p(R^{(z)} \mid (D_d^R)_A), z = 1, 2\}$ are the probability distributions of the response amplitudes, $R^{(z)}$, in the response amplitude domain, $(D_d^R)_A$; and $p((D_d^R)_A)$ is the occurrence probability

of $(D_d^R)_A$. Note that $\{p((D_d^R)_A)d(D_d^R)_A\}$ is equivalent to $\{p(A \mid D_d^A)dA\}$ which stands for the probability of the excitation amplitude being equal to A given that A belongs to D_d^A. The integration of Eq.(4.9) is carried out over the entire domain D_d^A. Thus, Eq.(4.9) can be rewritten as

$$p(R^{(z)} \mid D_d^R) = \int_{D_d^A} p\left(R^{(z)} \mid (D_d^R)_A\right) p(A \mid D_d^A)\, dA, \qquad z = 1,2 \tag{4.10}$$

The system characteristics obtained in Chapter 3 show that the system response may exhibit inter-domain transitions among co-existing attraction domains, D_d, due to variations in the excitation amplitude. In addition, within a response attraction domain, the system behavior exhibits domain dependent characteristics. As a result, the response amplitude probability transitions may occur among co-existing attraction domains. Moreover, within an attraction domain, the response amplitude probability transition is governed by a domain dependent probability transition density function.

4.3 Inter-Domain Transition of Response Amplitude Probability

4.3.1 Governing Equation of Inter-Domain Probability Transition

For a stationary Markov response process, the response inter-domain transition (or the amplitude jump phenomenon) among finite number of domains, D_d^R, can be modeled as a stationary Markov process with discrete states (Gillespie, 1992) or a stationary Markov chain (Ochi, 1990; Bouleau and Lépingle, 1994). To evaluate the probability, $p(D_d)$, of the system response being in an attraction domain D_d, or equivalently, $p(D_d^R)$ in Eq.(4.8), the

characteristics of the response inter-domain transition behavior obtained in Section 3.3 are employed.

The stochastic behavior of the response inter-domain transition (or amplitude jump) is characterized by an inter-domain transition probability matrix K. Thus, the governing equation of the probability inter-domain transition can be expressed as

$$\hat{p}(D^{(2)}) = K\,\hat{p}(D^{(1)}) \tag{4.11}$$

where, $\hat{p}(D^{(1)})$ and $\hat{p}(D^{(2)})$ are probability vectors of the system response being in each individual attraction domain in the current and the next excitation cycles, respectively. The dimensions of $\hat{p}$ and K are (n x 1) and (n x n), respectively, where n is the number of co-existing attraction domains. Thus, Eq.(4.11) can also be written as

$$\left\{ p_i(D_i^{(2)}) \right\} = \left[p_{ij}(i|j) \right] \left\{ p_j(D_j^{(1)}) \right\}, \qquad i,j = 1,\ldots,n \tag{4.12}$$

where, $p_{ij}(i|j)$, an element of the inter-domain transition probability matrix K, is a conditional probability that the system response is going to the i^{th} attraction domain given that it is currently in the j^{th} attraction domain; $p_i(D_i^{(2)})$ and $p_j(D_j^{(1)})$, which are the i^{th} and j^{th} elements of the probability vectors $\hat{p}(D^{(2)})$ and $\hat{p}(D^{(1)})$, respectively, stand for the probabilities of the system response being in the i^{th} and j^{th} attraction domains in the next and the current excitation cycles, respectively. When the system is in the primary resonance region, n = 2 and the co-existing attraction domains are the large amplitude (D_1 or D_L) and the small amplitude (D_2 or D_S) harmonic domains. When the system is in the subharmonic resonance region, n = 4 and

large amplitude harmonic, small amplitude harmonic, 1/2 subharmonic (D_3 or $D_{1/2}$) and 1/3 subharmonic (D_4 or $D_{1/3}$) attraction domains co-exist.

Note that under stationary condition, $\hat{p}(D^{(1)})$ is equal to $\hat{p}(D^{(2)})$. Thus, to obtain a stationary probability vector $\hat{p}(D) = \{p_i(D_i)\}$ from Eq.(4.11 or 4.12) is equivalent to obtain the eigenvector of the transition matrix K corresponding to the unit eigenvalue. In fact, the probability, $p(D_d)$, of the system response being in an attraction domain D_d is equal to the corresponding element of the normalized eigenvector $\hat{p}(D)$. In other words,

$$p(D_d) = \frac{p_d(D_d)}{\sum_{i=1}^{n} p_i(D_i)} \tag{4.13}$$

4.3.2 Evaluation of Transition Matrix K

The conditional probabilities, $p_{ij}(i|j)$, can be evaluated by considering the mechanism of the system response inter-domain transition behavior depicted in Section 3.3 and the stochastic behavior of the excitation amplitude characterized by Eqs.(4.4-6) in Section 4.2.2. For the system response to stay in the same attraction domain, D_d, in the next excitation cycle, the excitation amplitude must remain within the same domain, D_d^A, in the next cycle. The probability, $p(A|D_d^A)$, of the excitation amplitude being in the domain D_d^A can be expressed as

$$p(A|D_d^A) = \frac{p(A)}{\int_{D_d^A} p(A)\,dA}, \qquad A \in D_d^A \tag{4.14}$$

where, p(A) is a Rayleigh distribution. From Eqs.(4.4-6), the probability distribution, $p(A^{(2)} \mid A^{(1)} \in D_d^A)$, of the excitation amplitude in the next cycle given that the excitation amplitude belongs to D_d^A in the current cycle can be obtained by

$$p(A^{(2)} \mid A^{(1)} \in D_d^A) = \int_{D_d^A} p(A^{(2)} \mid A^{(1)})\, p(A^{(1)} \mid D_d^A)\, dA^{(1)} \tag{4.15}$$

Thus, the probability that the system response remains in the same attraction domain, D_d, in the next excitation cycle reads

$$p(R^{(2)} \in D_d^R \mid R^{(1)} \in D_d^R) = \int_{D_d^A} p(A^{(2)} \mid A^{(1)} \in D_d^A)\, dA^{(2)} \tag{4.16}$$

Note that $p(R^{(2)} \in D_d^R \mid R^{(1)} \in D_d^R)$ is equal to the diagonal elements of K, $p_{ii}(i|i)$, in Eqs.(4.11-12). The probability, $p(E_{dU})$, that the system response exits from the attraction domain D_d at the domain upper limit A_{dU} is equivalent to the probability that the excitation amplitude $A^{(2)}$ is greater than A_{dU}. Thus, from Eq.(4.15), $p(E_{dU})$ can be obtained by

$$p(E_{dU}) = 1 - \int_0^{A_{dU}} p(A^{(2)} \mid A^{(1)} \in D_d^A)\, dA^{(2)} \tag{4.17}$$

Accordingly, the probability, $p(E_{dL})$, that the system response exits from the attraction domain D_d at the domain lower limit A_{dL} can be obtained by

$$p(E_{dL}) = 1 - \int_{A_{dL}}^{\infty} p(A^{(2)} \mid A^{(1)} \in D_d^A)\, dA^{(2)} \tag{4.18}$$

Note that, after the system response exits from an attraction domain, there may exist multiple possible destination domains of the inter-domain transition. In this case, the transient-state system mean energy, or equivalently, the transient-state system response amplitude is employed to determine the attraction domain which the system will settle to during the inter-domain transition, as depicted in Section 3.3. The conditional probabilities $p_{ij}(i|j)$ in Eq.(4.12) depend on the domain exit probabilities, $p(E_{dL})$ and $p(E_{dU})$, and the probability that an attraction domain becomes the destination domain. Detailed procedure of the evaluation of $p_{ij}(i|j)$ is discussed in Appendix D.

4.4 Intra-Domain Transition of Response Amplitude Probability

In this section, the behavior of the response amplitude probability transition taking place within an attraction domain, D_d, i.e., intra-domain transition, is investigated. Recall from Section 4.2.2 that the response amplitude probability intra-domain transition is governed by a domain dependent transition density function.

4.4.1 Governing Equation of Probability Intra-Domain Transition

Recall from Eq.(4.10) that the conditional probability, $\{p(R^{(z)} \mid D_d^R), z=1, 2\}$, of the response amplitude, $R^{(z)}$, being in the domain D_d^R is an integral of the probability that $R^{(z)}$ is in the response amplitude domain $(D_d^R)_A$ corresponding to all the excitation amplitudes in the domain D_d^A. Thus, due to variations in the excitation amplitude, transitions of the response amplitude probability will occur among response amplitude domains, $(D_d^R)_A$, corresponding to different excitation amplitudes within D_d^A. From Eq.(4.7), the governing equation of the intra-domain probability transition from $(D_d^R)_A^{(1)}$ at the current excitation cycle to $(D_d^R)_A^{(2)}$ at

the next excitation cycle reads

$$p(R^{(2)}|A^{(1)},A^{(2)},D_d^R) = \int_{(D_d^R)_A^{(1)}} p(R^{(2)}|R^{(1)},A^{(1)},A^{(2)},D_d^R)\, p(R^{(1)}|(D_d^R)_A^{(1)})dR^{(1)} \tag{4.19}$$

where, $p(R^{(2)} \mid R^{(1)}, A^{(1)}, A^{(2)}, D_d^R)$ is a domain dependent response amplitude probability transition density function.

Note that the probability distribution of the response amplitude $p(R^{(2)} \mid (D_d^R)_A^{(2)})$ may be transited from all $p(R^{(1)} \mid (D_d^R)_A^{(1)}, A^{(1)} \in D_d^A)$ and is the union of all the possible transition. The events of these transitions are mutually exclusive and thus, according to the Bayes formula (Ochi, 1990), $p(R^{(2)} \mid (D_d^R)_A^{(2)})$ can be expressed as

$$p(R^{(2)}|(D_d^R)_A^{(2)}) = \int_{D_d^A} p(R^{(2)}|A^{(1)},A^{(2)},D_d^R)p(A^{(1)}|D_d^A)dA^{(1)} \tag{4.20}$$

By substituting Eqs.(4.19 and 4.20) into Eq.(4.10), the governing equation of the response amplitude probability inside-domain transition yields

$$p(R^{(2)}|D_d^R) = \int \left\{ \int \left[\int p(R^{(2)}|R^{(1)},A^{(1)},A^{(2)},D_d^R)\, p(R^{(1)}|(D_d^R)_A^{(1)})\, dR^{(1)} \right] p(A^{(1)}|D_d^A)\, dA^{(1)} \right\} p(A^{(2)}|D_d^A)\, dA^{(2)} \tag{4.21}$$

4.4.2 Evaluation of Intra-Domain Probability Transition

The procedure of evaluating Eq.(4.21) is discussed in this section. From a deterministic point of view, the variation in the response amplitude is a function of: (1) the

excitation amplitude and the response amplitude in the current excitation cycle, (2) variation in the response parameters (amplitude and phase angle), and (3) the system phase status (x, $\dot{x}$) at the time when the excitation parameter variation takes place, which is also considered as the initial condition of the following transient-state response. That is,

$$R^{(2)} = g(R^{(1)}, A^{(1)}, A^{(2)}, \Phi = \phi^{(2)} - \phi^{(1)}, X^{o}) \tag{4.22}$$

where, $R^{(1)}$ and $R^{(2)}$ are response amplitudes in the domains $(D_d^R)_A^{(1)}$ and $(D_d^R)_A^{(2)}$, respectively; Φ is the variation in the excitation phase angle; and X^o stands for the system initial condition. Note that the function g is domain dependent. If the response amplitude $R^{(1)}$, the excitation amplitudes $A^{(1)}$ and $A^{(2)}$ are fixed, then $R^{(2)}$ can be considered as a function of Φ and X^o only, i.e., $R^{(2)} = \bar{g}(\Phi, X^o)$ where $\bar{g}$ is a domain dependent function. As a result, the probability distribution of $R^{(2)}$ can be derived from the joint probability distribution of Φ and X^o through the functional relationship $R^{(2)} = \bar{g}(\Phi, X^o)$, given that $R^{(1)}$, $A_j^{(1)}$ and $A_i^{(2)}$ are fixed. However, up to today, an explicit expression of the function $\bar{g}$ (or g) is not available, and thus, a direct derivation of $p(R^{(2)} \mid R^{(1)}, A^{(1)}, A^{(2)}, D_d^R)$ from $p(\Phi, X^o \mid R^{(1)}, A^{(1)}, A^{(2)}, D_d^R)$ is not feasible. To obtain $p(R^{(2)} \mid R^{(1)}, A^{(1)}, A^{(2)}, D_d^R)$, numerical techniques are required.

To facilitate numerical evaluation of $p(R^{(2)} \mid R^{(1)}, A^{(1)}, A^{(2)}, D_d^R)$, the response amplitude domains $\{(D_d^R)_A^{(z)}, z=1,2\}$, the system initial condition X^o domain, the excitation phase angle difference Φ domain, and the excitation amplitude domain D_d^A are discretized. The value of $\bar{g}(\Phi_{up}, X_{uo}^{\ o}) = R_{ur2}^{(2)}$, given $R_{ur1}^{(1)}$, $A_j^{(1)}$ and $A_i^{(2)}$, can be obtained by direct numerical integration of Eq.(2.3), where the subscripts indicate sample points of their corresponding discretized random variables, Φ, X^o, $R^{(2)}$, $R^{(1)}$, and D_d^A, respectively. Thus, $p(\Phi_{up}, X_{uo}^{\ o} \mid R_{ur1}^{(1)}, A_j^{(1)}, A_i^{(2)}, D_d^R) = p(R_{ur2}^{(2)} \mid R_{ur1}^{(1)}, A_j^{(1)}, A_i^{(2)}, D_d^R)$.

The probability distribution of the phase difference Φ is characterized by Eq.(4.3) and depends on $A_j^{(1)}$ and $A_i^{(2)}$ only. The initial condition, X^o, is assumed to be uniformly distributed over the domain which is the phase trajectory of the current response cycle. In addition, Φ and X^o can be assumed as statistically independent because the excitation properties Φ is not affected by the system response and the uniformly distributed system initial condition is affected by neither the variation in the excitation parameters nor the system response. Thus,

$$p\left(R_{ur2}^{(2)} \middle| R_{ur1}^{(1)}, A_j^{(1)}, A_i^{(2)}, D_d^R \right)$$

$$= p\left(\Phi_{up}, X_{uo}^{o} \middle| R_{ur1}^{(1)}, A_j^{(1)}, A_i^{(2)}, D_d^R \right) = \frac{1}{m_X} \int_{\Phi_{up}-\Delta\Phi/2}^{\Phi_{up}+\Delta\Phi/2} \frac{p(A_j^{(1)}, A_i^{(2)}, \Phi)}{p(A_j^{(1)}, A_i^{(2)})} d\Phi \tag{4.23}$$

where, m_X is the total number of intervals in discretized X^o domain; $p(A_j^{(1)}, A_i^{(2)}, \Phi)$ and $p(A_j^{(1)}, A_i^{(2)})$ can be obtained by Eqs.(4.3-4). By varying Φ_{up} and $X_{uo}{}^o$ over their entire respective domains and lumping all computed $p(R_{ur2}^{(2)} | R_{ur1}^{(1)}, A_j^{(1)}, A_i^{(2)}, D_d^R)$, a probability vector of the response amplitude $\hat{p}(R^{(2)} | R_{ur1}^{(1)}, A_j^{(1)}, A_i^{(2)}, D_d^R)$ can be obtained.

Note that, after $\hat{p}(R^{(2)} | R_{ur1}^{(1)}, A_j^{(1)}, A_i^{(2)}, D_d^R)$ is obtained, the discrete form of Eq.(4.19) can be expressed as

$$\hat{p}(R^{(2)} | A_j^{(1)}, A_i^{(2)}, D_d^R) = \sum_{ur1=1}^{m_R} \hat{p}(R^{(2)} | R_{ur1}^{(1)}, A_j^{(1)}, A_i^{(2)}, D_d^R) p(R_{ur1}^{(1)} | (D_d^R)_A^{(1)}) \tag{4.24}$$

where, m_R is the number of intervals in the discretized $(D_d^R)_A^{(1)}$ domain. Accordingly, the discrete forms of Eqs.(4.20-21) can be expressed as

$$\hat{p}(R^{(2)}|(D_d^R)_A^{(2)}) = \sum_{j=1}^{m_A} \hat{p}(R^{(2)}|A_j^{(1)}, A_i^{(2)}, D_d^R)\, p(A_j^{(1)}|D_d^A) \tag{4.25}$$

$$\hat{p}(R^{(2)}|D_d^R) = \sum_{i=1}^{m_A} \hat{p}(R^{(2)}|(D_d^R)_A^{(2)})\, p(A_i^{(2)}|D_d^A) \tag{4.26}$$

where, m_A is the number of intervals in the discretized excitation amplitude domain, D_d^A and, from Eq.(4.14),

$$p(A_{j,i}^{(z)} \mid D_d^A) = \int_{A_{j,i}-\Delta A/2}^{A_{j,i}+\Delta A/2} p(A \mid D_d^A)\, dA, \qquad z = 1,2 \tag{4.27}$$

4.5 Stationary Response Amplitude Probability Distribution

To obtain the probability vector $\hat{p}(R^{(2)}|D_d^R)$ or $\hat{p}(R^{(2)}|(D_d^R)_A^{(2)})$ in Eq.(4.26), the probability $p(R_{url}^{(1)}|(D_d^R)_A^{(1)})$ in Eq.(4.24), or equivalently, the probability vector $\hat{p}(R^{(1)}|(D_d^R)_A^{(1)})$ and thus, $\hat{p}(R^{(1)}|D_d^R)$, needs to be known in advance. Note that, as $\hat{p}(R^{(2)}|(D_d^R)_A^{(2)})$ in Eq.(4.25), $\hat{p}(R^{(1)}|(D_d^R)_A^{(1)})$ is also a desired solution of the transition from its previous excitation cycle and thus, is unknown. However, due to stationarity of the response process, the $\hat{p}(R^{(2)}|(D_d^R)_A^{(2)})$ can be obtained by an iteration procedure.

Since the response process is stationary, $\hat{p}(R^{(2)}|D_d^R)$ is equal to $\hat{p}(R^{(1)}|D_d^R)$ because the response amplitude probability distribution is time invariant, as described in Section 4.2.2. By examining Eqs.(4.10 and 4.26), in order to have a time invariant $\{\hat{p}(R^{(z)}|D_d^R), z=1,2\}$,

$\hat{p}(R^{(2)}|(D_d^R)_A^{(2)})$ must be also time invariant because the excitation process is stationary and thus $p(A|D_d^A)$ is time invariant. As a result, $\hat{p}(R^{(2)}|(D_d^R)_A^{(2)})$ is equal to $\hat{p}(R^{(1)}|(D_d^R)_A^{(1)})$ when the response amplitudes $R^{(1)}$ and $R^{(2)}$ correspond to the same excitation amplitude A.

An iteration procedure may start with estimations of $\hat{p}(R^{(1)}|(D_d^R)_A^{(1)})$ corresponding to all excitation amplitude in D_d^A. For convenience and efficiency, the first estimation of $\hat{p}(R^{(1)}|(D_d^R)_A^{(1)})$ can be obtained by Eqs.(4.24-25) with the system responses being currently in their steady-states. That is,

$$\hat{y}(R^{(2)}|A_j^{(1)}, A_i^{(2)}, D_d^R) = \hat{p}(R^{(2)}|(R^{(S)})^{(1)}, A_j^{(1)}, A_i^{(2)}, D_d^R) \tag{4.28}$$

and

$$\tilde{p}(R^{(1)}|(D_d^R)_A^{(1)}) \approx \hat{y}(R^{(2)}|(D_d^R)_A^{(2)}) = \sum_{j=1}^{m_A} \hat{y}(R^{(2)}|A_j^{(1)}, A_i^{(2)}, D_d^R)\, p(A_j^{(1)}|D_d^A) \tag{4.29}$$

where, $(R^{(S)})^{(1)}$ in Eq.(4.28) is the steady-state response amplitude corresponding to the excitation amplitude $A_j^{(1)}$ and its occurrence probability is equal to 1; $\tilde{p}(R^{(1)}|(D_d^R)_A^{(1)})$ is an estimation of $\hat{p}(R^{(1)}|(D_d^R)_A^{(1)})$. Numerical results of Eq.(4.29) for the system in four different attraction domains are shown in Figs.4.1a-4.4a.

Let $\tilde{p}_{url}(R_{url}^{(1)}|(D_d^R)_A^{(1)})$ be an element of $\tilde{p}(R^{(1)}|(D_d^R)_A^{(1)})$, then the first iteration result obtained by Eq.(4.24) becomes

$$\tilde{p}(R^{(2)}|A_j^{(1)}, A_i^{(2)}, D_d^R) = \sum_{url=1}^{m_R} \hat{p}(R^{(2)}|R_{url}^{(1)}, A_j^{(1)}, A_i^{(2)}, D_d^R)\, \tilde{p}_{url}(R_{url}^{(1)}|(D_d^R)_A^{(1)}) \tag{4.30}$$

Numerical results of Eqs.(4.28 and 4.30) corresponding to the cases shown in Figs.4.1a-4.4a are presented in Figs.4.1b-4.4b. It can be observed that the results obtained by Eq.(4.28) agrees well with that by Eq.(4.30). The good agreements indicate that $\tilde{p}(R^{(1)}|(D_d^R)_A^{(1)})$ is a reasonable approximation to $\hat{p}(R^{(1)}|(D_d^R)_A^{(1)})$. This is because a substitution of Eq.(4.30) into Eq.(4.25) will produce probability distribution close to the results obtained by Eq.(4.29) when $R^{(1)}$ and $R^{(2)}$ correspond to the same excitation amplitude. Thus, the condition of stationary is satisfied.

By recognizing that $\tilde{p}(R^{(1)}|(D_d^R)_A^{(1)})$ is a reasonable approximation to $\hat{p}(R^{(1)}|(D_d^R)_A^{(1)})$, the approximate stationary response amplitude probability distribution within an attraction domain can be obtained from Eqs.(4.26 and 4.29) and expressed as

$$\tilde{p}(R^{(1)}|D_d^R) = \tilde{p}(R^{(2)}|D_d^R) = \sum_{j=1}^{m_A} \tilde{p}(R^{(1)}|(D_d^R)_A^{(1)})\, p(A_j^{(1)}|D_d^A) \tag{4.31}$$

In addition, from Eqs.(4.8, 4.13 and 4.31), the overall stationary response amplitude probability distribution can be approximated as

$$\tilde{p}(R^{(1)}) = \tilde{p}(R^{(2)}) = \sum_{d=1}^{n} \tilde{p}(R^{(1)}|D_d^R)\, p(D_d) \tag{4.32}$$

(a)

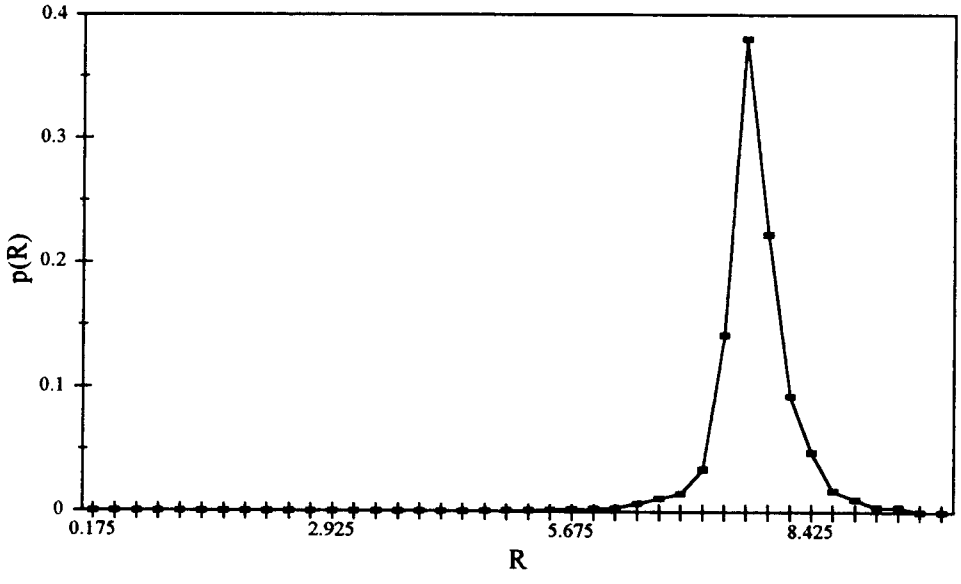

(b)

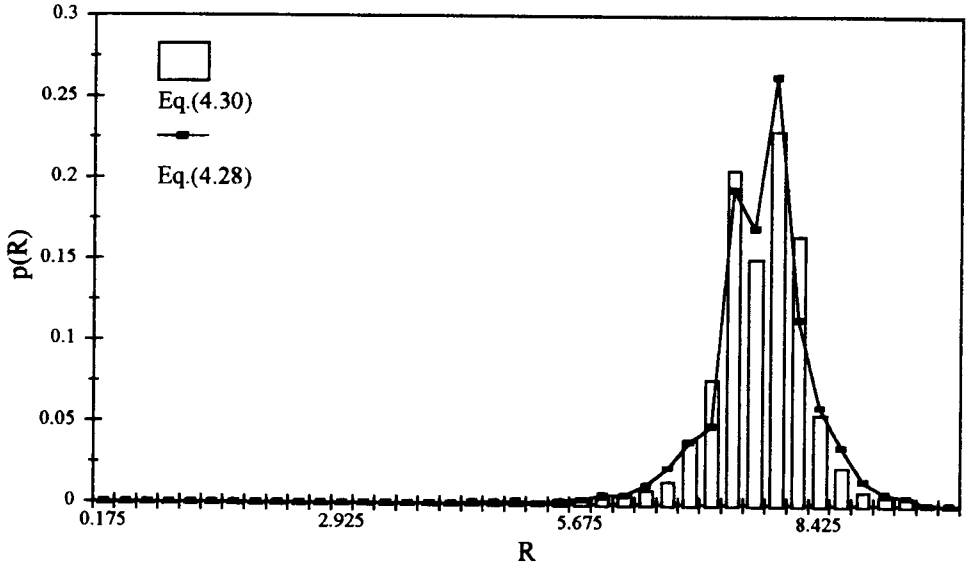

Figure 4.1 Response amplitude probability distribution in the large amplitude harmonic attraction domain. (a) $\tilde{p}(R^{(1)}|(D_1^R)_A^{(1)})$, and (b) $\hat{y}(R^{(2)}|A_j^{(1)}, A_i^{(2)}, D_1^R)$ from Eq.(4.28) and $\tilde{p}(R^{(2)}|A_j^{(1)}, A_i^{(2)}, D_1^R)$ from Eq.(4.30). $\{c_S = 0.05, a_1 = 1, a_3 = 0.3, \omega_f = 3.6, \gamma = 0.01, \sigma_f^2 = 157, A_j^{(1)} = 10, A_i^{(2)} = 7\}$.

(a)

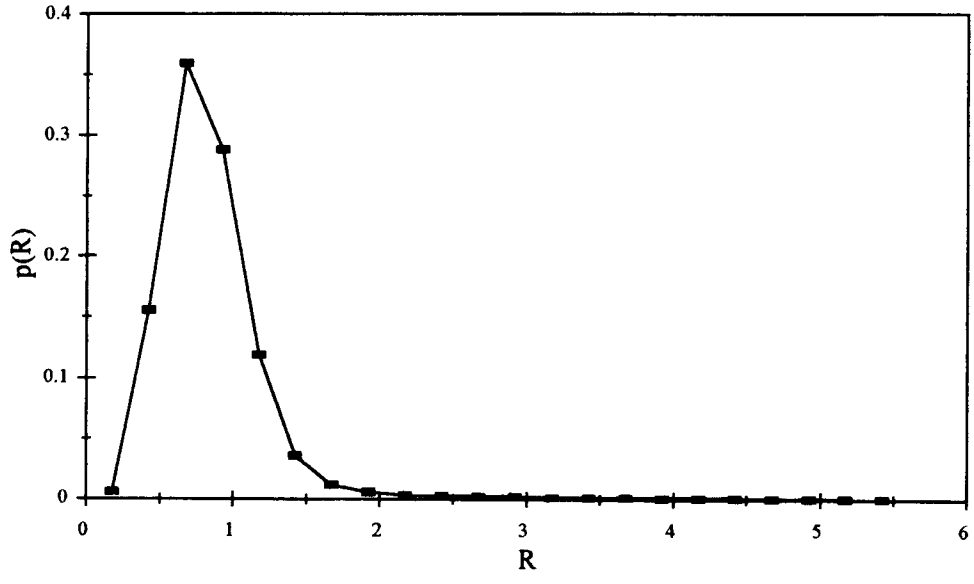

(b)

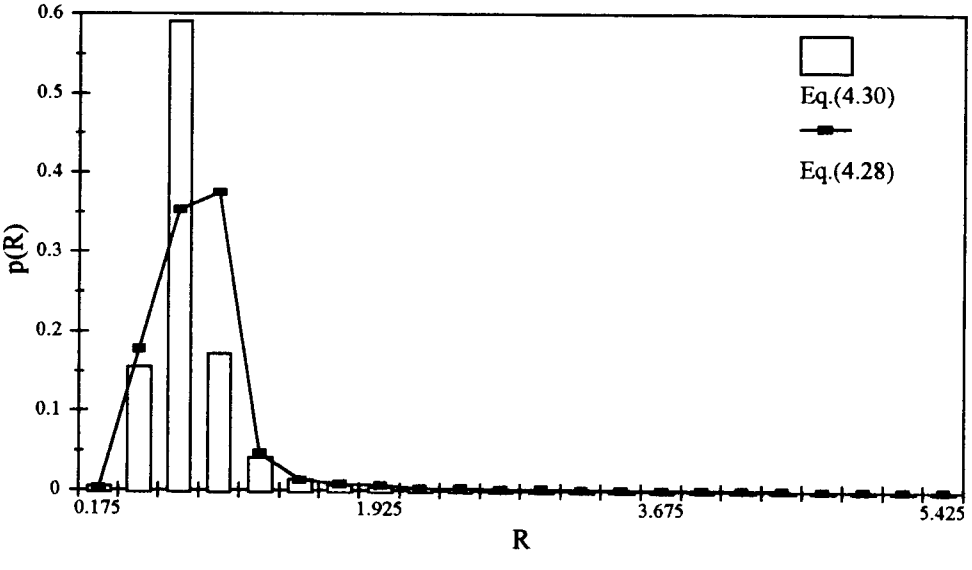

Figure 4.2 Response amplitude probability distribution in the small amplitude harmonic attraction domain. (a) $\tilde{p}(R^{(1)}|(D_2{}^R)_A{}^{(1)})$, and (b) $\hat{y}(R^{(2)}|A_j^{(1)}, A_i^{(2)}, D_2{}^R)$ from Eq.(4.28) and $\tilde{p}(R^{(2)}|A_j^{(1)}, A_i^{(2)}, D_2{}^R)$ from Eq.(4.30). $\{c_S = 0.05, a_1 = 1, a_3 = 0.3, \omega_f = 3.6, \gamma = 0.01, \sigma_f^2 = 157, A_j^{(1)} = 10, A_i^{(2)} = 7\}$.

(a)

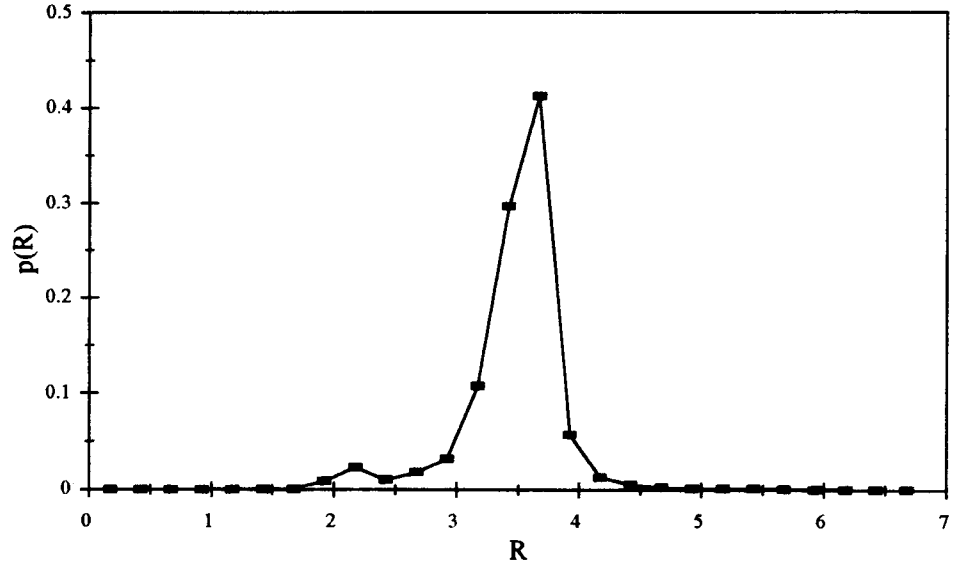

(b)

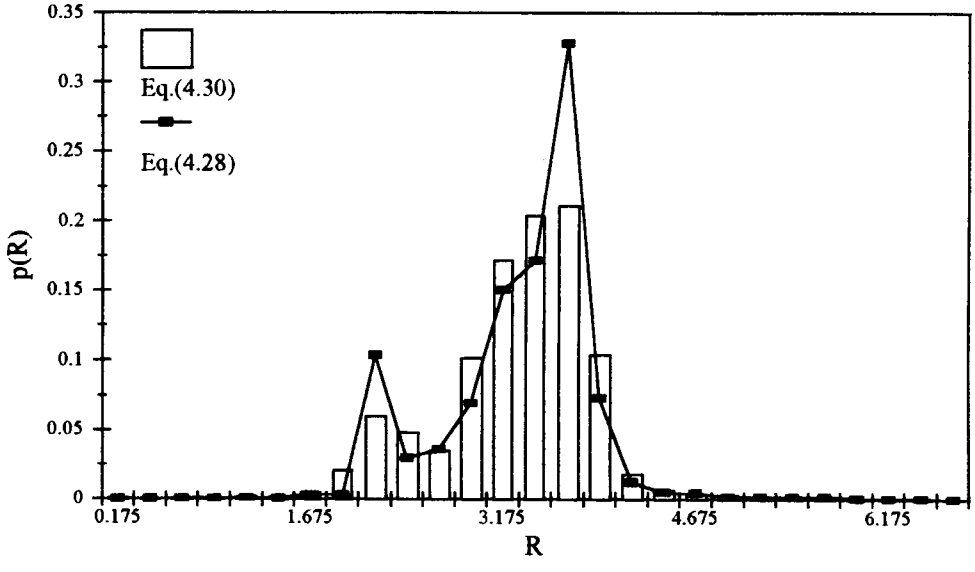

Figure 4.3 Response amplitude probability distribution in the 1/2 subharmonic attraction domain. (a) $\tilde{p}(R^{(1)}|(D_3^R)_A^{(1)})$, and (b) $\hat{y}(R^{(2)}|A_j^{(1)}, A_i^{(2)}, D_3^R)$ from Eq.(4.28) and $\tilde{p}(R^{(2)}|A_j^{(1)}, A_i^{(2)}, D_3^R)$ from Eq.(4.30). $\{c_S = 0.05, a_1 = 1, a_3 = 0.3, \omega_f = 3.6, \gamma = 0.01, \sigma_f^2 = 157, A_j^{(1)} = 10, A_i^{(2)} = 7\}$.

{a)

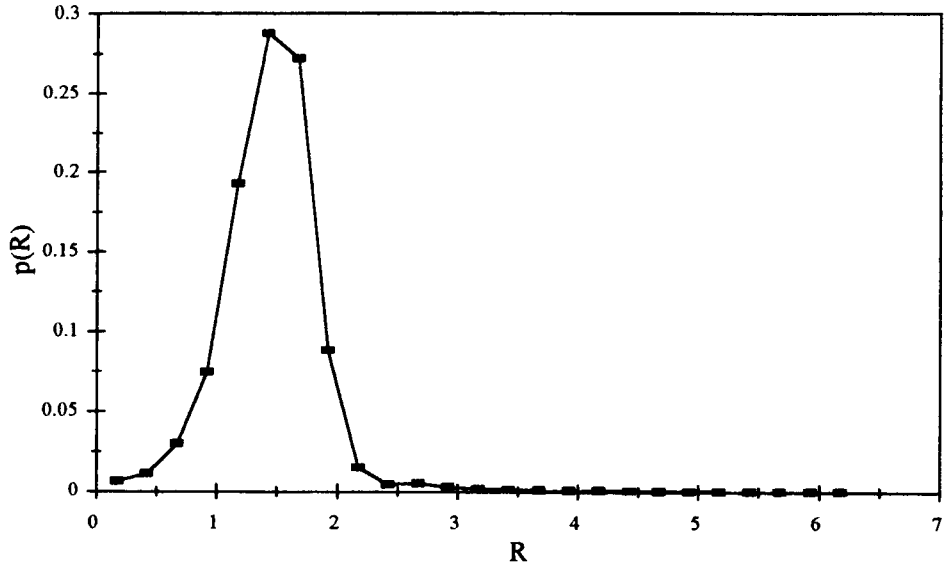

(b)

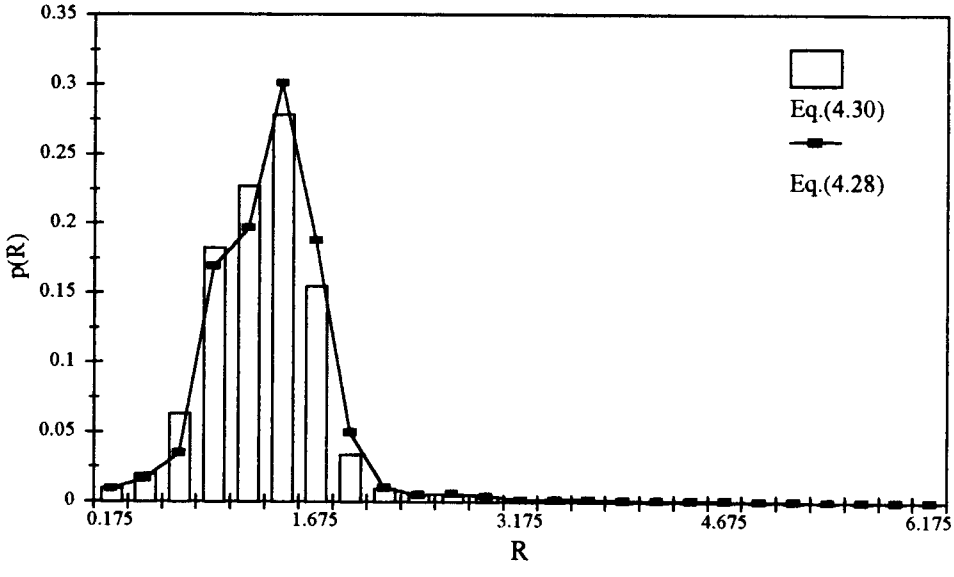

Figure 4.4 Response amplitude probability distribution in the 1/3 subharmonic attraction domain. (a) $\tilde{p}(R^{(1)}|(D_4^R)_A^{(1)})$, and (b) $\hat{y}(R^{(2)}|A_j^{(1)}, A_i^{(2)}, D_4^R)$ from Eq.(4.28) and $\tilde{p}(R^{(2)}|A_j^{(1)}, A_i^{(2)}, D_4^R)$ from Eq.(4.30). $\{c_S = 0.05, a_1 = 1, a_3 = 0.3, \omega_f = 3.6, \gamma = 0.01, \sigma_f^2 = 157, A_j^{(1)} = 10, A_i^{(2)} = 7\}$.

5. STOCHASTIC RESPONSE BEHAVIOR AND PREDICTIONS

Response behaviors of the nonlinear structural system subject to narrowband stochastic excitations is investigated via simulations to verify the stochastic system characteristics assumed in the development of the semi-analytical procedure. In addition, to demonstrate the accuracy of the procedure, predicted response amplitude probability distributions are presented and compared to simulation results. Numerical simulations are conducted by directly integrating Eq.(2.3) with the narrowband excitation f(t) modeled by the Shinozuka (1970) formulation (Section 2.3.3, Eq.(2.11)).

5.1 Stochastic Response Behavior

5.1.1 Jump Phenomena and Subharmonic Responses

Jump Phenomena -- The system response under a narrowband excitation (shown in Fig.5.1a) exhibits amplitude jumps between two distinct levels. To depict the mechanism of the jump phenomenon, an amplitude response map is employed. The map is obtained by plotting the excitation amplitudes versus the corresponding measured response amplitudes, as shown in Fig.5.1b. In addition, the corresponding amplitude response curves of the system (Section 3.1) are presented as the solid lines in the figure (see Fig.3.1 for a clear demonstration). From the figure, it is revealed that the characteristics of the response inter-domain transition (jump phenomenon) behavior depicted in Section 3.3 is preserved in a narrowband excitation environment. Namely, the system response goes from the large amplitude domain to the small amplitude domain when the excitation amplitude A varies from greater than to less than the

(a)

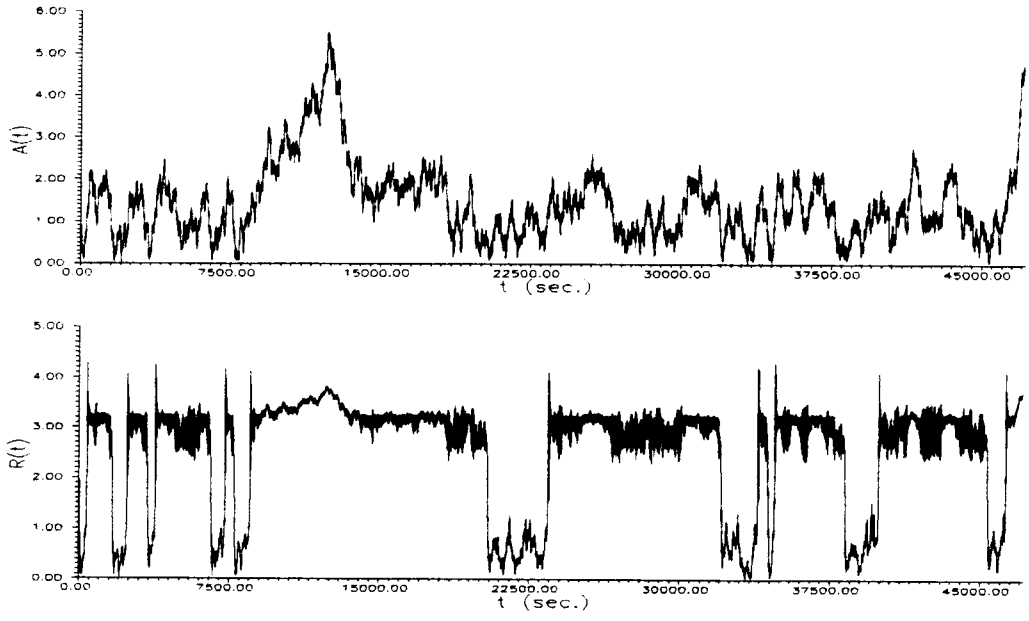

(b)

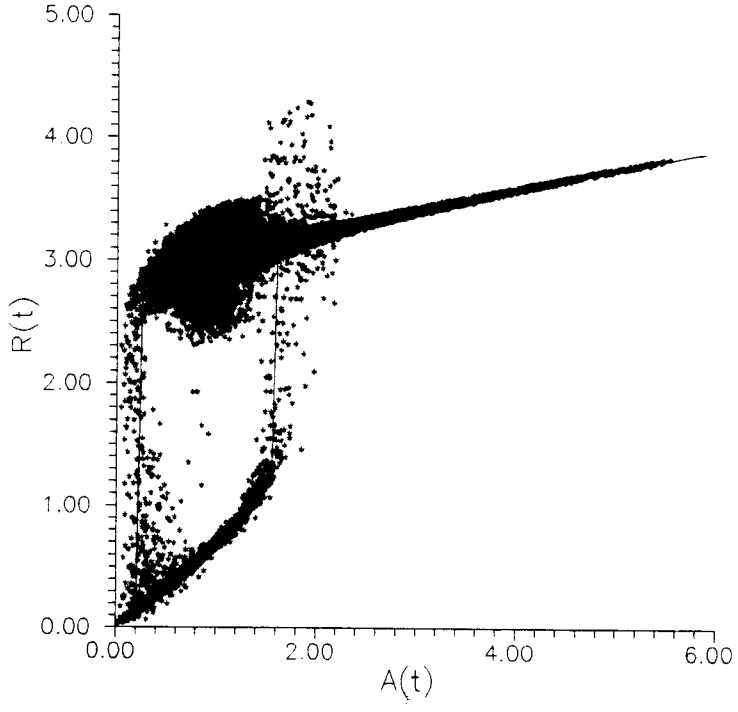

Figure 5.1 (a) Time series of a narrowband excitation (top) and corresponding response (bottom). (b) Amplitude response map corresponding to (a). $\{c_S = 0.05, a_1 = 1, a_3 = 0.3, \omega_f = 1.6, \sigma_f^2 = 1.57, \gamma = 0.001\}$.

large amplitude domain lower bound A_{1L}. Similarly, the system response goes from the small amplitude domain to the large amplitude domain when the excitation amplitude, A, varies from less than to greater than the small domain upper bound A_{2U}.

Subharmonic Responses -- Repeated occurrence of the 1/2 and 1/3 subharmonic responses under narrowband excitations can be observed in Figs.5.2a and 5.2b. The system responses oscillate at two distinct amplitude levels (i.e., a similar jump phenomenon to that in the primary resonance region shown in Fig.5.1a). Existence of the subharmonic responses is obscured in the time series due to the response amplitude domains D_d^R (d =2,3,4) overlapping among the small amplitude harmonic, 1/2 and 1/3 subharmonic domains (Section 3.2.3). However, the existence of these responses can be detected through their corresponding amplitude response maps (Figs.5.3a and 5.3b) by observing that some of the points stay closely to the subharmonic amplitude response curves (shown as the solid lines, see also Fig.3.3 for clear demonstration). Note that, for an excitation amplitude A, the corresponding points in the neighborhood of a response amplitude curve form the response amplitude domain $(D_d^R)_A$ in the attraction domain D_d.

From the amplitude response maps, it is observed that the system response may enter the 1/2 or the 1/3 subharmonic domain when an exit from the large amplitude harmonic domain occurs. As a result, the subharmonic responses (1/2 or 1/3) may occur repeatedly, although the duration of stay in each visit of the system response in these domains may be short. In addition, a response inter-domain transition from the 1/2 subharmonic domain to the large amplitude harmonic domain is also observed in Fig.5.3b when an exit from the 1/2 subharmonic domain occurs at the domain upper boundary. Thus, the response inter-domain

(a)

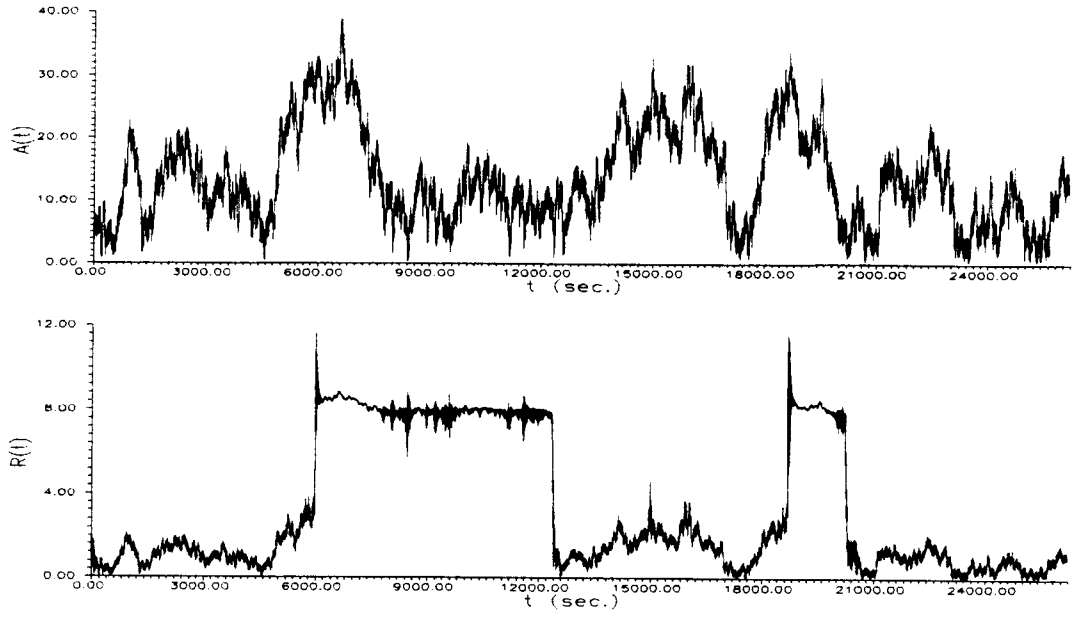

(b)

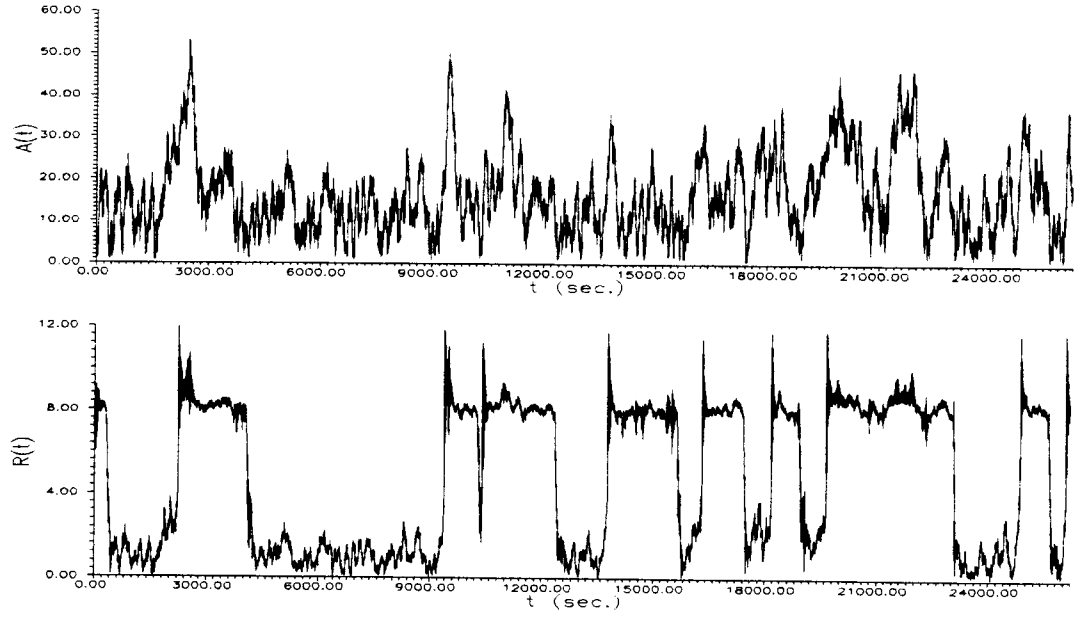

Figure 5.2 (a) and (b), system response in the subharmonic resonance region. Time series of narrowband excitation amplitude (top) and corresponding response amplitude (bottom). $\{c_S = 0.05, a_1 = 1, a_3 = 0.3, \omega_f = 3.6, \sigma_f^2 = 157, \gamma =$ (a) 0.001, (b) 0.005 $\}$.

(a)

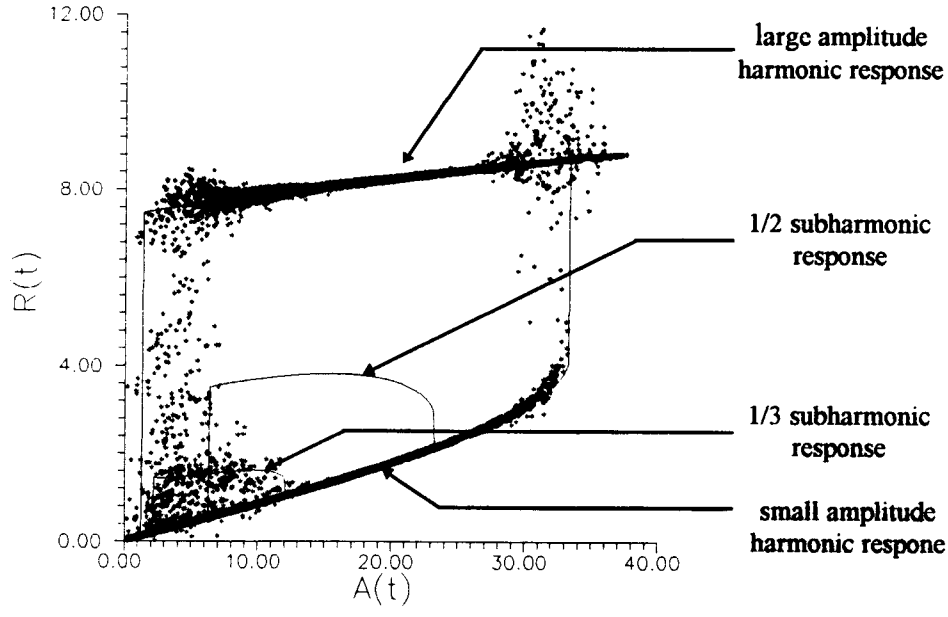

(b)

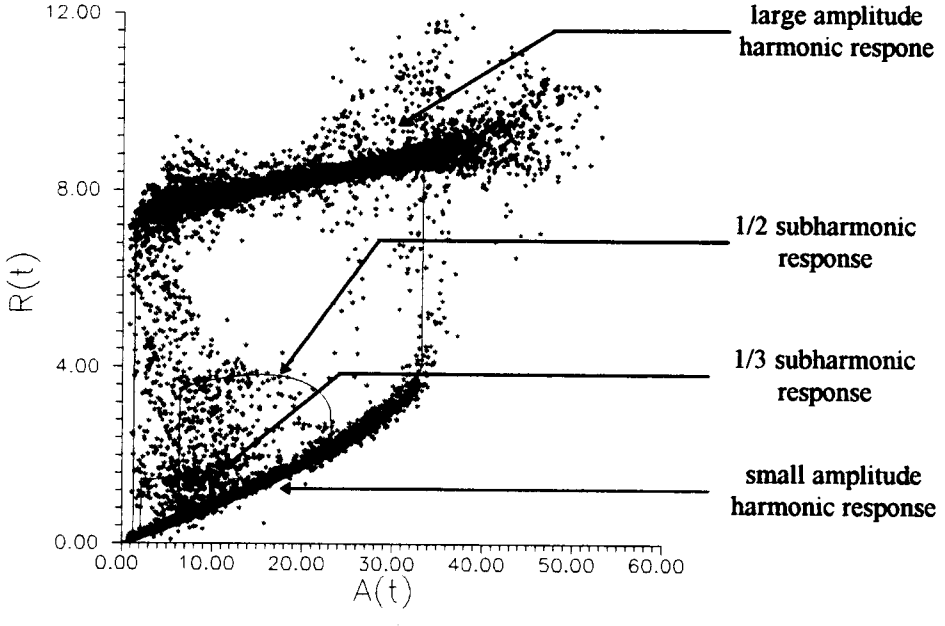

Figure 5.3 (a) and (b): Amplitude response maps correspond to the time series shown in Figs.5.2(a) and 5.2(b), respectively.

transition behavior depicted in Section 3.3 is also preserved in the narrowband excitation environment when the system is in the subharmonic resonance region.

Note that the existence of the 1/3 subharmonic response under a narrowband excitation was also observed in simulations conducted in previous studies (Davies and Rajan, 1988; Francescutto, 1991) when an extremely small excitation bandwidth and special system initial conditions are employed. However, it was concluded that the 1/3 subharmonic response only exists in the beginning of a response realization and, once it disappears, it will not be observed. The contradiction in the conclusion of repeated occurrence of the subharmonic response is mainly due to different simulation durations employed. In this study, the simulation duration is equal to 12,000 excitation cycles which is significantly longer than those employed in previous studies (600 excitation cycles).

5.1.2 Attraction Domain Dependency

Dependency of the system response characteristics on the attraction domains D_d can be observed in the amplitude response maps (Figs.5.1b, and 5.3a-b). Degrees of the response amplitude concentration in $(D_d^R)_A$ are found to depend on the attraction domains D_d. Note that the randomness in the excitation is independent of the response attraction domains. Therefore, dependency of the degree of response amplitude concentration in $(D_d^R)_A$ on the response attraction domain D_d indicates the dependency of the system characteristics and thus, the intra-domain probability transition behavior on D_d.

5.1.3 Effect of Varying Excitation Bandwidth

The effect of varying excitation bandwidth on the response behavior is demonstrated in Figs.5.4-5. It is observed that randomness in the excitation increases when the excitation bandwidth increases. Due to the increasing excitation randomness, the response time series exhibits more frequent amplitude jumps between two distinct levels. In addition, the total time of the response in higher amplitude level is also observed to increase as the excitation bandwidth increases. As a result, the probability of the system response in the higher (lower) amplitude level increases (decreases) as the excitation bandwidth increases. Therefore, the response inter-domain transition probability and thus, the response amplitude probability distribution is related to the excitation bandwidth. Note that, for the system in the primary resonance region (Fig.5.4), the higher and lower amplitude levels correspond to the large amplitude domain, D_1^R, and small amplitude domain, D_2^R, respectively. When the system is in the subharmonic resonance region, the lower amplitude level shown in Fig.5.5 includes the small amplitude harmonic domain, D_2^R, the 1/2 subharmonic domain, D_3^R, and 1/3 subharmonic attraction domain, D_4^R, as depicted in Section 5.1.1. Whereas, the higher amplitude level corresponds to the large amplitude harmonic domain, D_1^R.

In the amplitude response maps shown in Figs.5.6-7, an effect of increasing excitation bandwidth on the system response behavior is demonstrated by the decrease in the degrees of the response amplitude concentration in the domains $(D_d^R)_A$. As a result, the variance of the response amplitude in D_d^R increases with increasing excitation bandwidth. Therefore, the response intra-domain probability transition and thus, the response amplitude probability distribution is also affected by variations in the excitation bandwidth.

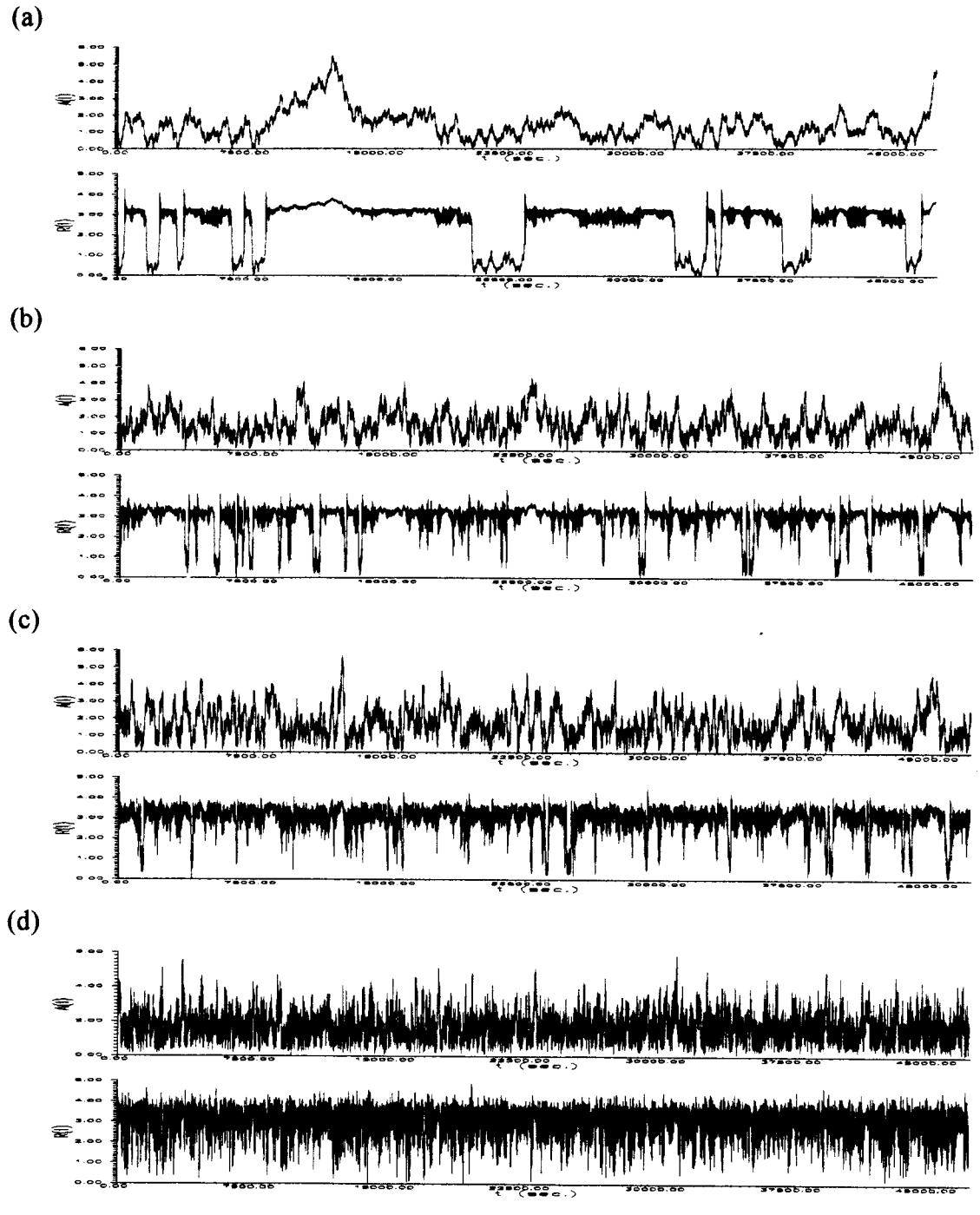

Figure 5.4 (a), (b), (c) and (d): system response under varying excitation bandwidth in the primary resonance region. Time series of narrowband excitation amplitude (top) and corresponding response amplitude (bottom). $\{c_S = 0.05, a_1 = 1, a_3 = 0.3, \omega_f = 1.6, \sigma_f^2 = 1.57, \gamma =$ (a) 0.001, (b) 0.005, (c) 0.01, and (d) 0.05 $\}$.

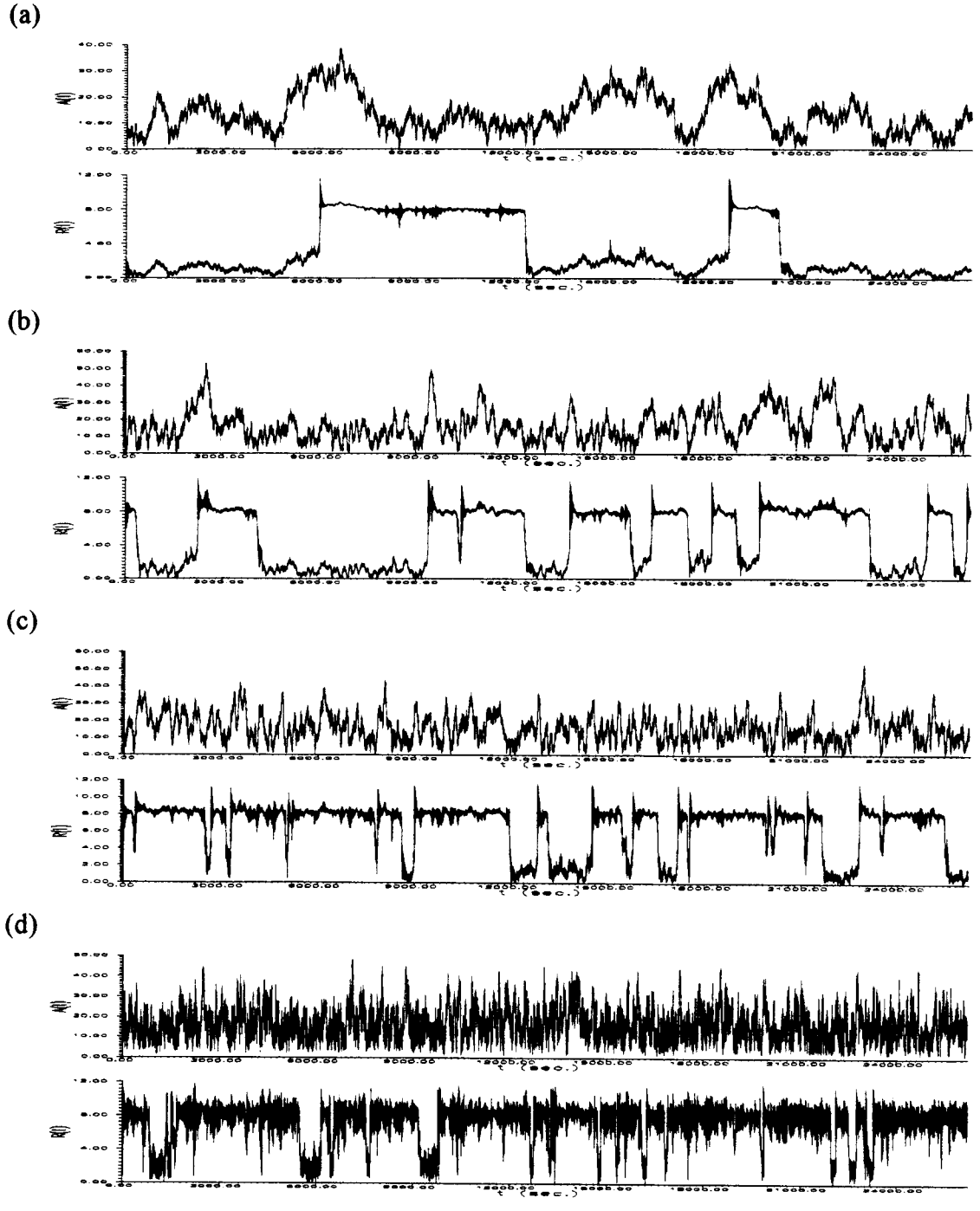

Figure 5.5 (a), (b), (c) and (d): system response under varying excitation bandwidth in the subharmonic resonance region. Time series of narrowband excitation amplitude (top) and corresponding response amplitude (bottom). $\{c_S = 0.05, a_1 = 1, a_3 = 0.3, \omega_f = 3.6, \sigma_f^2 = 157, \gamma =$ (a) 0.001, (b) 0.005, (c) 0.01, and (d) 0.05 $\}$.

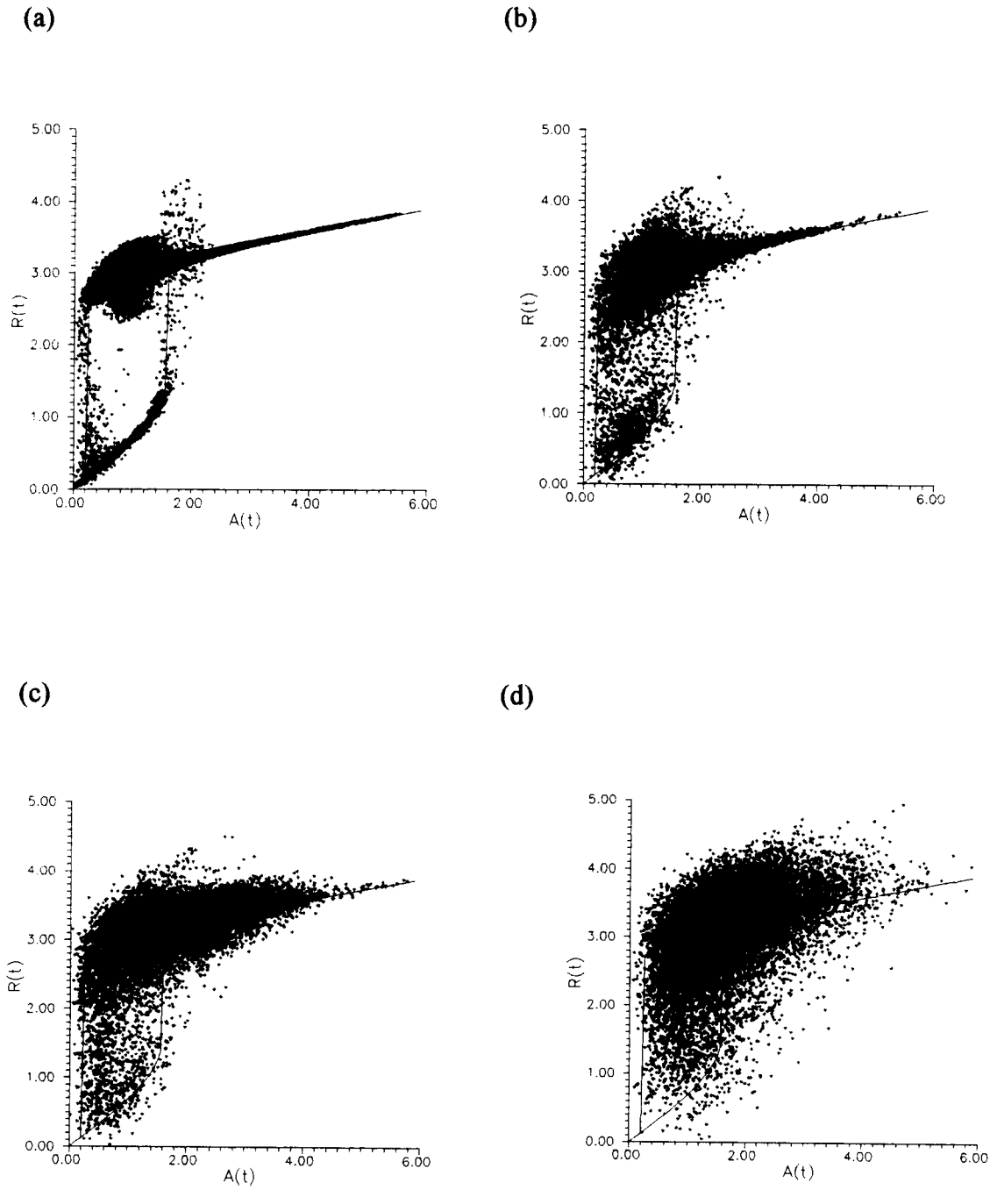

Figure 5.6 (a), (b), (c) and (d): Amplitude response maps correspond to the time series shown in Figs.5.4(a) - (d), respectively.

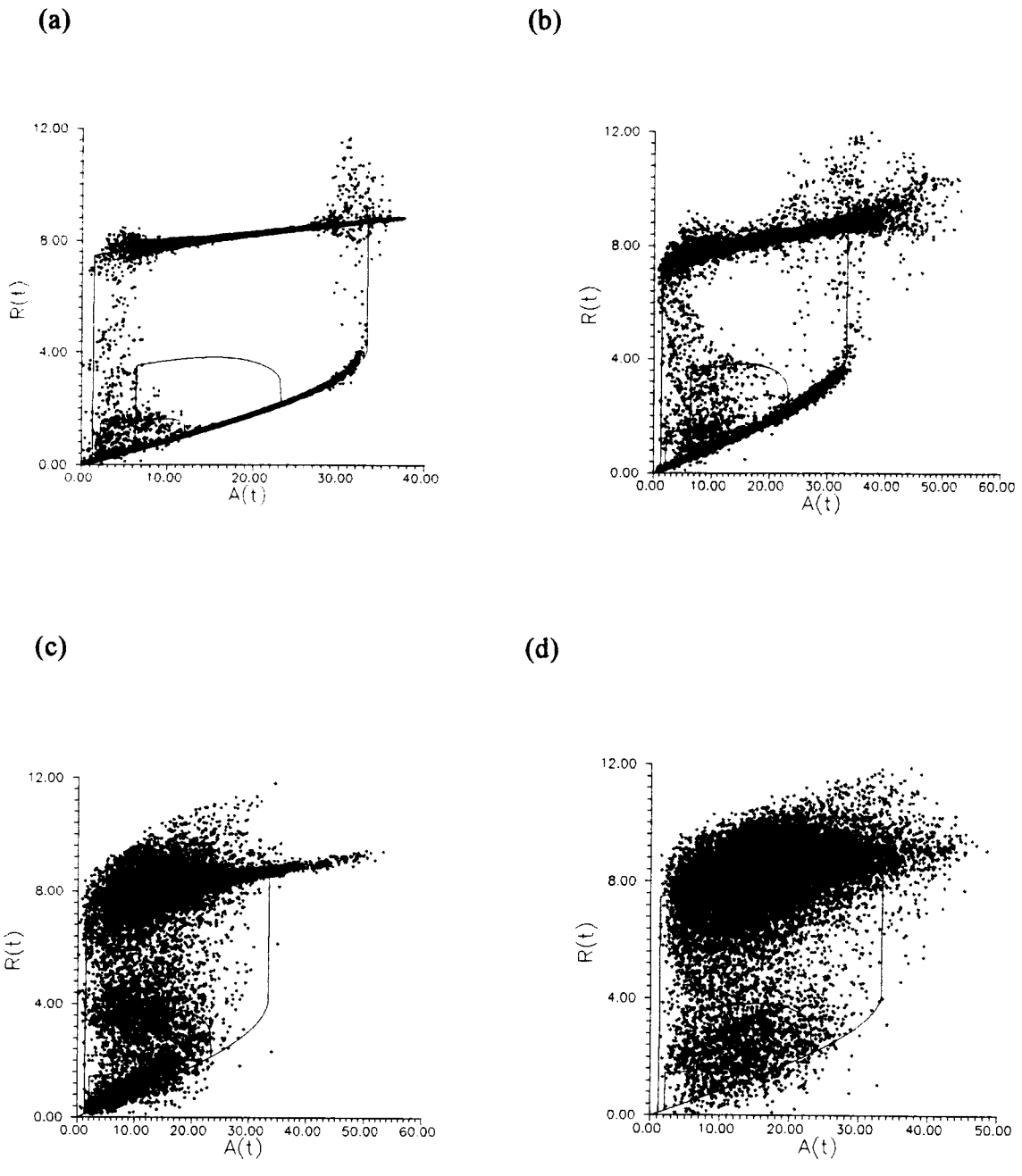

Figure 5.7 (a), (b), (c) and (d): Amplitude response maps correspond to the time series shown in Figs.5.5(a) - (d), respectively.

Note that a less obvious effect of varying the excitation bandwidth on the response behavior is the shifting of the domain boundaries, A_{dL} and A_{dU}, which are employed to characterize the response inter-domain transition behavior. In Figs.5.6-7, the domain boundaries correspond to the excitation peak (or central) frequency, ω_f, which is assumed to be constant. As a result, A_{dL} and A_{dU} are also assumed to be time invariant. However, when the excitation bandwidth increases, variations in the excitation frequency may induce shifts of these boundaries and thus affect the response inter-domain transition probability.

5.1.4 Effect of Varying Excitation Variance

By reducing the variance of the excitation process (or the input energy level), the total time of the system response in the lower amplitude level increases as shown in Figs.5.8-9. The excitation bandwidth employed is fixed in these cases, and thus, the randomness in the excitations shows no significant change. Consequently, the frequency of the response amplitude jumps is approximately unchanged. However, the system response stays longer in the lower amplitude level in every visit with decreasing excitation variance. That is, the probability of the system response in the lower (higher) amplitude level increases (decreases) as the excitation variance decreases. Therefore, the response inter-domain transition probability is affected by the excitation variance. Note that, in the amplitude response maps shown in Figs.5.10-11, the density of the points in the lower part increases as the excitation variance decreases. Variations in the density of the amplitude response maps also demonstrate the influence of varying excitation variance on the system response.

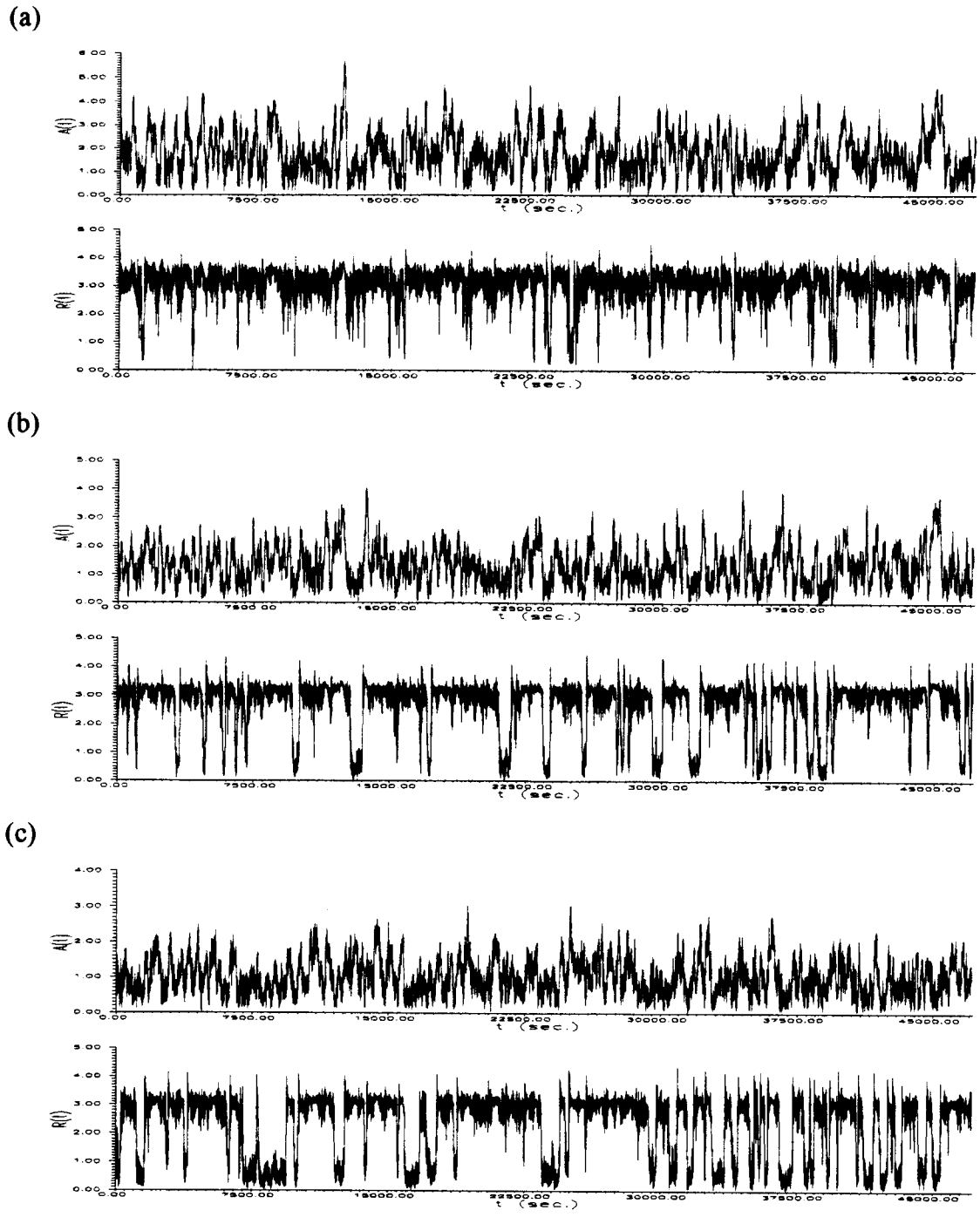

Figure 5.8 (a), (b) and (c): system response under varying excitation variance in the primary resonance region. Time series of narrowband excitation amplitude (top) and corresponding response amplitude (bottom). $\{c_S = 0.05, a_1 = 1, a_3 = 0.3, \omega_f = 1.6, \gamma = 0.01, \sigma_f^2 =$ (a) 1.57, (b) 0.94, and (c) 0.63$\}$.

(a)

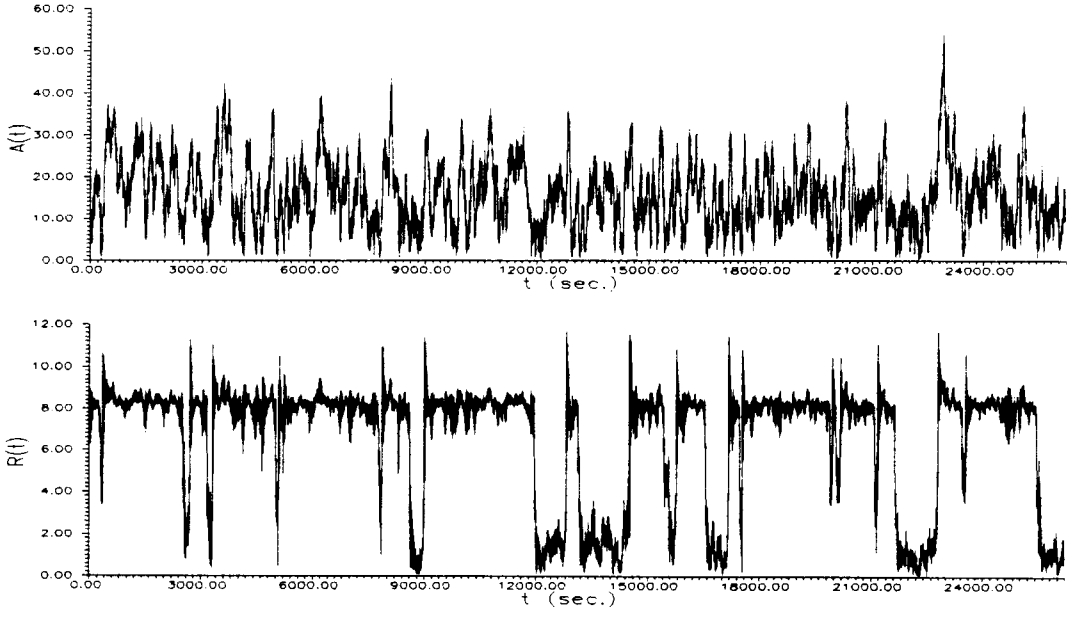

(b)

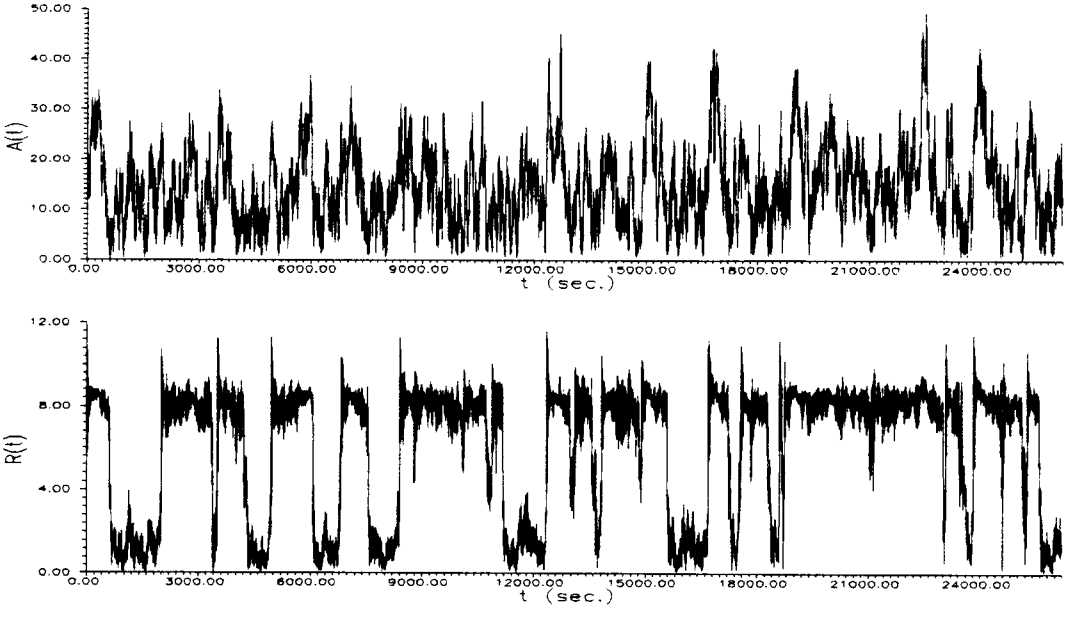

Figure 5.9 (a) and (b): system response under varying excitation variance in the subharmonic resonance region. Time series of narrowband excitation amplitude (top) and corresponding response amplitude (bottom). $\{c_S = 0.05, a_1 = 1, a_3 = 0.3, \omega_f = 3.6, \gamma = 0.01, \sigma_f^2 =$ (a) 157, and (b) 125$\}$.

(a)

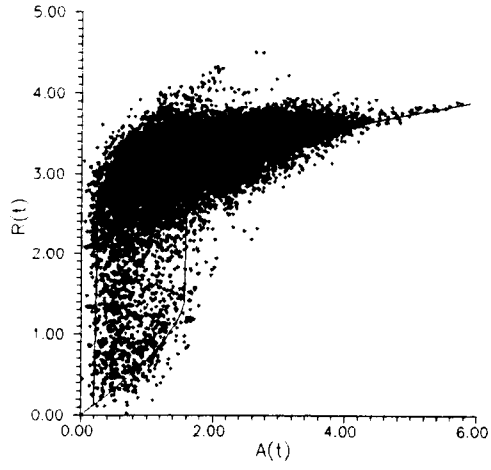

(b)

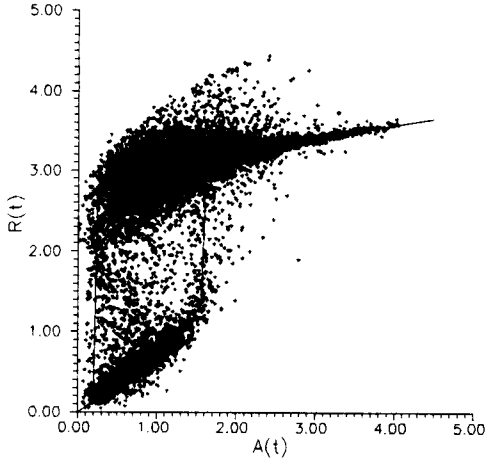

(c)

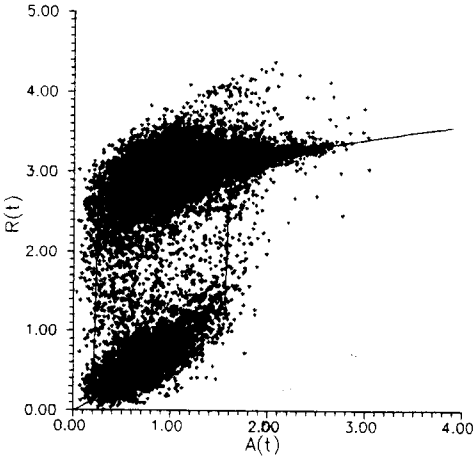

Figure 5.10 (a), (b) and (c): Amplitude response maps correspond to the time series shown in Figs.5.8(a) - (c), respectively.

(a)

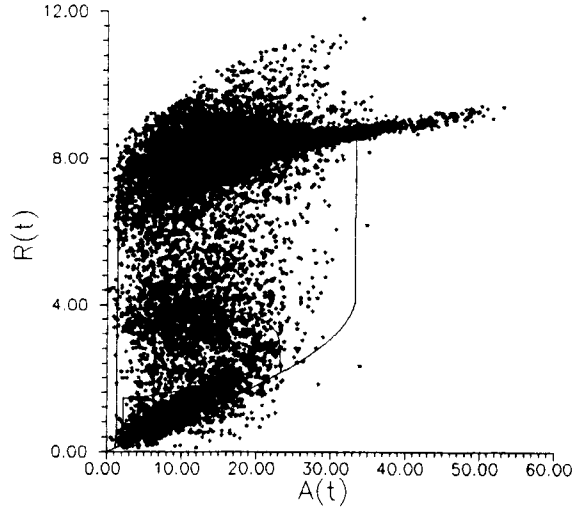

(b)

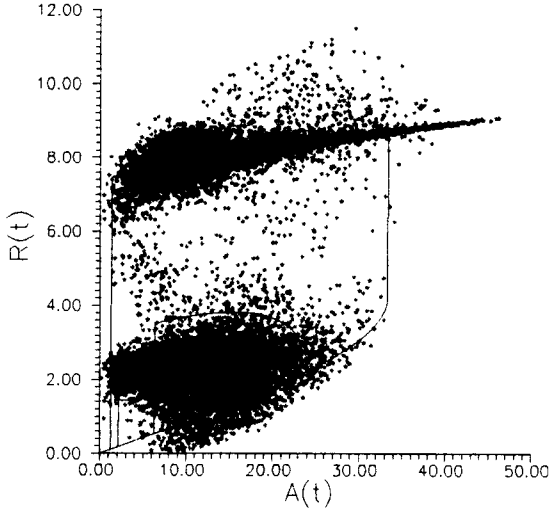

Figure 5.11 (a) and (b): Amplitude response maps correspond to the time series shown in Figs.5.9(a) - (b), respectively.

5.2 Predictions of Stochastic Nonlinear Response Behavior

The capability of the proposed semi-analytical method in characterizing the stochastic nonlinear response behavior depicted above will be investigated in this section through several case studies. In addition, to demonstrate the accuracy of the semi-analytical procedure in predicting the response amplitude probability distribution, prediction results in each case will be presented and compared to simulation results.

5.2.1 Primary Resonance Region

Response Characteristics -- To validate the proposed method in characterizing the stochastic response behavior in the primary resonance region, prediction results of the system responses in six cases with various excitation parameter sets (see Table 5.1 below) are examined. Note that the system damping, linear and nonlinear restoring force parameters c_S, a_1 and a_3,

Case	(i)	(ii)	(iii)	(iv)	(v)	(vi)
System Parameters	c_S=0.05, a_1=1, a_3=0.3 Eq.(2.3)					
Excitation Parameters, Eq.(2.5)						
ω_f	1.6	1.6	1.6	1.6	1.6	1.6
γ	0.001	0.005	0.01	0.05	0.01	0.01
σ_f^2	1.57	1.57	1.57	1.57	0.94	0.63
Domain Boundaries, Fig.3.1						
A_{1L}	0.25	0.25	0.25	0.25	0.25	0.25
A_{2U}	1.6	1.6	1.6	1.6	1.6	1.6

Table 5.1 Parameters of the systems considered in the primary resonance region.

respectively, are fixed. To investigate the influence of varying the degree of excitation randomness on the response behavior, the excitation bandwidth γ is increased from cases (i) to (iv), with fixed excitation intensity (i.e., fixed variance σ_f^2). On the other hand, to investigate the response behavior under varying excitation intensity, the excitation variance σ_f^2 is varied in cases (iii), (v) and (vi), with the excitation bandwidth γ held fixed.

In the primary resonance region, two attraction domains (large amplitude harmonic domain, D_1, and small amplitude harmonic domain, D_2) co-exist as depicted in Section 3.1. The probabilities $p(D_1)$ and $p(D_2)$ of the system response being in the domains D_1 and D_2, respectively, are calculated according to Eq.(4.13) in Section 4.3 and the procedure discussed in Appendix D.1. In addition, the approximate stationary response amplitude probability distributions in attraction domains $\tilde{p}(R|D_d^R)$ (d=1,2) can be obtained by Eq.(4.31), and thus, the overall distribution is obtained by Eq.(4.32).

(1) *Effects of Varying Excitation Randomness on Response Inter-Domain Transition*: The system response behavior under increasing degree of excitation randomness (i.e. increasing excitation bandwidth parameter γ) with a constant excitation intensity (i.e., variance σ_f^2) is investigated in cases (i) through (iv). For these cases, the normalized parameters $\rho'=|\rho|/\sigma_f^2$ and $\lambda'=|\lambda|/\sigma_f^2$ (see Eq.(4.2)), the response probability inter-domain transition matrices K, and the normalized eigenvectors corresponding to the unit eigenvalues are listed in Table 5.2. Note that ρ' and λ' are the normalized auto-correlation and cross-correlation, respectively, of the cosine and sine components of the excitation envelop process with time lag equal to the central excitation period (Ochi, 1990). A decrease in ρ' and an increase in λ' indicate a decrease in the correlation between the respective cosine and sine components of two

Case	γ	ρ'	λ'	Transition Matrix, K	Normalized Eigenvector
(i)	0.001	0.999	0.00029	$\begin{bmatrix} 0.9942 & 0.0284 \\ 0.0058 & 0.9716 \end{bmatrix}$	$\begin{Bmatrix} p_1(D_1) \\ p_2(D_2) \end{Bmatrix} = \begin{Bmatrix} 0.831 \\ 0.169 \end{Bmatrix}$
(ii)	0.005	0.990	0.00126	$\begin{bmatrix} 0.9889 & 0.0563 \\ 0.0111 & 0.9437 \end{bmatrix}$	$\begin{Bmatrix} p_1(D_1) \\ p_2(D_2) \end{Bmatrix} = \begin{Bmatrix} 0.836 \\ 0.164 \end{Bmatrix}$
(iii)	0.010	0.981	0.00251	$\begin{bmatrix} 0.986 & 0.0803 \\ 0.014 & 0.9197 \end{bmatrix}$	$\begin{Bmatrix} p_1(D_1) \\ p_2(D_2) \end{Bmatrix} = \begin{Bmatrix} 0.851 \\ 0.149 \end{Bmatrix}$
(iv)	0.050	0.907	0.01210	$\begin{bmatrix} 0.9815 & 0.1758 \\ 0.0185 & 0.8242 \end{bmatrix}$	$\begin{Bmatrix} p_1(D_1) \\ p_2(D_2) \end{Bmatrix} = \begin{Bmatrix} 0.905 \\ 0.095 \end{Bmatrix}$

Table 5.2 Effects of varying excitation bandwidth on response inter-domain transition probability in the primary resonance region.

consecutive excitation amplitudes. Observed in Table 5.2 that as the excitation bandwidth parameter γ increases, ρ' decreases and λ' increases. Thus, the randomness in the processes of excitation amplitude cosine and sine components is increased as expected. As a result, from Eqs.(B.5-6), the randomness in the excitation amplitude and the excitation phase angle is increased as the excitation bandwidth increases. Therefore, dependency of the stochastic behavior of the excitation parameters on the excitation bandwidth is confirmed. For the transition matrices K, both $p_{11}(1|1)$ and $p_{22}(2|2)$ decrease with increasing excitation bandwidth. However, the rate of decreasing (0.53% from case (i) to case (ii)) in $p_{11}(1|1)$ is lower than that in $p_{22}(2|2)$ (2.87% from case (i) to case (ii)). As a result, the calculated probability of the system response in the large (small) amplitude attraction domain increases

(decreases) with increasing excitation bandwidth as demonstrated in the last column of Table 5.2. Therefore, the stochastic response behavior observed in Section 5.1.3 under varying excitation bandwidth is captured by the semi-analytical procedure.

(2) *Effects of Varying Excitation Randomness on Response Intra-Domain Transition*: To investigate the effects of varying excitation randomness on the response amplitude probability transition within a given domain (i.e., intra-domain transition probability), the variances σ_d^2 (d=1,2) of the response amplitude within attraction domains D_d^R (d=1, 2) are evaluated numerically from the analytical conditional probability distributions $\tilde{p}(R|D_d^R)$ (d=1,2), Eq.(4.31). The results for cases (i) though (iv) are tabulated in Table 5.3. In both the large amplitude domain, D_1^R, and the small amplitude domain, D_2^R, the predicted variances of the response amplitude probability distribution increase with increasing excitation bandwidth. This observation is in accordance with the response behavior observed in Section 5.1.3. In addition, in each case, the variance of the response amplitude in both the large and the small amplitude attraction domains (computed from the analytical probability distribution obtained

Variance σ_d^2 of Response Amplitude within Attraction Domain				
case	(i)	(ii)	(iii)	(iv)
γ	0.001	0.005	0.010	0.050
σ_1^2	0.0347	0.0928	0.1449	0.4130
σ_2^2	0.1147	0.2013	0.2805	0.5251

Table 5.3 Effects of varying excitation bandwidth on the variance of the response amplitude within the large amplitude and small amplitude attraction domains, D_1 and D_2, respectively, in the primary resonance region.

using the proposed method) are significantly different, reflecting the domain dependency of the system response characteristics. Thus, the validity of the proposed method in the analysis of stochastic response behavior under varying excitation bandwidth is confirmed.

(3) *Effects of Varying Excitation Intensity on Response Inter-Domain Transition*: The effects of varying excitation intensity (i.e., variance σ_f^2) on the system response behavior under constant excitation bandwidth γ are investigated in this section. For cases (iii), (v) and (vi)), the values of the normalized parameters $\rho'=|\rho|/\sigma_f^2$ and $\lambda'=|\lambda|/\sigma_f^2$, the response probability inter-domain transition matrices K, and the normalized eigenvectors corresponding to the unit eigenvalues are tabulated in Table 5.4.

Observed that, when the excitation variance σ_f^2 decreases (with fixed excitation bandwidth $\gamma = 0.01$), the parameters ρ' and λ' remain approximately constant. Recall from

Case	σ_f^2	ρ'	λ'	Transition Matrix, K	Normalized Eigenvector
(iii)	1.57	0.981	0.00251	$\begin{bmatrix} 0.986 & 0.0803 \\ 0.014 & 0.9197 \end{bmatrix}$	$\begin{Bmatrix} p_1(D_1) \\ p_2(D_2) \end{Bmatrix} = \begin{Bmatrix} 0.851 \\ 0.149 \end{Bmatrix}$
(v)	0.94	0.983	0.00252	$\begin{bmatrix} 0.9797 & 0.045 \\ 0.0203 & 0.955 \end{bmatrix}$	$\begin{Bmatrix} p_1(D_1) \\ p_2(D_2) \end{Bmatrix} = \begin{Bmatrix} 0.689 \\ 0.311 \end{Bmatrix}$
(vi)	0.63	0.978	0.00251	$\begin{bmatrix} 0.9739 & 0.0233 \\ 0.0261 & 0.9767 \end{bmatrix}$	$\begin{Bmatrix} p_1(D_1) \\ p_2(D_2) \end{Bmatrix} = \begin{Bmatrix} 0.472 \\ 0.528 \end{Bmatrix}$

Table 5.4 Effects of varying excitation variance on response inter-domain transition probability in the primary resonance region.

discussion in (1) above that variations in the ρ' and λ' indicate variations in the randomness of the excitation parameter (amplitude and phase angle) processes. Therefore, the randomness in the excitation parameter processes is generally unaffected by the variation in the excitation variance. This result is in accordance with that observed in Section 5.1.4. However, when the excitation intensity (i.e., variance) decreases, the excitation amplitudes become small and the excitation amplitude probability (Rayleigh) distribution is shifted to left (small amplitude level). Thus, the stochastic behavior of the excitation amplitude is affected accordingly.

In the transition matrices K, variations in the values of elements $p_{ij}(i|j)$ $(i,j=1,2)$ also reflect the influence of varying excitation variance on the excitation amplitude behavior. When the excitation amplitude decreases (from case (iii) to (v) to (vi)), the probability that the system response exits from the large amplitude domain increases and the probability of the system response staying in the small amplitude domain also increases. Thus, the value of $p_{11}(1|1)$ in the transition matrix K decreases while $p_{22}(2|2)$ increases, when the excitation variance decreases. As a result, the probability of the system response in the large (small) amplitude attraction domain decreases (increases) with decreasing excitation variance as shown in the last column of Table 5.4. Therefore, the stochastic response behavior observed in Section 5.1.4 under varying excitation variance is predicted by the semi-analytical procedure and the validity of the proposed method is confirmed.

Response Amplitude Probability Distribution -- To demonstrate the capability and accuracy of the semi-analytical procedure in predicting the response behavior, the response amplitude probability distributions predicted by the method (i.e., the results obtained by Eq.(4.32)) and

simulation results are presented in Fig.5.12 for the six cases examined. In each case, a total of 15 simulations are conducted. Each of the simulations consists of 12,000 excitation cycles and thus, each of the response amplitude histograms is obtained from a total of 180,000 data cycles. Good agreements are observed in all six cases. Specifically, locations of the mode in the probability distributions and the probability masses associated with the modes are predicted accurately.

(1) *Effects of Varying Excitation Randomness on Response Amplitude Probability Distribution*: As the excitation randomness (i.e., bandwidth parameter γ) increases from cases (i) to (iv), Fig.5.13a shows that the response amplitude probability mass in the higher (lower) amplitude level increases (decreases) in accordance with the response behavior observed in Section 5.1.3. The same trend of variations in the response amplitude probability distribution due to varying excitation bandwidth is also accurately predicted by the method as shown in Fig.5.13b. In addition, variations in the probability distribution from bi-modal to uni-modal due to varying excitation bandwidth are also accurately captured. The convergence of two modes into a single mode in the probability distribution reflects the combined effects of increasing probability in the higher amplitude level (i.e., probability mass shifting to the right) and increasing response amplitude probability variance in each of the individual attraction domains with increasing excitation bandwidth.

(2) *Effects of Varying Excitation Variance on Response Amplitude Probability Distribution*: As the excitation variance decreases from cases (iii) to (v) to (vi), Fig.5.14a show that the response amplitude probability mass in the higher (lower) amplitude level decreases

(a) case (i)

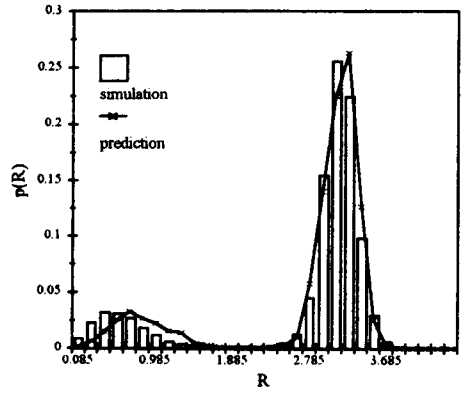

(b) case (ii)

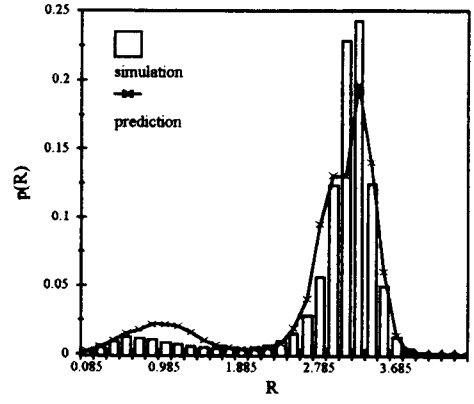

(c) case (iii)

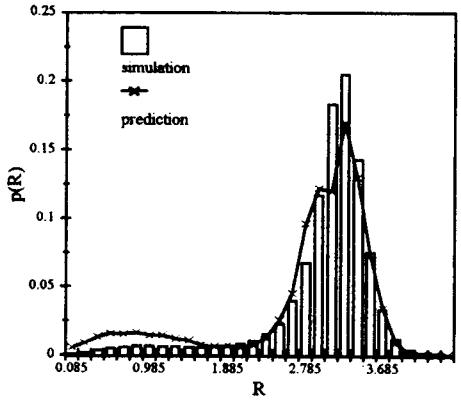

(d) case (iv)

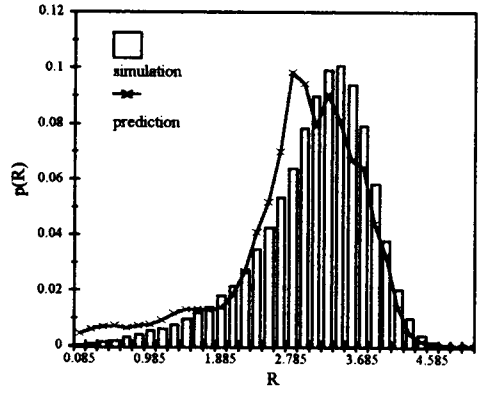

(e) case (v)

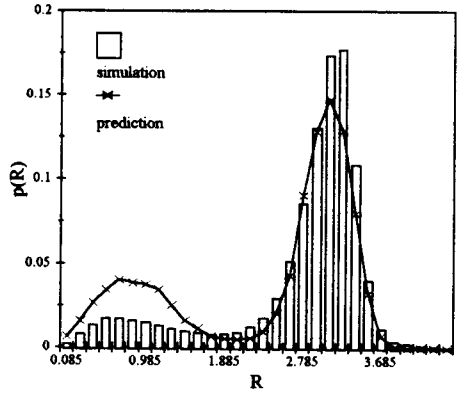

(f) case (vi)

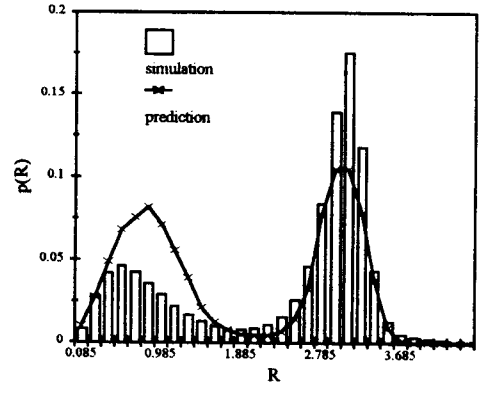

Figure 5.12 (a)-(f): Response amplitude probability distributions of case (i)-(vi), respectively. {parameters used are listed in Table 5.1}.

(a)

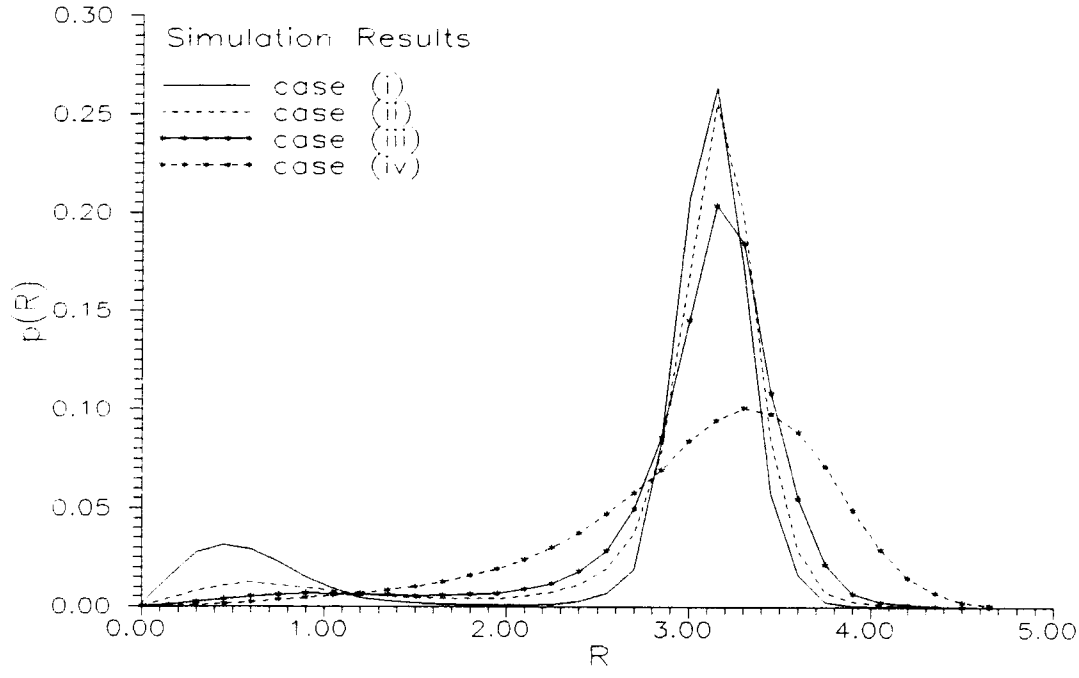

(b)

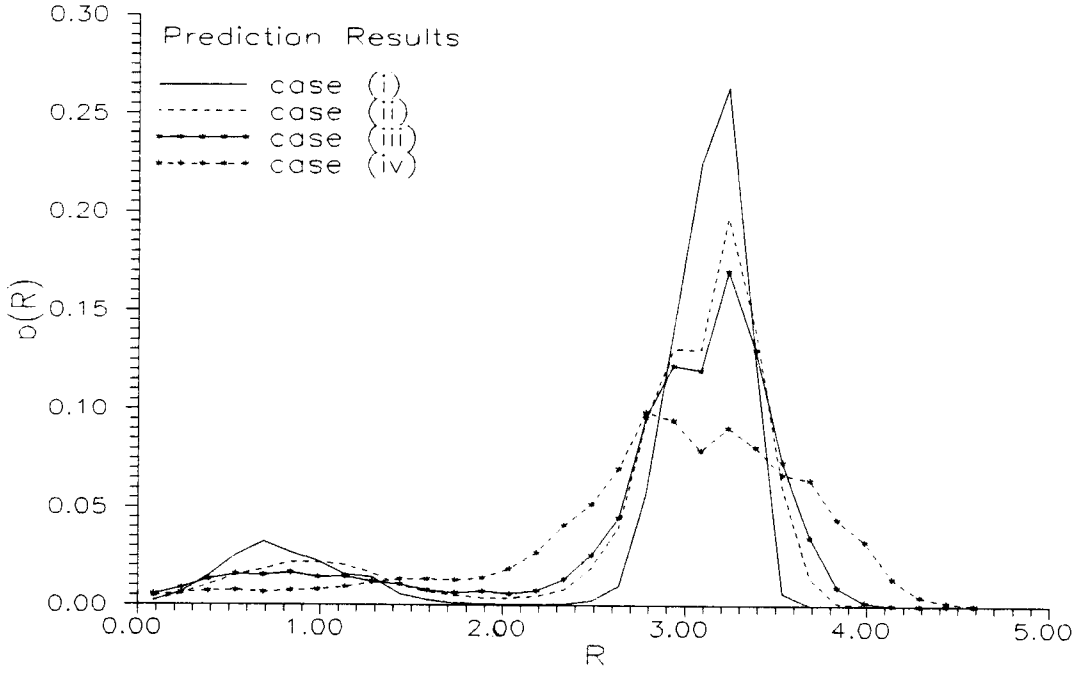

Figure 5.13 Variations in the response amplitude probability distribution under varying excitation bandwidth in the primary resonance region. (a) simulation results, (b) prediction results.

(a)

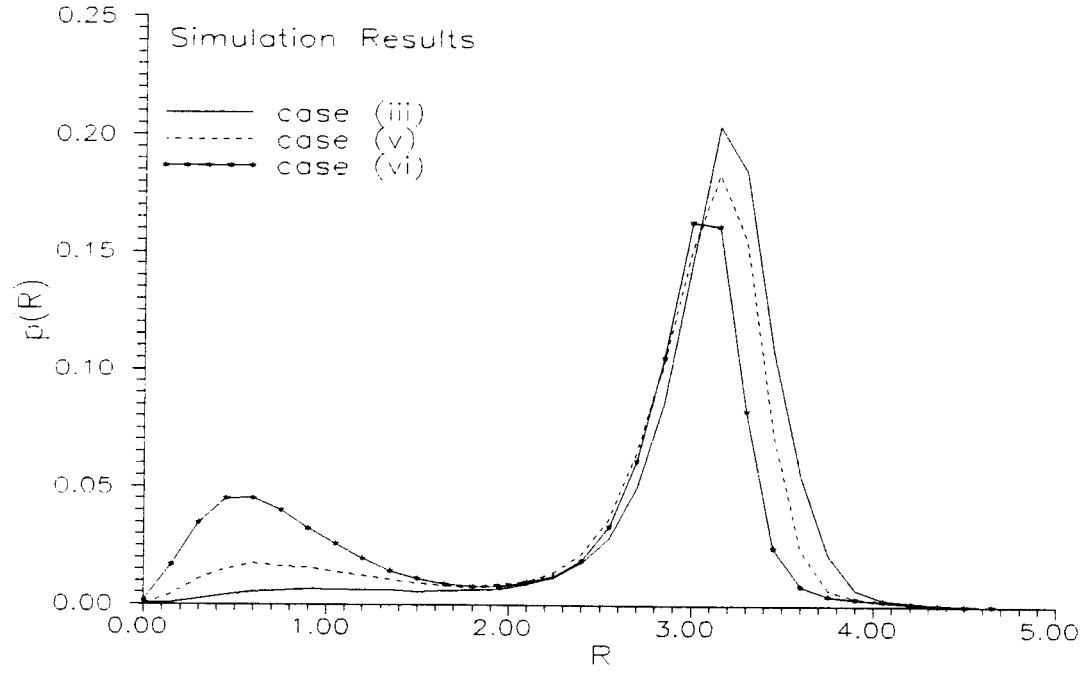

(b)

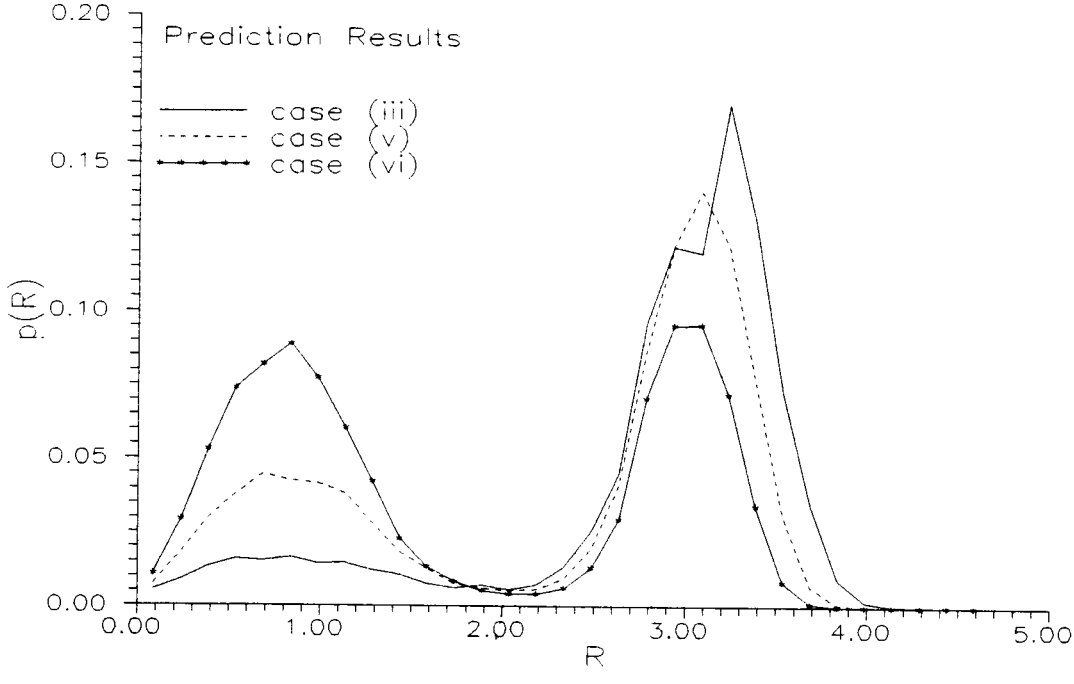

Figure 5.14 Variations in the response amplitude probability distribution under varying excitation variance in the primary resonance region. (a) simulation results, (b) prediction results.

(increases) in accordance with the response behavior observed in Section 5.1.4. This variation in the response amplitude probability distribution is also accurately captured by the proposed semi-analytical procedure as demonstrated in Fig.5.14b.

5.2.2 Subharmonic Resonance Region

Response Characteristics -- To verify the proposed method in characterizing the stochastic response behavior in the subharmonic resonance region, analytical prediction of the system response in five cases, (vii)-(xi), with various excitation parameter sets (see Table 5.5 below) are examined and compared to simulation results. The system parameters damping, linear and

Case	(vii)	(viii)	(ix)	(x)	(xi)
System Parameters	c_s=0.05, a_1=1, a_3=0.3 Eq.(2.3)				
Excitation Parameters, Eq.(2.5)					
ω_f	3.6	3.6	3.6	3.6	3.6
γ	0.001	0.005	0.01	0.05	0.01
σ_f^2	157	157	157	157	125
Domain Boundaries, Fig.3.3					
A_{1L}	1.4	1.4	1.4	1.4	1.4
A_{2U}	33.3	33.3	33.3	33.3	33.3
A_{3U}	23	23	23	23	23
A_{3L}	6.4	6.4	6.4	6.4	6.4
A_{4U}	12	12	12	12	12
A_{4L}	2.2	2.2	2.2	2.2	2.2

Table 5.5 Parameters of the systems considered in the subharmonic resonance region.

nonlinear restoring force parameters c_s, a_1 and a_3, respectively, are held constant for these cases. To isolate the effects of varying the degree of excitation randomness on the response behavior, the excitation bandwidth γ is increased from cases (vii) to (ix), while the excitation intensity (i.e., variance σ_f^2) is fixed. Also, to examine the effect of varying excitation intensity on the response behavior, the excitation variance σ_f^2 is decreased from cases (ix) to (xi) as the excitation randomness (i.e., bandwidth γ) remains constant.

In the subharmonic resonance region, the co-existing attraction domains are the large amplitude harmonic (D_1), the small amplitude harmonic (D_2), the 1/2 subharmonic (D_3) and the 1/3 subharmonic (D_4) domains (Section 3.1). The probability $p(D_d)$ of the response being in each of the four co-existing attraction domains D_d, d=1,2,3,4, respectively, are evaluated according to Eq.(4.13) and the procedure discussed in Appendix D.2. The approximate stationary response amplitude probability distribution $\tilde{p}(R|D_d^R)$ in each attraction domains D_d, d=1,2,3,4, are obtained by Eq.(4.31), and thus, the overall probability distribution is obtained by Eq.(4.32).

(1) *Effects of Varying Excitation Randomness on Response Inter-Domain Transition*: The system response behavior under increasing degree of excitation randomness (i.e., increasing γ) with constant excitation intensity (i.e., constant σ_f^2) is investigated in cases (vii) through (x). For these four cases, the normalized parameters $\rho'=|\rho|/\sigma_f^2$ and $\lambda'=|\lambda|/\sigma_f^2$, the response probability inter-domain transition matrices K, and the normalized eigenvectors corresponding to the unit eigenvalues are listed in Table 5.6.

Observed that, in the subharmonic resonance region, trends of variations in the values of ρ' and λ' are similar to those in the primary resonance region. That is, when the excitation

Case	γ	ρ'	λ'	Transition Matrix, K	Normalized Eigenvector
(vii)	0.001	0.999	0.00011	$\begin{bmatrix} 0.9979 & 0.0014 & 0.0014 & 0 \\ 0.0005 & 0.9986 & 0.0116 & 0.0385 \\ 0.0001 & 0 & 0.9802 & 0.0008 \\ 0.0015 & 0 & 0.0068 & 0.9607 \end{bmatrix}$	$\begin{Bmatrix} p_1(D_1) \\ p_2(D_2) \\ p_3(D_3) \\ p_4(D_4) \end{Bmatrix} = \begin{Bmatrix} 0.399 \\ 0.586 \\ 0.001 \\ 0.014 \end{Bmatrix}$
(viii)	0.005	0.996	0.00056	$\begin{bmatrix} 0.9959 & 0.0031 & 0.0039 & 0 \\ 0.0006 & 0.9969 & 0.0143 & 0.0742 \\ 0.0004 & 0 & 0.9566 & 0.0098 \\ 0.0031 & 0 & 0.0252 & 0.916 \end{bmatrix}$	$\begin{Bmatrix} p_1(D_1) \\ p_2(D_2) \\ p_3(D_3) \\ p_4(D_4) \end{Bmatrix} = \begin{Bmatrix} 0.426 \\ 0.547 \\ 0.009 \\ 0.018 \end{Bmatrix}$
(ix)	0.010	0.992	0.00112	$\begin{bmatrix} 0.9949 & 0.0044 & 0.0063 & 0 \\ 0.0008 & 0.9956 & 0.0195 & 0.0949 \\ 0.0017 & 0 & 0.939 & 0.0216 \\ 0.0026 & 0 & 0.0352 & 0.8835 \end{bmatrix}$	$\begin{Bmatrix} p_1(D_1) \\ p_2(D_2) \\ p_3(D_3) \\ p_4(D_4) \end{Bmatrix} = \begin{Bmatrix} 0.462 \\ 0.504 \\ 0.018 \\ 0.016 \end{Bmatrix}$
(x)	0.050	0.958	0.00549	$\begin{bmatrix} 0.9935 & 0.0097 & 0.0183 & 0 \\ 0.001 & 0.9903 & 0.0389 & 0.1532 \\ 0.0047 & 0 & 0.8679 & 0.0846 \\ 0.0008 & 0 & 0.0749 & 0.7622 \end{bmatrix}$	$\begin{Bmatrix} p_1(D_1) \\ p_2(D_2) \\ p_3(D_3) \\ p_4(D_4) \end{Bmatrix} = \begin{Bmatrix} 0.608 \\ 0.352 \\ 0.029 \\ 0.011 \end{Bmatrix}$

Table 5.6 Effects of varying excitation bandwidth on response inter-domain transition probability in the subharmonic resonance region.

bandwidth parameter γ increases, ρ' decreases but λ' increase. Thus, according to the previous discussion in the primary resonance region (1), dependency of the stochastic behavior of the excitation parameters (amplitude and phase angle) on the excitation bandwidth is confirmed also in the subharmonic resonance region.

In the transition matrix K, as the excitation randomness (i.e., bandwidth parameter γ) increases, the decreasing values of diagonal elements indicate increasing probability of the response exit from the current attraction domain. The off-diagonal elements, except the zero entries and $p_{41}(4|1)$, are increasing in different rates (e.g., 121% in $p_{12}(1|2)$, 178% in $p_{13}(1|3)$) with increasing degree of excitation randomness. That is, the probability that an attraction domain becomes the destination domain of the transition from another domain is increasing as the degree of excitation randomness increases. The probability $p_{41}(4|1)$ increases from cases (vii) to (viii) but decreases from cases (viii) through (x). These various rates in the variations in $p_{ij}(i|j)$ (i,j = 1,2,3,4) reflect the complexity of the response inter-domain transition behavior in the subharmonic resonance region. However, even under such complex response interactive behavior among competitive attraction domains, the trends of variation in the probability $p_d(D_d)$ (d=1,2,3,4), that the system response is in an attraction domain, are still captured by the proposed method. In the last column of Table 5.6, the probability of the response being in the large amplitude harmonic domain, $p_1(D_1)$, increases with increasing excitation bandwidth. Whereas, the probability that the responses are in either the small amplitude harmonic, the 1/2 subharmonic or the 1/3 subharmonic domains (which in this case is equal to the disjoint sum of the probabilities $p_d(D_d)$, d=2,3,4) decreases as the excitation bandwidth increases. Recall from Section 5.1.3 that the response higher amplitude level consists of the large amplitude response, whereas, the lower amplitude level consists of the small amplitude response and the (1/2 and 1/3) subharmonic responses. Thus, the trends of variation in the $p_d(D_d)$ observed in Table 5.6 agree with the stochastic response behavior described in Section 5.1.3. Hence, the validity of the proposed method in analyzing the

response behavior under varying excitation bandwidth is also confirmed in the subharmonic resonance region.

(2) *Effects of Varying Excitation Randomness on Response Intra-Domain Transition*: To investigate the influence of varying excitation randomness on the response intra-domain transition behavior, the variances σ_d^2 (d=1,2,3,4) of the response amplitude probability distribution within attraction domains D_d^R (d=1,2,3,4) are calculated from $\tilde{p}(R|D_d^R)$ (d=1,2,3,4) (Eq.(4.31)). The results obtained for cases (vii) to (x) are tabulated in Table 5.7. In all the four co-existing attraction domains, D_d^R (d=1,2,3,4), the predicted variance σ_d^2 (d=1,2,3,4) increases with increasing excitation bandwidth, which is in accordance with the response behavior observed in Section 5.1.3. In addition, in each case, the variance σ_d^2 (d=1,2,3,4) varies with attraction domains, reflecting the domain dependency of the system

Variance σ_d^2 of Response Amplitude within Attraction Domain				
Cases	(vii)	(viii)	(ix)	(x)
γ	0.001	0.005	0.010	0.050
σ_1^2	0.0883	0.1623	0.2370	1.8192
σ_2^2	0.4738	0.5364	0.9796	2.1156
σ_3^2	0.4489	0.6716	0.8203	1.6155
σ_4^2	0.0397	0.1100	0.1885	0.8431

Table 5.7 Effects of varying excitation bandwidth on the variance of the response amplitude within the co-existing attraction domains D_d^R (d=1,2,3,4), respectively, in the subharmonic resonance region.

response characteristics. Thus, in the subharmonic resonance region, the proposed method in the analysis of stochastic response behavior under varying excitation bandwidth is also validated.

(3) *Effects of Varying Excitation Intensity on Response Inter-Domain Transition*: In the subharmonic resonance region, the effects of varying excitation intensity (i.e., variance σ_f^2) on the system response behavior are investigated in cases (ix) and (xi). For these two cases, the values of normalized parameters $\rho'=|\rho|/\sigma_f^2$ and $\lambda'=|\lambda|/\sigma_f^2$, the response probability inter-domain transition matrices K, and the normalized eigenvectors corresponding to the unit eigenvalues are listed in Table 5.8.

Case	σ_f^2	ρ'	λ'	Transition Matrix, K	Normalized Eigenvector
(ix)	157	0.992	0.00112	$\begin{bmatrix} 0.9949 & 0.0044 & 0.0063 & 0 \\ 0.0008 & 0.9956 & 0.0195 & 0.0949 \\ 0.0017 & 0 & 0.939 & 0.0216 \\ 0.0026 & 0 & 0.0352 & 0.8835 \end{bmatrix}$	$\begin{Bmatrix} p_1(D_1) \\ p_2(D_2) \\ p_3(D_3) \\ p_4(D_4) \end{Bmatrix} = \begin{Bmatrix} 0.462 \\ 0.504 \\ 0.018 \\ 0.016 \end{Bmatrix}$
(xi)	125	0.997	0.00113	$\begin{bmatrix} 0.9936 & 0.0021 & 0.0040 & 0 \\ 0.0010 & 0.9979 & 0.0138 & 0.0894 \\ 0.0015 & 0 & 0.946 & 0.0155 \\ 0.0039 & 0 & 0.0362 & 0.8951 \end{bmatrix}$	$\begin{Bmatrix} p_1(D_1) \\ p_2(D_2) \\ p_3(D_3) \\ p_4(D_4) \end{Bmatrix} = \begin{Bmatrix} 0.243 \\ 0.733 \\ 0.011 \\ 0.013 \end{Bmatrix}$

Table 5.8 Effects of varying excitation variance on response inter-domain transition probability in the subharmonic resonance region.

Again, trends of variation in the values of ρ' and λ' are similar to those in the primary resonance region. That is, little changes in the values of ρ' and λ' (less than 0.6%) are observed when the excitation variance σ_f^2 decreases (20%) from cases (ix) to (xi). According to the previous discussion in the primary resonance region (3), the randomness in the excitation is not affected by the variations in the excitation intensity but the behavior of the excitation amplitude still depends on the excitation variance.

In the transition matrices K, as the excitation variance decreases, the probability $p_{11}(1|1)$ decreases, whereas, $p_{ii}(i|i)$ (i = 2,3,4) increase. The complexity of the transition behavior is reflected by the variations in the other elements of K. For example, $p_{21}(2|1)$, $p_{41}(4|1)$, $p_{43}(4|3)$ and $p_{34}(3|4)$ increase with decreasing excitation variance, but $p_{31}(3|1)$, $p_{12}(1|2)$, $p_{13}(1|3)$, $p_{23}(2|3)$ and $p_{24}(2|4)$ decrease. Under such complex response inter-domain transitions, the trends of variation in the probabilities that the response is in the higher and lower amplitude levels, respectively, is still accurately predicted as shown in the last column of Table 5.8. That is, $p_1(D_1)$ decreases but $\sum p_i(D_i)$ (i=2,3,4) increases with decreasing excitation variance σ_f^2. This result agrees with the response characteristics observed in Section 5.1.4. Therefore, in this aspect, the proposed semi-analytical method is also validated in the subharmonic resonance region.

Response Amplitude Probability Distribution -- To demonstrate the prediction capability of the semi-analytical procedure, the response amplitude probability distributions predicted by the method (i.e., the results obtained by Eq.(4.32)) and simulation results are presented in Fig.5.15 for the five cases examined in the subharmonic resonance region. In each case, a total of 15 simulations are conducted. In each simulation, a duration equal to 15,000

(a) case (vii)

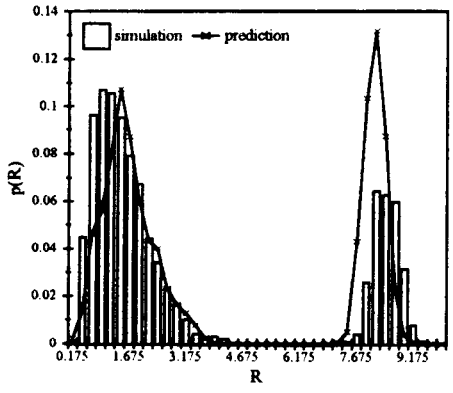

(b) case (viii)

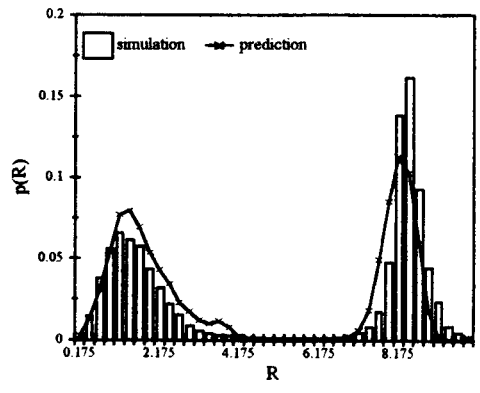

(c) case (ix)

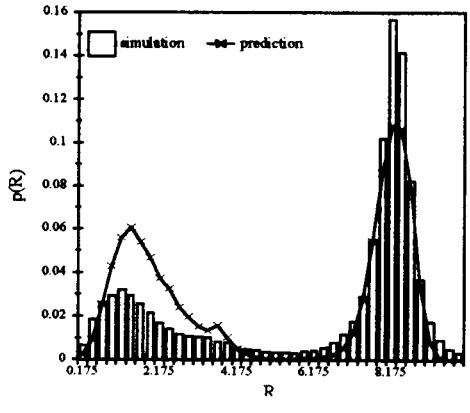

(d) case (x)

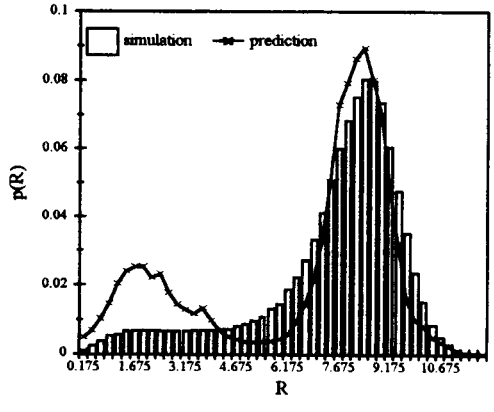

(e) case (xi)

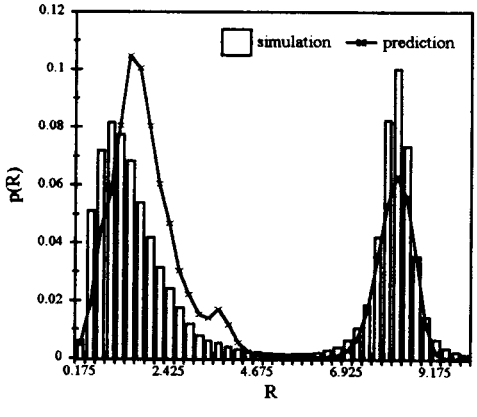

Figure 5.15 (a)-(e): Response amplitude probability distributions of case (vii)-(xi), respectively. {parameters used are listed in Table 5.5}.

excitation cycles is employed and thus, for each case, the response amplitude histogram is obtained from a total of 225,000 data cycles. Again, good agreements are observed in all five cases. Specifically, the locations of the modes in the probability distributions and the probability masses associated with each mode are predicted accurately.

(1) *Effects of Varying Excitation Randomness on Response Amplitude Probability Distribution*: As the degree of excitation randomness (i.e., bandwidth parameter γ) increases from cases (vii) to (x), Figs.5.16a shows that the response amplitude probability mass in the higher (lower) level increases (decreases) in accordance with the response behavior observed in Section 5.1.3. Note that, in case (x), although the simulation result appear to show only a single mode located in the higher amplitude level in the probability distribution, the long tail of the distribution in the lower amplitude level actually indicates the existence of a less obvious mode in that region. This trend of variations in the response amplitude probability distribution is predicted by the proposed method as shown in Fig.5.16b. The less consistent match in the results of case (x) in the lower amplitude level is probably due to insufficient samples in that region.

(2) *Effects of Varying Excitation Intensity on Response Amplitude Probability Distribution*: As the excitation variance decreases from cases (ix) to (xi), Figs.5.17a shows that the response amplitude probability mass in the higher (lower) level decreases (increases) in accordance with the response behavior observed in Section 5.1.4. By the proposed semi-analytical procedure, the same trend of variations in the response amplitude probability distribution due to changes in excitation variance is captured as shown in Fig.5.17b.

(a)

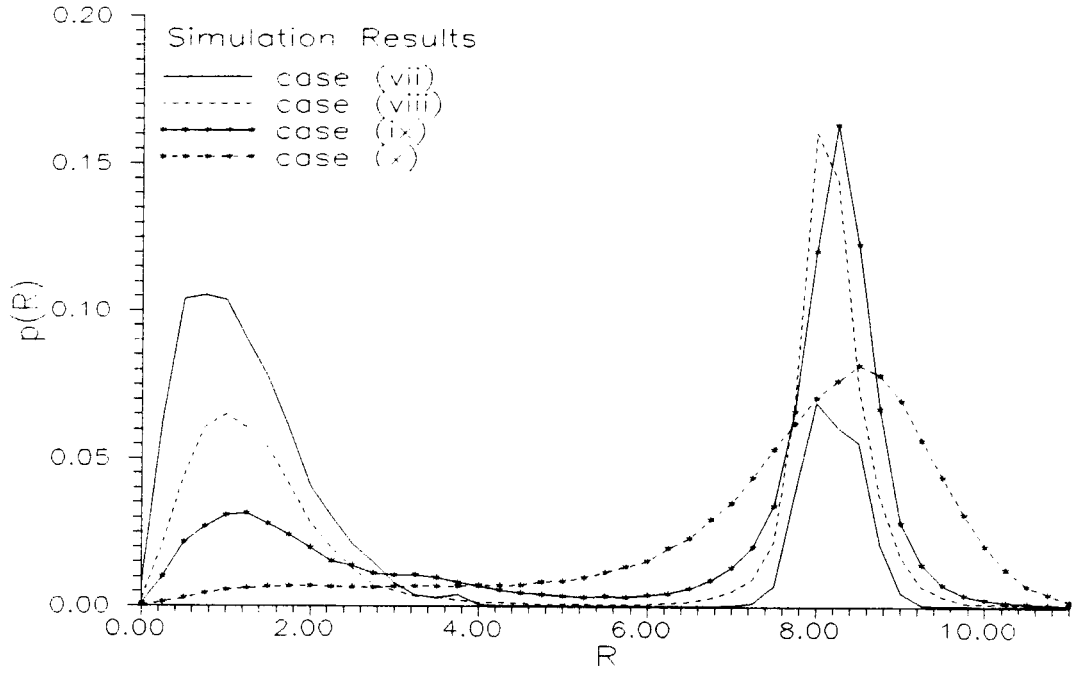

(b)

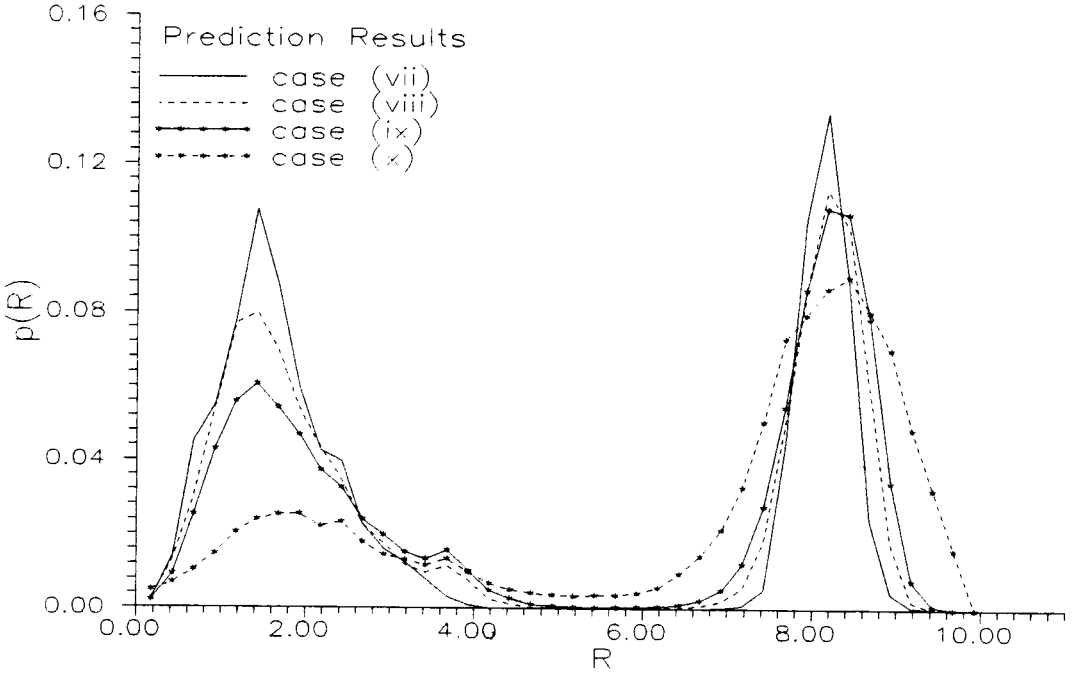

Figure 5.16 Variations in the response amplitude probability distribution under varying excitation bandwidth in the subharmonic resonance region. (a) simulation results, (b) prediction results.

(a)

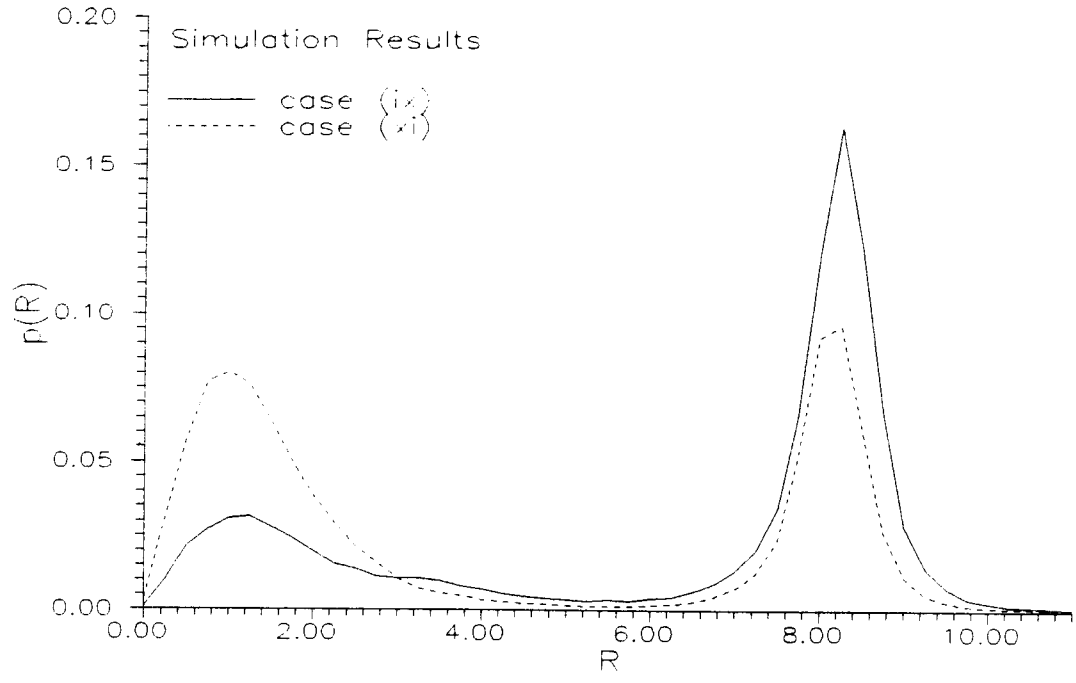

(b)

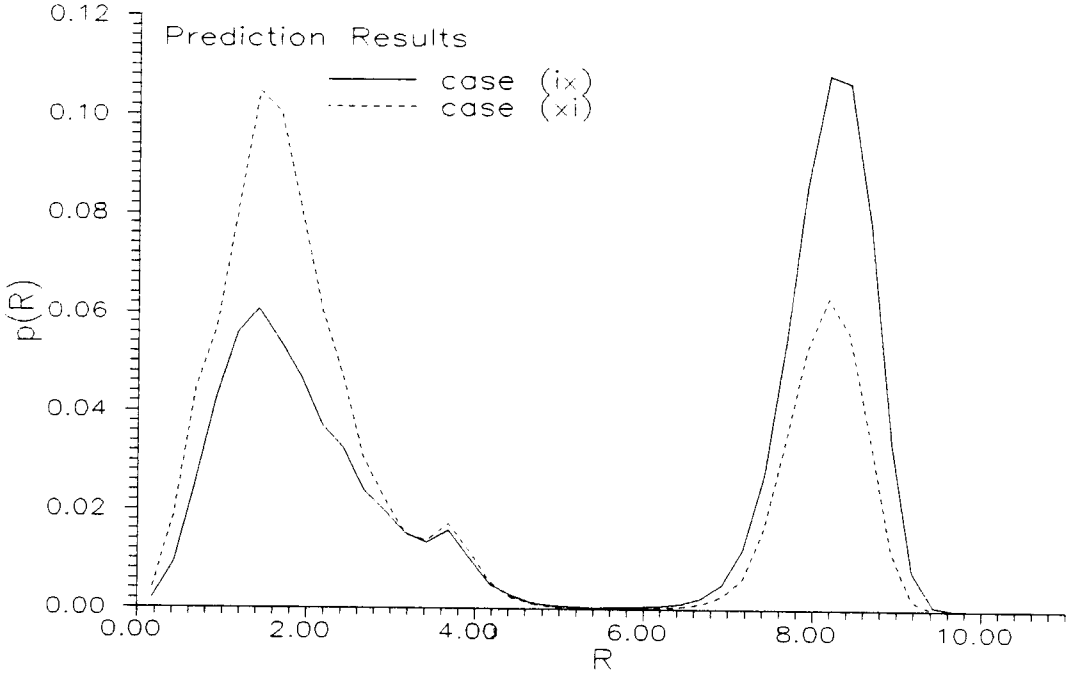

Figure 5.17 Variations in the response amplitude probability distribution under varying excitation variance in the subharmonic resonance region. (a) simulation results, (b) prediction results.

Therefore, from the results shown above and in Section 5.2.1, the validity of the proposed method is confirmed and the resulting semi-analytical procedure has demonstrated the capability of accurately characterizing the nonlinear system response behavior under narrowband excitations.

5.3 Comparisons with Existing Analytical Prediction Results

In this section, to demonstrate an improvement in the prediction accuracy, the response amplitude probability distributions predicted by the proposed semi-analytical method are compared with those obtained by two existing analytical methods and simulation histograms. The two analytical methods are stochastic averaging method (Davis and Liu, 1990) and quasi-harmonic method (Koliopulos and Bishop, 1993).

5.3.1 Existing Analytical Prediction of Response Amplitude Probability Distribution

For the Duffing type nonlinear system represented in Eq.(2.3) subject to a narrowband excitation modeled as in Eq.(2.7), the predictive results of the response amplitude probability distribution obtained by the stochastic averaging method and the quasi-harmonic method are respectively shown as following:

(1). stochastic averaging method: The suggested form of the response amplitude probability distribution can be expressed as (Davis and Liu, 1990; Koliopulos and Bishop, 1993):

$$p(y) = C \exp\left\{ \frac{-2\nu^2 \delta}{(\epsilon + \delta)\eta} y \left[(\epsilon + \delta)^2 + \frac{(\nu^2 - 1)^2}{4\nu^2} - \frac{3(\nu^2 - 1)y}{16\nu^2} + \frac{9y^2}{192\nu^2} \right] \right\} \qquad (5.1)$$

and,

$$y = \frac{a_3}{a_1} R^2, \quad \delta = \frac{s_C}{2\sqrt{a_1}}, \quad \eta = \frac{a_3 \sigma_f^2}{a_1^3}, \quad \epsilon = \frac{\gamma}{2\sqrt{a_1}}, \quad \nu = \frac{\omega_f}{\sqrt{a_1}} \tag{5.2}$$

where, R is the response amplitude; s_C, a_1, and a_3 are structural damping, linear stiffness and nonlinear stiffness coefficients, respectively; γ, ω_f, and σ_f^2 are excitation bandwidth parameter, central frequency and variance, respectively.

(2). quasi-harmonic method: A relationship between the randomly varying narrowband excitation amplitude A and its corresponding response amplitude R is obtained as (Koliopulos and Bishop, 1993):

$$y^3 + \frac{8}{3}(1-\nu^2)y^2 + \frac{16}{9}\left[(1-\nu^2)^2 + 4\delta^2\nu^2\right]y = \frac{32}{9}\theta, \qquad \theta = \frac{A^2 a_3}{2a_1^3} \tag{5.3}$$

where, scaled parameters y, δ and ν are defined in Eq.(5.2). The response amplitude probability distribution can be obtained by a probability transformation rule between the random variables θ and y through the functional relationship defined in Eq.(5.3) (Ochi, 1990). The probability density function of θ is obtained as (Koliopulos and Bishop, 1993):

$$p(\theta) = \frac{1}{\eta} e^{-\frac{\theta}{\eta}}, \qquad \eta = \frac{a_3 \sigma_f^2}{a_1^3} \tag{5.4}$$

Note that Eq.(5.3) is a third-degree polynomial equation. Thus, for a given θ, there may exist three real solutions. As discussed in Section 3.1.1, the real solutions with the smallest and the largest magnitudes correspond to the co-existing stable (physically observable) small and large amplitude steady-state responses. The real intermediate magnitude solution, associated with the unstable steady-state response, is physically unobservable. In this case, the probability mass associated with θ will be transferred and distributed to the smallest and the largest values of y, respectively, by a ratio κ determined by the following equation (Dimentberg, 1988; Koliopulos and Bishop, 1993):

$$\kappa = \frac{Ei\left(\frac{\theta_{max}}{\eta}\right) - Ei\left(\frac{\theta_{min}}{\eta}\right)}{\ln\left(\frac{\theta_{max}}{\theta_{min}}\right)} - 1, \qquad Ei(x) = \int_{-\infty}^{x} \frac{e^{v}}{v} dv \tag{5.5}$$

where θ_{max} and θ_{min} are the respective upper and lower bounds of θ which corresponds to multiple solutions of Eq.(5.1).

5.3.2 Comparisons of Analytical Predictions and Simulation Results

In this section, the prediction capabilities of the proposed semi-analytical method developed in Chapter 4 and the stochastic averaging method presented by Davies and Liu (1990) and the quasi-harmonic method presented by Koliopulos and Bishop (1993) are examined. In particular, the response amplitude probability distributions predicted by these methods for two specific excitation bandwidths selected by Koliopulos and Bishop (1993) are compared. In both cases, (a) and (b), the system and the excitation parameters are: $\{c_s =$

0.16, $a_1 = 1$, $a_3 = 0.3$, $\omega_f = 2$, $\sigma_f^2 = 3.05\}$, whereas, the excitation bandwidth parameter are $\gamma = 0.02$, and $\gamma = 0.08$, respectively. Note that corresponding to these system and excitation parameters, the scaled parameters employed in the stochastic averaging and the quasi-harmonic methods are $\{\nu = 2, \delta = 0.08, \varepsilon = \gamma/(2\sqrt{a_1}) = 0.01, \eta = 0.91\}$ and $\{\nu = 2, \delta = 0.08, \varepsilon = 0.04, \eta = 0.91\}$, respectively.

Prediction results of the semi-analytical, stochastic averaging and quasi-harmonic methods are shown in Fig.(5.18a) for case (a) and Fig.(5.18b) for case (b), respectively. Comparisons are also made with the response amplitude histograms obtained from simulations conducted through the procedure described in Section 5.2.1. It can be observed that, in both cases, probability distribution predictions obtained by the semi-analytical method show better agreements with the simulation histograms than those obtained by the stochastic averaging and quasi-harmonic methods. In addition, when the excitation bandwidth increases from case (a) to case (b), variations in the response amplitude histograms are accurately captured by the semi-analytical method. However, the trend of variation in the response amplitude probability distribution due to varying excitation bandwidth is not predicted by either the stochastic averaging method and the quasi-harmonic method. Therefore, by modeling the response inter-domain and intra-domain transitions, the proposed semi-analytical method demonstrates that better accuracy in the prediction of the response amplitude probability distribution is obtained.

(a)

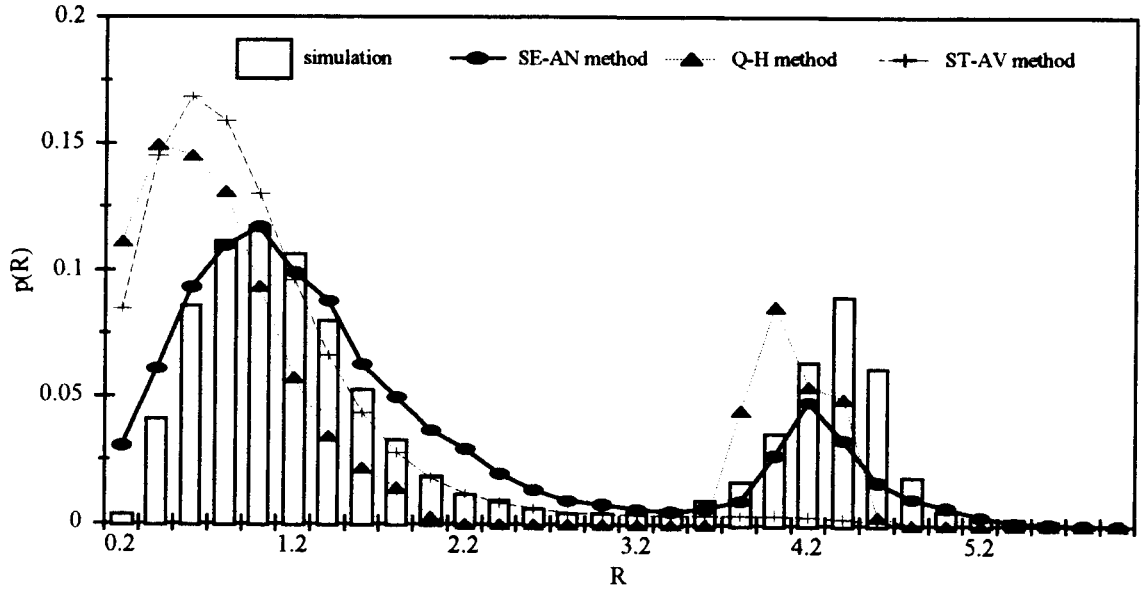

(b)

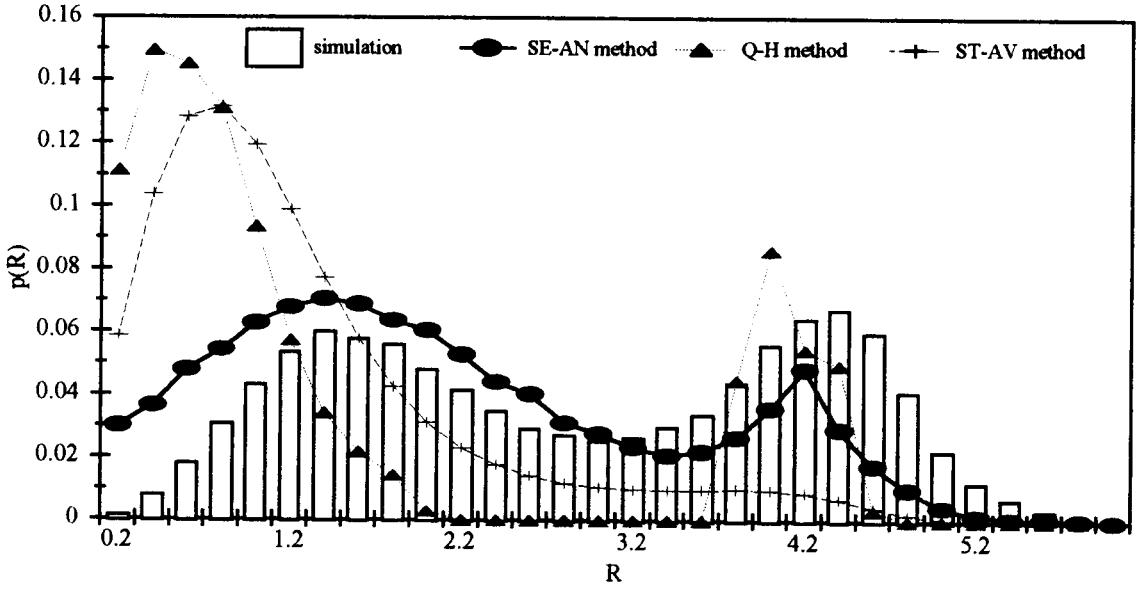

Figure 5.18 Response amplitude histogram and probability distributions predicted by the semi-analytical (SE-AN), quasi-harmonic (Q-H) and stochastic averaging (ST-AV) methods, respectively. $\{c_S = 0.16, a_1 = 1, a_3 = 0.3, \omega_f = 2, \sigma_f^2 = 3.05\}$. (a) $\gamma = 0.02$, and (b) $\gamma = 0.08$.

6. SUMMARY, CONCLUDING REMARKS AND FUTURE RESEARCH

6.1 Summary

Response behavior of a nonlinear system subject to narrowband excitations in the primary and subharmonic resonance regions is investigated in this study. The structural system is modeled as a single-degree-of-freedom Duffing type nonlinear oscillator. Typical deterministic response behavior including primary resonance, 1/2 and 1/3 subharmonic responses and the jump phenomena is demonstrated in detail in Chapter 2. In addition, the characteristics of narrowband processes are described.

To investigate the system behavior under successive variations in the excitation parameters, qualitative characterizations of the nonlinear system transient-state response behavior under deterministic excitation are performed through and interpreted from an energy evolution point of view in Chapter 3. Distinct response behavior patterns are observed depending on the response attraction domains which co-exist under certain excitation parameters (amplitude and phase angle). Response amplitude domains associated with some of the co-existing attraction domains are found to overlap. In addition, the response amplitude domains corresponding to different excitation amplitudes within an individual attraction domain also overlap. Due to the co-existence of distinct response attraction domains, complex response inter-domain transition behavior is induced when the excitation amplitude crosses domain boundaries defined in the amplitude response curves. To determine the destination domain of the inter-domain transition, the system transient-state mean energy is employed.

A semi-analytical procedure in analyzing the stochastic response behavior of the nonlinear system under narrowband excitations is proposed in Chapter 4. The methodology is developed based on the understanding of the nonlinear system response characteristics gained in Chapter 3 and the assumptions of the narrowband stochastic excitation described in Chapter 2. The system transient-state response characteristics under deterministic excitation (discussed in Chapter 3) are assumed to be preserved under narrowband random excitations. In addition, both the excitation amplitude and the response amplitude processes are approximated as stationary Markov processes. The response amplitude probability inter-domain transition is modeled as a stationary Markov chain. The developed formulation of the governing probability transition matrix is directly related to the excitation bandwidth and variance (energy level), as well as the amplitude jump phenomena of a nonlinear system. The probability of the system response being in an attraction domain can be obtained by solving the eigenvector of the probability transition matrix corresponding to the unit eigenvalue.

The governing equation for the response amplitude probability intra-domain transition between response amplitude domains corresponding to two excitation amplitudes is also formulated based on the Markovian approximation. The probability transition density function depends on the system transient-state response characteristics as well as the excitation bandwidth and variance. Numerical integration of the system response governing equation (Eq.(2.3)) is employed to obtain the transient-state response amplitude at this stage. This is because an explicit quantitative expression for the evaluation of the transient-state response amplitude is still lacking at present. Evaluation of the response amplitude intra-domain transition is then performed through statistical techniques. To facilitate numerical evaluation of the response amplitude intra-domain probability transition, the governing

equation is discretized. To obtain the stationary response amplitude probability distribution in each attraction domain, an iteration procedure is developed. It is demonstrated that a close approximation of the solution to the iterative procedure can be obtained by the one-step probability transition of the steady-state response process. That is, the steady-state solution is used as the initial estimation for the iteration process.

To gain an in-depth understanding of the stochastic response behavior under narrowband excitation and to verify the methodology proposed, numerical simulations are conducted in Chapter 5. Under narrowband random excitation, the response behavior including the response amplitude jump phenomena and the dependence of the response characteristics on attraction domains is observed to follow closely those under deterministic excitation. Repeated occurrence of the (1/2 and 1/3) subharmonic responses is observed in long duration simulations. In addition, influences of varying excitation bandwidth and variance on the response behavior are examined. Good agreements in both qualitative and quantitative aspects between the prediction and simulation results demonstrate the capability and validity of the method proposed. Moreover, comparisons of the accuracy of prediction results by the proposed semi-analytical method and two existing analytical (stochastic averaging and quasi-harmonic) method are conducted against simulation histograms. The results obtained by the semi-analytical method show better agreements than those predicted by the other methods.

6.2 Concluding Remarks

The main goal of this study is to develop a method to predict the response behavior of a nonlinear system subject to narrowband excitations in both the primary and the

subharmonic resonance regions. Based on the results of this study, the following are concluded:

1. Nonlinear system response characteristics under deterministic excitations are generally preserved under narrowband excitation environment. However, due to the random nature of the narrowband process, excitation parameters (amplitude and phase angle) vary slowly. These slow variations can be approximated by a succession of finite discrete changes in the system excitation parameters. Thus, transient-state response characteristics are employed to interpret the system response behavior under narrowband excitations.

2. The probability of the system response being in different attraction domains is related to the response inter-domain transition (or amplitude jump) phenomena. This probability transition behavior can be characterized by the excitation amplitude domain boundaries as well as the excitation bandwidth and variance. Note that the locations of the domain boundaries are determined by the excitation frequency which is assumed to be equal to the central frequency of the narrowband process and is a constant, in this study. Thus, the locations of the domain boundaries are time invariant. However, when the excitation bandwidth increases, variations in the excitation frequency may shift the domain boundaries significantly thus affecting the response inter-domain transition behavior.

3. The system response characteristics, and thus, the response amplitude probability intra-domain transition depends on the response attraction domains considered. In addition, the intra-domain probability transition also depends on the excitation amplitude and the excitation bandwidth.

4. Subharmonic (1/2 and 1/3) responses can occur repeatedly in the response process. Long duration simulations show that, when the system response exits from the large

amplitude harmonic domain, the randomly varying excitation amplitude may lead the system to the 1/2 or 1/3 subharmonic domains. In addition, an exit of the system response from a subharmonic domain may also lead the system to the small amplitude harmonic domain or another subharmonic domain.

5. The proposed semi-analytical method is capable of accurately characterizing the stochastic response behavior of the nonlinear system subject to narrowband excitations by predicting the response amplitude probability distribution and capturing the trends of variations in the response amplitude statistical properties. In both the primary and the subharmonic resonance regions, good agreements between the response amplitude probability distributions predicted by the semi-analytical method and obtained from simulation results are observed both qualitatively and quantitatively. In addition, trends of the variations in the probability masses associated with the modes with variations in excitation parameters (bandwidth, variance) are captured.

6. The analysis of the response behavior under narrowband excitations has been successfully extended to the subharmonic resonance region. In previous studies, analytical methods can only predict the response behavior in the primary resonance region where only two attraction domains co-exist. In this study, the developed method has demonstrated its capability of accurately predicting more complex response behavior in the subharmonic resonance region where four attraction domains co-exist.

7. A significant improvement in the accuracy of predicting response amplitude probability distributions is achieved by the proposed semi-analytical method. This is because the stochastic nonlinear response behavior under narrowband excitation is accurately

characterized by the semi-analytical method through modeling the response inter-domain and intra-domain transitions.

6.3 Recommended Future Research

The methodology proposed in this study has successful demonstrated the feasibility of characterizing the stochastic response behavior of a nonlinear system under narrowband excitations. More general, time efficient and accurate methods along the same line may be developed in the future. Following are suggestions for potential extensions of this study:

(1) Analytical and Quantitative System Response Characteristics Description -- Up to now, the transient-state response behavior can only be characterized qualitatively, in general. Numerical integrations of the system equation of motion (Eq.(2.3)) need to be employed to determine the transient-state response amplitudes and thus, the response amplitude intra-domain probability transition in this study. This procedure of numerical evaluations can be quite time consuming. For example, by using a Pentium 166 PC (personal computer), run time of the FORTRAN program to obtain the approximation of $\hat{p}(R^{(1)}|D_d^R)$ by Eq.(4.31) with $m_a = 15$ for all the co-existing attraction domains, D_d^R, may take up to 48 hours to complete a single case. Thus, an analytical expression of function g in Eq.(4.22) (or $\bar{g}$ in Section 4.4.2) will significantly improve the efficiency of the semi-analytical procedure in analyzing the stochastic response behavior.

(2) Inclusion of Influence of Excitation Frequency Variations -- Finite variations in the excitation frequency may induce significant shifts of the excitation amplitude domain boundaries, which in turn affects the response inter-domain transition behavior. The

excitation amplitude domain boundaries defined in this study correspond to the constant excitation peak frequency. Thus, the excitation amplitude domain boundaries are also constant. However, the oscillating excitation frequency is actually varying from cycle to cycle and its variation is governed by the excitation phase process. When the excitation bandwidth is small, the variations in the excitation frequency may be negligible and the excitation amplitude boundaries may be reasonably considered as constant. However, when the excitation bandwidth increases, the variations in the excitation frequency may be significant enough to shift the excitation amplitude domain boundaries obviously and affect the response inter-domain transition behavior. Therefore, to improve the accuracy of the method, the behavior of the excitation amplitude domain boundary shifts due to variations in the excitation frequency should be investigated. In addition, the influence of domain boundary shifts on the response inter-domain transition behavior should be incorporated in the semi-analytical procedure.

(3). Extension to Superharmonic Resonance Region -- In this study, the analysis of the stochastic response behavior under narrowband excitations has been successfully extended from the primary resonance region to the subharmonic resonance region. However, for the analysis of the stochastic response behavior in general cases, the developed method should be extended to the superharmonic resonance region. To achieve this extension, the deterministic system response characteristics in the superharmonic resonance region should be studied in depth.

BIBLIOGRAPHY

Berger, M.S. (1990). Mathematical Structures of Nonlinear Science. Kluwer Academic Publishers, Boston.

Burton, T.D. and Rahman, Z. (1986). On the multi-Scale Analysis of Strongly Nonlinear Forced Oscillators. International Journal of Nonlinear Mech., 21, 135-146.

Bouleau, N. and Lépingle, D. (1994). Numerical Methods for Stochastic Processes. John Wiley and Sons, Inc..

Choi, H.S. and Lou, J.Y.K. (1991). Nonlinear Behavior of an Articulated Lading Platform. App. Ocean res., 13, 63

Clough, R.W. and Penzien, J. (1993). Dynamics of Structures, 2nd Edition. McGraw-Hill, Inc..

Crandall, S.H. and Mark, W.D. (1963). Random Vibration in Mechanical Systems. Academic Press, New York.

Davies, H.G. and Nandlall, D. (1986). Phase Plane for Narrow-Band Random Excitation of a Duffing Oscillartor. Journal of Sound and Vibration, 104, 277-283.

Davies, H.G. and Liu, Q. (1990). The Response Envelope Probability Density Function of a Duffing Oscillator with Random Narrow-Band Excitation. Journal of Sound and Vibration, 139, 1-8.

Davies, H.G. and Rajan, S. (1988). Random Superharmonic and Subharmonic Response: Multiple Time Scaling of a Duffing Oscillator. Journal of Sound and Vibration, 126, 195-208.

Dean, R.G. and Dalrymple, R.A. (1984). Water Wave Mechanics for Engineers and Scientists. Prentice-Hall, NJ.

Dimentberg, M.F. (1971). Oscillations of a System with Nonlinear Cubic Characteristics under Narrow Band Random Excitation. Mechanics and Solids, 6, 142-146.

Dimentberg, M.F. (1988). Statistical Dynamics of Nonlinear and Time-Varying Systems. John Wiley & Sons Inc.

Drazin, P.G. (1992). Nonlinear Systems. Cambridge University Press.

Francescutto, A. (1991). On the Probability of Large Amplitude Rolling and Capsizing as a Consequence of Bifurcations. OMAE 1991, Vol. II, 91-96.

Francescutto, A. (1993). Nonlinear Ship Rolling in the Presence of Narrow Band Excitation. OMAE 1993, Vol. 1, 93-102.

Gillespie, D.T. (1992). Markov Processes. Academic Press, Inc., San Diego.

Gottlieb, O. and Yim, S. (1992). Nonlinear Oscillations, Bifurcations and Chaos in a Multi-Point Mooring System with a Geometric Nonlinearity. Applied Ocean Research, Elsevier Scinece Publishers Ltd. (241-257).

Guckenheimer, J. and Holmes, P. (1986). Nonlinear Oscillations, Dynamical Systems and Bifurcation of Vector Fields. Springer-Verlag, New York.

Hagedorn, P. (1988). Nonlinear Oscillations. Oxford, New York.

Hsieh, S., Shaw, S.W. and Troesch, A.W. (1993). A Predictive Method for vessel capsize in Random Sea. Nolinear Dynarmics of Marine Vehicles, OMAE Vol. 1, 103-123.

Hughes, S.A. (1984). The TMA Shallow-Water Spectrum Description and Applications. U.S. Army Engineer Waterways Experiment Station, Vicksburg, MS.

Humar, J.L. (1990). Dynamics of Structures. Prentice Hall, Englewood Cliffs, NJ.

Isaacson, M. and Phadke, A. (1994). Chaotic Motion of a Nonlinear Moored Structure. Fourth Intenrnational Offshore and Polar Engineering Conference, Osaka, Japan, 3, 338-345.

Jordan, D.W. and Smith, P. (1987). Nonlinear Ordinary Differential Equations, Second Edition. Clarendon Press, Oxford.

Koliopulos, P.K. and Bishop, S.R. (1993). Quasi-Harmonic Analysis of the Behavior of a Hardening Duffing Oscillator Subjected to Filtered White Noise. Nonlinear Dynamics, 4, 279-288.

Koliopulos, P.K.,Bishop, S.R., Stefanou, G.D. (1991). Response Statistics of Nonlinear System underVariations of Excitation Bandwidth. Computational Stochastic Mechanics, Elsevier Applied Science, London, 335-348.

Koliopulos, P.K. and Langley, R.S. (1993). Improved Stability Analysis of The Response of a Duffing Oscillator under Filtered White Noise. International Journal of Non-Linear Mechanics, 28, 145-155.

Langley, R.S. (1986). On Various Definitions of the Envelope of a Random Process. Journal of Sound and Vibration, 105, 503-512.

Lin, H. and Yim, S.C.S. (1995). Noisy Nonlinear Motions of Moored Systems. Part I: Analysis and Simulation. Journal of Waterways, Port, Coastal, and Ocean Engineering, 123 (5), 287-295.

Lin, Y.K. (1967). Probabilistic Theory of Structural Dynamics. McGraw-Hill, New York.

Lutes, L.D. and Sarkani, S. (1997). Stochastic Analysis of Structural and Mechanical Vibrations. Prentice Hall.

Lyon, R.H., Heckl, M. and Hazelgrove, C.B. (1961). Response of Hard-Spring Oscillator to Narrow-Band Excitation. Journal of the Acoustical Society of America, 33, 1401-1411.

Nayfeh, A.H. and Mook, D.T. (1979). Nonlinear Oscillations. Wiley, New York.

Newland, D.E. (1993). An Introduction to Random Vibrations, Spectral & Wavelet Analysis. (3rd Ed.) Longman, New York.

Nigam, N.C. (1983). Introduction to Random Vibrations. The MIT Press, London.

Ochi, M. K. (1990). Applied Probability and Stochastic Processes in Engineering and Physical Sciences. John Wiley and Sons, New York.

Roberts, J. B. and Spanos, P.D. (1986). Stochastic Averaging: An Approximate Method of Solving Random Vibration Problems. International Journal of Non-Linear Mechanics, 21, 111-134.

Roberts, J.B. and Spanos, P.D. (1990). Random Vibration and Statistical Linearization. John Wiley and Sons, New York.

Rice, S.O. (1954). Selected Papers on Noise and Stochastic Processes, Mathematical Analysis of Random Noise. Dover, New York.

Richard, K. and Anand, G.V. (1983). Nonlinear Resonance in Strings under Narrow-Band Random Excitation, Part I: Planar Response and Stability. Journal of Sound and Vibration, 86, 85-98.

Rajan, S. and Davies, H.G. (1988). Multiple Time Scaling of the Response of a Duffing Oscillator to Narrow-Band Random Excitation. Journal of Sound and Vibration, 123, 497-506.

Shinozuka, M. and Deodatis, G. (1991). Simulation of Stochastic Processes by Spectral Representation. Appl Mech Rev, Vol 44, no 4, 191-203.

Shinozuka, M. (1971). Simulation of Multivariate and Multidimensional Random Processes. Journal of the Acoustical Society of America, 49, 357-367.

Soong, T.T. and Grigoriu M. (1993). Random Vibration of Mechanical and Structural Systems. Prentice Hall.

Stratonovich, R.L. (1963). Topics in the Theory of Random Noise. Gordon and Breach, New York.

Thompson, J.M.T., Bokaian, A.R. and Ghaffari, R. (1984). Subharmonic and Chaotic Motions of Compliant Offshore Structures and Articulated Mooring Towers. Journal of Energy Resources Tech., 106, 191-198.

Thompson, J.M.T., and Stewart, H.B. (1986). Nonlinear Dynamics and Chaos. Joh Wiley and Sons, New York.

Virgin, L.N. and Bishop, S.R. (1988). Complex Dynamics and Chaotic Responses in the Time Domain Simulations of a Floating Structure. Ocean Engineering, 15, 71-90.

Wiggins, S. (1990). Introduction to Applied Nonlinear Dynamical Systems and Chaos. Springer-Verlag, New York.

Yim, S., Myrum, M.A., Gottlieb, O., Lin, H. And Shih, I. (1993). Summary and Preliminary Analysis of Nonlinear Oscillations in a Submerged Mooring System Experiment. ONR Report No. OE-93-03.

Yim, S. and Lin, H. (1992). Probabilistic Analysis of a Chaotic Dynamical System. Applied Chaos, 219-241. John Wiley and Sons, New York.

APPENDICES

APPENDIX A
FLOWCHART OF THE SEMI-ANALYTICAL PROCEDURE

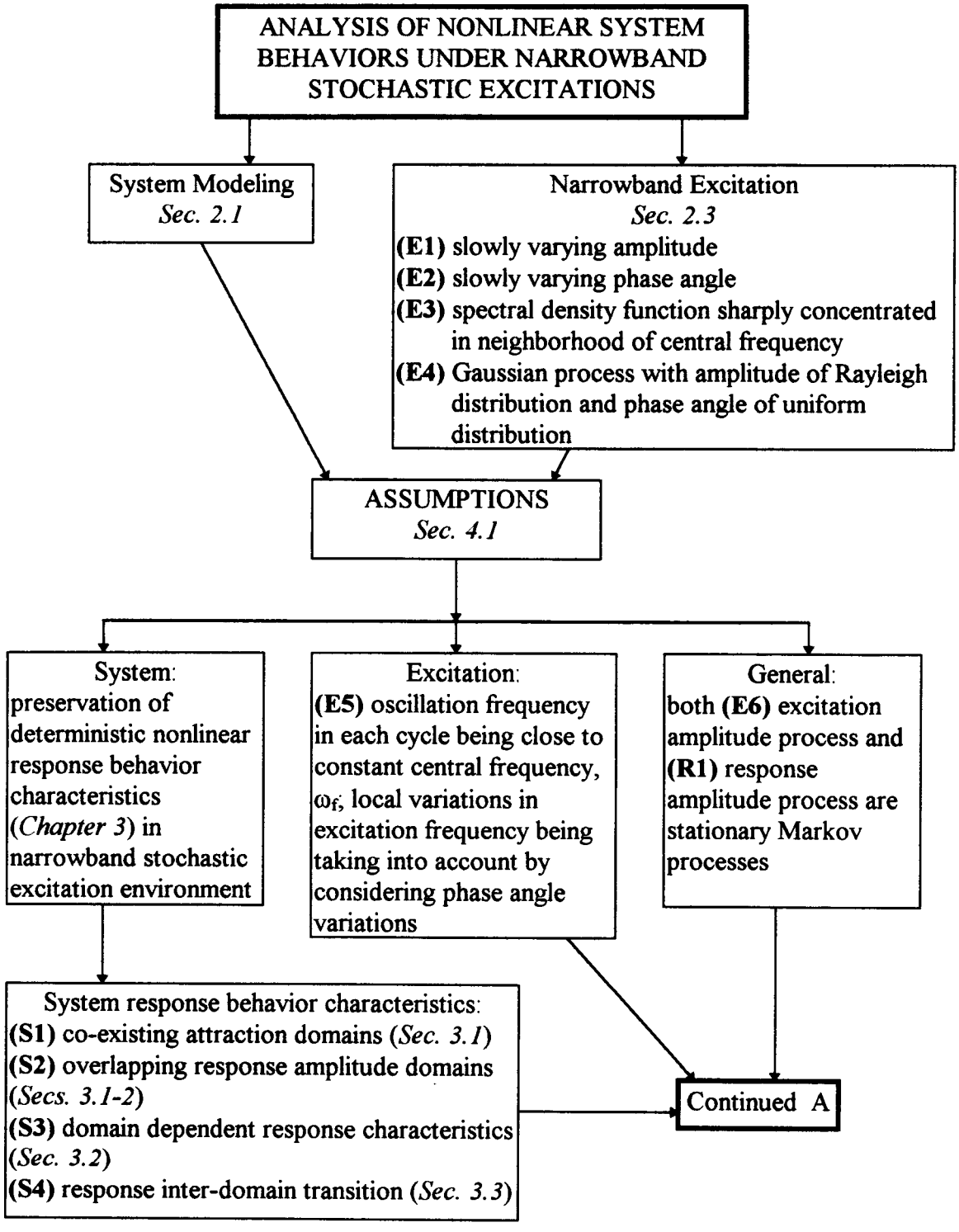

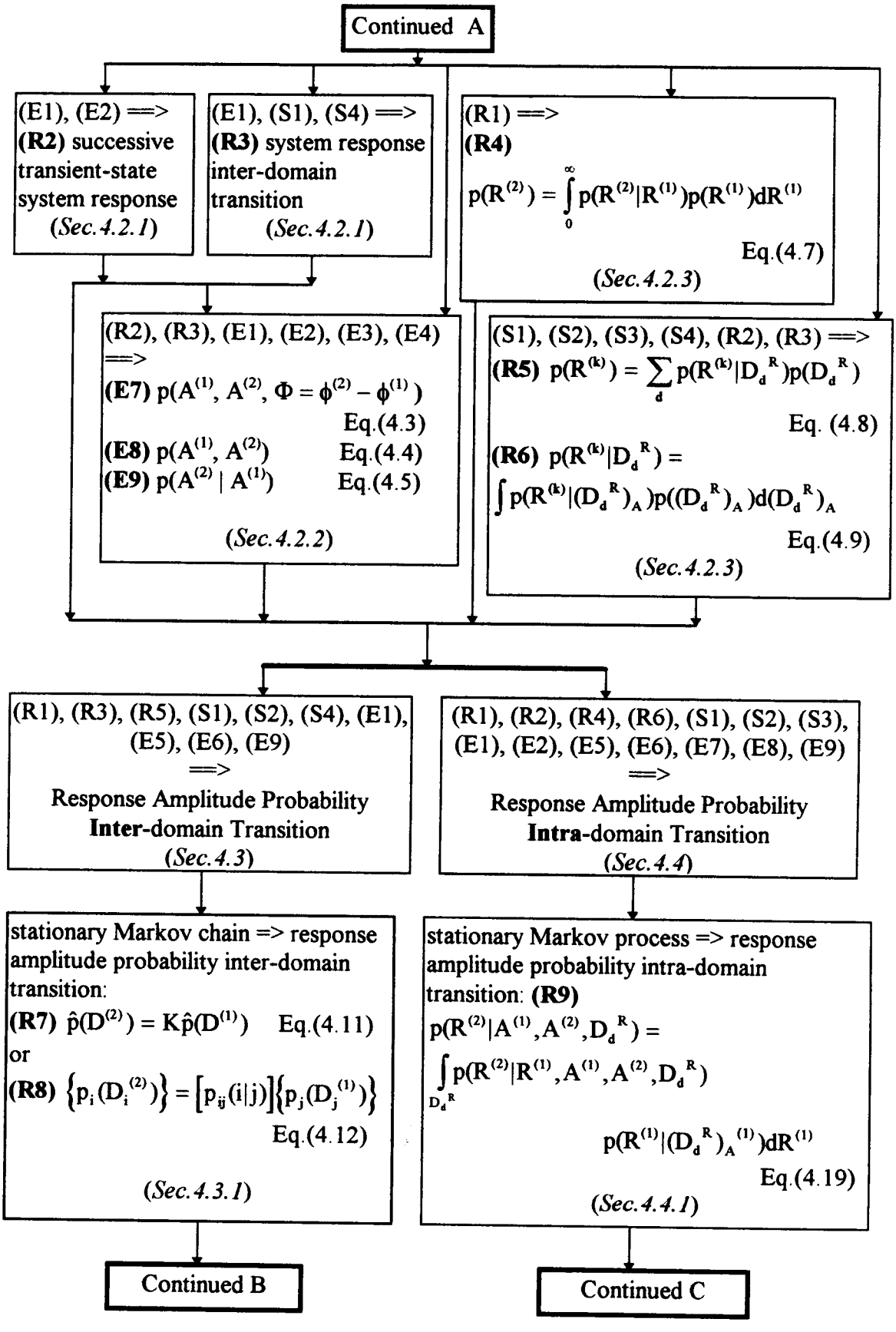
Continued A
(E1), (E2) ==> **(R2)** successive transient-state system response (*Sec.4.2.1*)
(E1), (S1), (S4) ==> **(R3)** system response inter-domain transition (*Sec.4.2.1*)
(R1) ==> **(R4)** $p(R^{(2)}) = \int_0^\infty p(R^{(2)}|R^{(1)})p(R^{(1)})dR^{(1)}$ Eq.(4.7) (*Sec.4.2.3*)
(R2), (R3), (E1), (E2), (E3), (E4) ==> **(E7)** $p(A^{(1)}, A^{(2)}, \Phi = \phi^{(2)} - \phi^{(1)})$ Eq.(4.3) **(E8)** $p(A^{(1)}, A^{(2)})$ Eq.(4.4) **(E9)** $p(A^{(2)} \mid A^{(1)})$ Eq.(4.5) (*Sec.4.2.2*)
(S1), (S2), (S3), (S4), (R2), (R3) ==> **(R5)** $p(R^{(k)}) = \sum_d p(R^{(k)}|D_d{}^R)p(D_d{}^R)$ Eq. (4.8) **(R6)** $p(R^{(k)}|D_d{}^R) = \int p(R^{(k)}|(D_d{}^R)_A)p((D_d{}^R)_A)d(D_d{}^R)_A$ Eq.(4.9) (*Sec.4.2.3*)
(R1), (R3), (R5), (S1), (S2), (S4), (E1), (E5), (E6), (E9) ==> Response Amplitude Probability **Inter**-domain Transition (*Sec.4.3*)
(R1), (R2), (R4), (R6), (S1), (S2), (S3), (E1), (E2), (E5), (E6), (E7), (E8), (E9) ==> Response Amplitude Probability **Intra**-domain Transition (*Sec.4.4*)
stationary Markov chain => response amplitude probability inter-domain transition: **(R7)** $\hat{p}(D^{(2)}) = K\hat{p}(D^{(1)})$ Eq.(4.11) or **(R8)** $\{p_i(D_i^{(2)})\} = [p_{ij}(i|j)]\{p_j(D_j^{(1)})\}$ Eq.(4.12) (*Sec.4.3.1*)
stationary Markov process => response amplitude probability intra-domain transition: **(R9)** $p(R^{(2)}|A^{(1)},A^{(2)},D_d{}^R) = \int_{D_d{}^R} p(R^{(2)}|R^{(1)},A^{(1)},A^{(2)},D_d{}^R)\, p(R^{(1)}|(D_d{}^R)_A{}^{(1)})dR^{(1)}$ Eq.(4.19) (*Sec.4.4.1*)
Continued B
Continued C

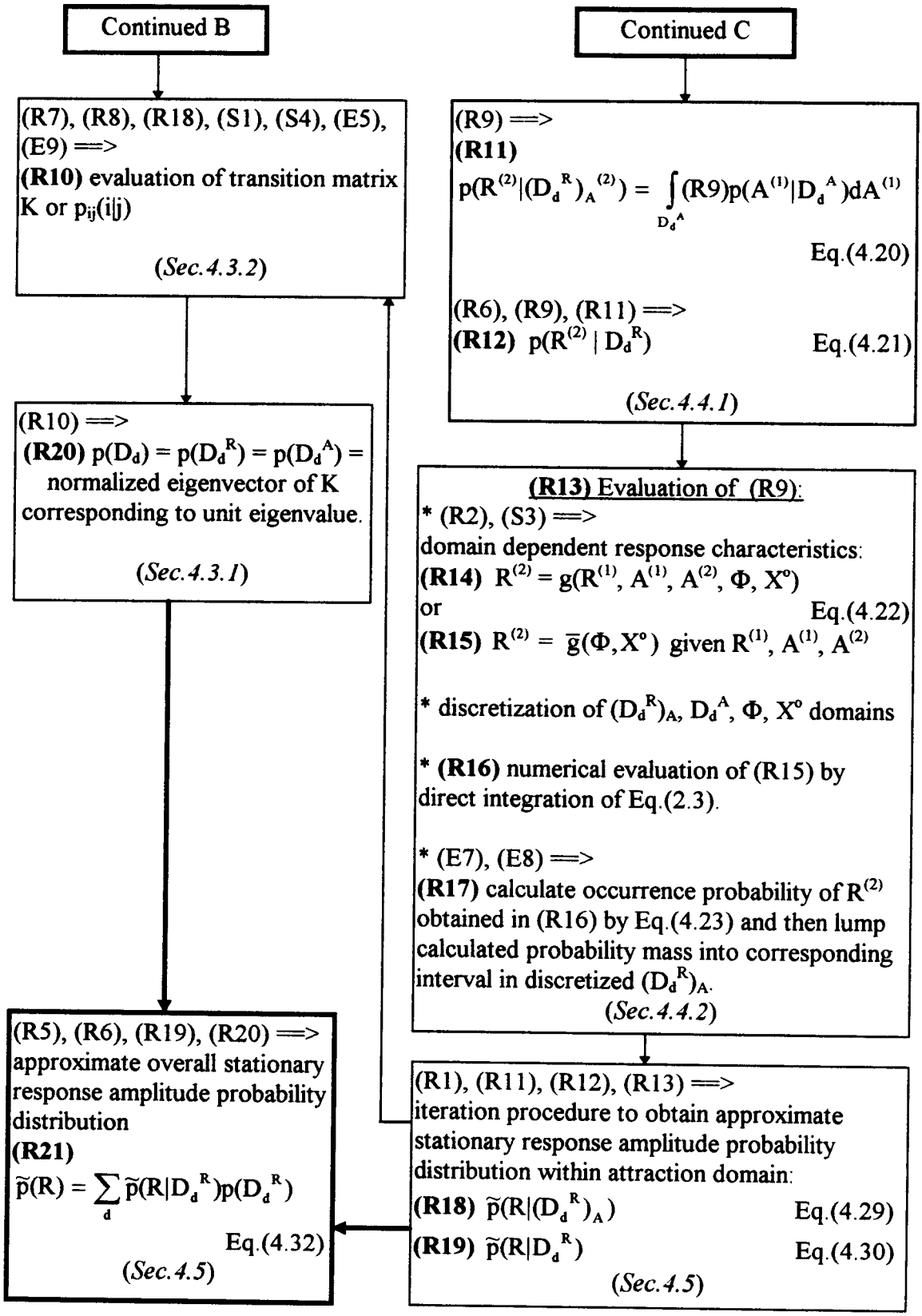
Continued B
Continued C
(R7), (R8), (R18), (S1), (S4), (E5), (E9) ==>
(R10) evaluation of transition matrix K or $p_{ij}(i|j)$
(Sec.4.3.2)
(R9) ==>
(R11)
$p(R^{(2)}|(D_d^R)_A^{(2)}) = \int_{D_d^A} (R9)p(A^{(1)}|D_d^A)dA^{(1)}$
Eq.(4.20)
(R6), (R9), (R11) ==>
(R12) $p(R^{(2)} | D_d^R)$ Eq.(4.21)
(Sec.4.4.1)
(R10) ==>
(R20) $p(D_d) = p(D_d^R) = p(D_d^A)$ = normalized eigenvector of K corresponding to unit eigenvalue.
(Sec.4.3.1)
(R13) Evaluation of (R9):
* (R2), (S3) ==>
domain dependent response characteristics:
(R14) $R^{(2)} = g(R^{(1)}, A^{(1)}, A^{(2)}, \Phi, X^o)$
or Eq.(4.22)
(R15) $R^{(2)} = \bar{g}(\Phi, X^o)$ given $R^{(1)}, A^{(1)}, A^{(2)}$
* discretization of $(D_d^R)_A$, D_d^A, Φ, X^o domains
* (R16) numerical evaluation of (R15) by direct integration of Eq.(2.3).
* (E7), (E8) ==>
(R17) calculate occurrence probability of $R^{(2)}$ obtained in (R16) by Eq.(4.23) and then lump calculated probability mass into corresponding interval in discretized $(D_d^R)_A$.
(Sec.4.4.2)
(R5), (R6), (R19), (R20) ==>
approximate overall stationary response amplitude probability distribution
(R21)
$\tilde{p}(R) = \sum_d \tilde{p}(R|D_d^R)p(D_d^R)$
Eq.(4.32)
(Sec.4.5)
(R1), (R11), (R12), (R13) ==>
iteration procedure to obtain approximate stationary response amplitude probability distribution within attraction domain:
(R18) $\tilde{p}(R|(D_d^R)_A)$ Eq.(4.29)
(R19) $\tilde{p}(R|D_d^R)$ Eq.(4.30)
(Sec.4.5)

APPENDIX B
ENVELOPE AND PHASE PROCESSES OF A NARROWBAND PROCESS

The classical definition of the envelope of narrowband processes was presented by Rice (1954) and applied to derive the statistical properties of ocean wave. The Rice definition of an envelope process is based on the Fourier series expansion of a stationary Gaussian zero-mean narrowband random process about some fixed carrier frequency ω_r chosen near the peak frequency ω_f. Then, f(t) can be expressed as (Langley, 1986)

$$f(t) = f_c(t)\cos(\omega_r t) - f_s(t)\sin(\omega_r t) \tag{B.1}$$

$$f_c(t) = \sum_n \left\{a_n \cos\left[(\omega_n - \omega_r)t\right] + b_n \sin\left[(\omega_n - \omega_r)t\right]\right\} \tag{B.2}$$

$$f_s(t) = \sum_n \left\{a_n \sin\left[(\omega_n - \omega_r)t\right] - b_n \cos\left[(\omega_n - \omega_r)t\right]\right\} \tag{B.3}$$

where, a_n and b_n are the Fourier coefficients and ω_n is the corresponding frequency. Eq.(B.1) can be rewritten as

$$f(t) = A(t)\cos\left[\omega_r t + \phi(t)\right] \tag{B.4}$$

with

$$A(t) = \sqrt{f_c^2(t) + f_s^2(t)}, \qquad \phi(t) = \tan^{-1}\left(\frac{f_s(t)}{f_c(t)}\right) \tag{B.5, B.6}$$

such that f(t) is represented by a cosine function with time dependent amplitude and phase.

The rate of change of the phase angle will afftect the absolute frequency, hence the result frequency is also time dependent. The functions A(t) and $\phi(t)$ defined in Eqs.(B.5-6) are Rice's definitions of envelope and phase processes. Note that the narrowband process, f(t),defined in Eq.(B.4) is oscillating at the frequency ω_r, instead of ω_f, with slowly varying amplitude and phase. The yet unknown frequency ω_r has been shown by Langley (1986) to be equal to the mean frequency, $\omega_1 = m_1/m_0$, of f(t), where

$$m_n = \int_0^\infty \omega^n S_{ff}(\omega)\, d\omega \tag{B.7}$$

and $S_{ff}(\omega)$ is the one-sided spectral density function of f(t). However, numerical evaluation of ω_1 shows that $\omega_1 \approx \omega_f$ for a general narrowband process.

Alternate definitions of the envelope and phase processes were derived based on the Hilber transform of f(t) (Dugundji, 1958; Stratonovich, 1963). The narrowband process, f(t), is represented by a carrier frequency ω_f and two slowly varying processes, $f_c(t)$ and $f_s(t)$, which can be obtained as (Stratonovich, 1963)

$$f_c(t) = f(t)\cos(\omega_f t) + \bar{f}(t)\sin(\omega_f t) \tag{B.8}$$

$$f_s(t) = -f(t)\sin(\omega_f t) + \bar{f}(t)\cos(\omega_f t) \tag{B.9}$$

where, $\bar{f}(t)$ is the Hilber transform of f(t). Thus, the Stratonovich's definitions of the envelope and the phase processes can be expressed as Eqs.(B.5-6) with $f_c(t)$ and $f_s(t)$ defined as Eqs.(B.8-9). Note that Langley (1986) has shown that the two definitions based on the Fourier expansion and the Hilber transform are equivalent.

By assuming f(t) to be a zero-mean Gaussian random process with variance σ_f^2, the $f_c(t)$ and $f_s(t)$ are found to be statistically independent zero-mean Gaussian processes with variance σ_f^2 (Langley, 1986; Ochi, 1990). The joint probability density function of $f_c(t)$ and $f_s(t)$ thus reads

$$p(f_c, f_s) = \frac{1}{2\pi\sigma_f^2} \exp\left[-\frac{f_c^2 + f_s^2}{2\sigma_f^2}\right], \qquad -\infty < f_c, f_s < \infty \tag{B.10}$$

When $f_c(t)$ and $f_s(t)$ are transformed to A(t) and $\phi(t)$ by Eqs.(B.5-6), the joint probability density function of A(t) and $\phi(t)$ can be obtained from Eq.(B.10) and expressed as (Ochi, 1990)

$$p(A, \phi) = \frac{A}{2\pi\sigma_f^2} \exp\left[-\frac{A^2}{2\sigma_f^2}\right], \qquad 0 \le A < \infty, \quad 0 \le \phi \le 2\pi \tag{B.11}$$

APPENDIX C
APPROXIMATE SOLUTION OF A DUFFING SYSTEM

C.1 Harmonic Solution

By the harmonic balance method, the first order approximate solution of the harmonic response is expressed as

$$x(t) = R_c(t)\cos(\omega t) + R_s(t)\sin(\omega t) \tag{C.1}$$

where $R_c(t)$ and $R_s(t)$ are the amplitudes of the cosine and sine components of the response process x(t), respectively, and are time dependent in general. Substitution of Eq.(C.1) and Eq.(2.2) into Eq.(2.1) yields

$$\left\{\left[a_1 - \omega^2 + \frac{3}{4}a_3(R_c^2 + R_s^2)\right]R_c + C_S\omega R_s - A\cos(\phi) + C_S\dot{R}_c + 2\omega\dot{R}_s\right\}\cos(\omega t)$$

$$+\left\{\left[a_1 - \omega^2 + \frac{3}{4}a_3(R_c^2 + R_s^2)\right]R_s - C_S\omega R_c + A\sin(\phi) - 2\omega\dot{R}_c + C_S\dot{R}_s\right\}\sin(\omega t) = 0 \tag{C.2}$$

where the higher order derivatives of $R_c(t)$ and $R_s(t)$ are discarded because these amplitudes are assumed to vary slowly (Jordan and Smith, 1987). In Eq.(C.2), the coefficient of each harmonic component is equal to zero, and thus, $R_c(t)$ and $R_s(t)$ can be solved from the following coupled first order differential equations,

$$\dot{R}_c = \frac{-1}{C_S^2 + 4\omega^2}\left\{(r + 2\omega^2)C_S R_s + (C_S^2 - 2r)\omega R_s - \left[C_S\cos(\phi) + 2\omega\sin(\phi)\right]A\right\} \qquad (C.3)$$

$$\dot{R}_s = \frac{1}{C_S^2 + 4\omega}\left\{(C_S^2 - 2r)\omega R_c - (2\omega^2 + r)C_S R_s + \left[2\omega\cos(\phi) - C_S\sin(\phi)\right]A\right\} \qquad (C.4)$$

where,

$$r = a_1 - \omega^2 + \frac{3}{4}a_3(R_c^2 + R_s^2) \qquad (C.5)$$

Eq.(C.1) can be rewritten as

$$x(t) = R(t)\cos[\omega t + \varphi(t)] \qquad (C.6)$$

with the response amplitude R(t) and phase $\varphi(t)$ expressed as

$$R(t) = \sqrt{R_c^2(t) + R_s^2(t)}, \qquad \varphi(t) = \tan^{-1}\left(\frac{R_s(t)}{R_c(t)}\right) \qquad (C.7, C.8)$$

Note that, when the system response reaches steady state, $R_c(t)$ and $R_s(t)$, and thus R(t) and $\varphi(t)$, become constant. In addition, time derivatives of $R_c(t)$ and $R_s(t)$ are equal to zero and Eqs.(C.3- 4) become two coupled simultaneous algebraic equations. Solving the algebraic equations for $R_c(t)$ and $R_s(t)$ to obtain the constant response amplitude and phase yields

$$\left[\left(a_1 - \omega^2 + \frac{3}{4}a_3R^2\right)^2 + C_S^2\omega^2\right]R^2 = A^2 \qquad (C.9)$$

$$\varphi = \tan^{-1}\left(\frac{-r\sin(\phi) + C_S\omega\cos(\phi)}{C_S\omega\sin(\phi) + r\cos(\phi)} \right) \qquad (C.10)$$

C.2 Subharmonic Solutions

C.2.1 1/2 subharmonic response

To solve Eq.(2.1) for the 1/2 subharmonic response under deterministic excitation f(t) (Eq.(2.2)) by the harmonic balance method, the first order approximate solution of the response is expressed as

$$x(t) = R_0(t) + R_{c1}(t)\cos(\omega t) + R_{s1}(t)\sin(\omega t) + R_{c2}(t)\cos(\frac{1}{2}\omega t) + R_{s2}(t)\sin(\frac{1}{2}\omega t) \qquad (C.11)$$

where, R_0, R_{c1}, R_{s1}, R_{c2} and R_{s2} are the amplitude of their associated harmonic and subharmonic components, respectively, and are time dependent quantities in general. For simplicity, the time parameter t is neglected henceforth. By substituting Eq.(C.11) into Eq.(2.1) and following the same procedure as in the primary resonance region (i.e., similar to Eq.(C.2)), the amplitudes R_0, R_{c1}, R_{s1}, R_{c2} and R_{s2} can be solved from the following five coupled simultaneous first order differential equations,

$$\dot{R}_{c1} = \frac{-C_S z_1 + 2\omega z_2}{C_S^2 + 4\omega^2}, \qquad \dot{R}_{s1} = \frac{-2\omega z_1 - C_S z_2}{C_S^2 + 4\omega^2} \qquad (C.12, C.13)$$

$$\dot{R}_0 = -\frac{z_0}{C_S}, \qquad \dot{R}_{c2} = \frac{-C_S z_3 + \omega z_4}{\omega^2 + C_S^2}, \qquad \dot{R}_{s2} = \frac{-\omega z_3 - C_S z_4}{\omega^2 + C_S^2} \qquad \text{(C.14, C.15, C.16)}$$

where,

$$z_0 = a_1 R_0 + a_3\left(R_0^3 + \frac{3}{2}R_0 p_1 + \frac{3}{4}R_{c1} p_2 + \frac{3}{2}R_0 p_3 + \frac{3}{2}R_{c2} R_{s1} R_{s2}\right)$$

$$z_1 = \left(a_1 - \omega^2\right) + a_3\left(\frac{3}{2}R_0 p_2 + \frac{3}{4}R_{c1} p_4 + \frac{3}{2}R_{c1} p_5 + 3R_0^2 R_{c1}\right) + C_S \omega R_{s1} - A\cos(\phi)$$

$$z_2 = \left(a_1 - \omega^2\right)R_{s2} + a_3\left[\frac{3}{4}R_{s1} p_4 + \frac{3}{2}R_{s1} p_5 + 3R_0\left(R_0 R_{s1} + R_{c2} R_{s2}\right)\right] - C_S \omega R_{c1} + A\sin(\phi)$$

$$z_3 = \left(a_1 - \frac{\omega^2}{4}\right) R_{c2} + a_3\left[\frac{3}{2}R_{c2} p_4 + \frac{3}{4}R_{c2} p_5 + 3R_0\left(R_0 R_{c2} + R_{c1} R_{c2} + R_{s1} R_{s2}\right)\right] + \frac{1}{2}C_S \omega R_{s2}$$

$$z_4 = \left(a_1 - \frac{\omega^2}{4}\right) R_{s2} + a_3\left[\frac{3}{2}R_{s2} p_4 + \frac{3}{4}R_{s2} p_5 + 3R_0\left(R_0 R_{s2} + R_{c2} R_{s1} - R_{c1} R_{s2}\right)\right] - \frac{1}{2}C_S \omega R_{c2}$$

$$p_1 = R_{c1}^2 + R_{c2}^2, \quad p_2 = R_{c2}^2 - R_{s2}^2, \quad p_3 = R_{s1}^2 + R_{s2}^2, \quad p_4 = R_{c1}^2 + R_{s1}^2, \quad p_5 = R_{c2}^2 + R_{s2}^2$$

C.2.2 1/3 subharmonic response

An approximate solution for the 1/3 subharmonic response can also be obtained by the harmonic balance method following the same procedure as in the 1/2 subharmonic

response. The first order approximation of the response x(t) can be expressed as

$$x(t) = R_{c1}(t)\cos(\omega t) + R_{s1}(t)\sin(\omega t) + R_{c3}(t)\cos(\frac{1}{3}\omega t) + R_{s3}(t)\sin(\frac{1}{3}\omega t) \qquad (C.17)$$

where, R_{c1}, R_{s1}, R_{c3} and R_{s3} are the amplitude of their associated harmonic and subharmonic components, respectively, and are time dependent in general. Again, for simplicity, the time parameter t is neglected in the following derivation. Substituting Eq.(C.17) into Eq.(2.1) and following the same procedure as in the 1/2 subharmonic response case, the amplitudes R_{c1}, R_{s1}, R_{c3} and R_{s3} can be obtained by solving the following four coupled simultaneous first order differential equations,

$$\dot{R}_{c1} = \frac{-C_s z_1 + 2\omega z_2}{C_S^2 + 4\omega^2}, \qquad \dot{R}_{s1} = \frac{-2\omega z_1 - C_S z_2}{C_S^2 + 4\omega^2} \qquad (C.18, C.19)$$

$$\dot{R}_{c3} = \frac{-9C_S z_3 + 6\omega z_4}{9C_S^2 + 4\omega^2}, \qquad \dot{R}_{s2} = \frac{-6\omega z_3 - 9C_S z_4}{9C_S^2 + 4\omega^2} \qquad (C.20, C.21)$$

where,

$$z_1 = r_c R_{c1} + C_S \omega R_{s1} + \frac{1}{4} a_3 \left(R_{c3}^3 - 3R_{c3}R_{s3}^2\right) - A\cos(\phi)$$

$$z_2 = -C_S \omega R_{c1} + r_c R_{s1} + \frac{1}{4} a_3 \left(3R_{c3}^2 R_{s3} - R_{s3}^2\right) + A\sin(\phi)$$

$$z_3 = r_s R_{c3} + \frac{1}{3} C_S \omega R_{s3} + \frac{3}{4} a_3 \left[\left(R_{c3}^2 - R_{s3}^2 \right) R_{c1} + 2 R_{s1} R_{c3} R_{s3} \right]$$

$$z_4 = -\frac{1}{3} C_S \omega R_{c3} + r_s R_{s3} + \frac{3}{4} a_3 \left[-2 R_{c1} R_{c3} R_{s3} + \left(R_{c3}^2 - R_{s3}^2 \right) R_{s1} \right]$$

$$r_c = a_1 - \omega^2 + \frac{3}{4} a_3 \left[R_{c1}^2 + R_{s1}^2 + 2 \left(R_{c3}^2 + R_{s3}^2 \right) \right]$$

$$r_s = a_1 - \frac{1}{9} \omega^2 + \frac{3}{4} a_3 \left[2 \left(R_{c1}^2 + R_{s1}^2 \right) + R_{c3}^2 + R_{s3}^2 \right]$$

APPENDIX D
EVALUATION OF INTER-DOMAIN PROBABILITY TRANSITION MATRIX

D.1 Primary Resonance Region

In the primary resonance region, two attraction (large amplitude, D_L or D_1, and small amplitude harmonic, D_S or D_2) domains co-exist. The conditional probabilities $p_{11}(1|1)$ and $p_{22}(2|2)$ in Eq.(4.12) are obtained by Eq.(4.16). Note that, in this region, an exit from one domain will lead the system response to another domain (Section 3.3). Thus, $p_{21}(2|1)$ and $p_{12}(1|2)$ in Eq.(4.12) are the complements of $p_{11}(1|1)$ and $p_{22}(2|2)$, respectively. In other words,

$$p_{21}(2|1) = 1 - p_{11}(1|1), \qquad p_{12}(1|2) = 1 - p_{22}(2|2) \tag{D.1}$$

D.2 Subharmonic Resonance Region

In the subharmonic resonance region, the system response inter-domain transition behavior is more complicated than that in the primary resonance region due to an increase in the number of co-existing attraction domains as depicted in Section 3.3. In addition, under narrowband excitation, an exit from the large amplitude domain may lead the system response not only to the small amplitude domain but also to the 1/2 and 1/3 subharmonic domains.

There are four attraction (large amplitude harmonic, D_L or D_1, small amplitude harmonic, Ds or D_2, 1/2 subharmonic, $D_{1/2}$ or D_3, and 1/3 subharmonic, $D_{1/3}$ or D_4) domains co-existing (Section 3.3). The four diagonal elements of matrix K, $p(L|L) = p_{11}(1|1)$, $p(S|S) = p_{22}(2|2)$, $p(1/2|1/2) = p_{33}(3|3)$, and $p(1/3|1/3) = p_{44}(4|4)$, can also be obtained by Eq.(4.16). Evaluation of the rest elements of K is discussed in the following:

1. p(L|1/3), p(1/2|S), p(1/3|S) According to the response inter-domain transition behavior depicted in Section 3.3, these three conditional probabilities are equal to zeros. That is,

$$p_{14}(1|4) = p_{32}(3|2) = p_{42}(4|2) = 0 \tag{D.2}$$

2. p(L|S) This probability is equal to the complement of p(S|S) as in the primary resonance region. Thus,

$$p_{12}(1|2) = 1 - p_{22}(2|2) \tag{D.3}$$

3. p(1/3|1/2) When the system is in the 1/2 subharmonic domain, D_3, an exit from the domain at the lower boundary A_{3L} leads the system to the 1/3 subharmonic domain, D_4. Therefore, from Eq.(4.18), $p(1/3|1/2) = p_{43}(4|3)$ can be calculated as

$$p_{43}(4|3) = 1 - \int_{A_{3L}}^{\infty} p(A^{(2)}|A^{(1)} \in D_3^A)\, dA^{(2)} \tag{D.4}$$

4. p(L|1/2) and p(S|1/2) An exit of the system response from the 1/2 subharmonic domain, D_3, at the upper boundary A_{3U} may lead the system to the large (D_1) or the small (D_2)

amplitude harmonic domain. The probability of the exit $p(E_{3U})$ can be calculated from Eq.(4.17). The probability that the system response goes to the large amplitude harmonic domain after the exit, $p(L|E_{3U})$, can be approximated by the probability that the system transient-state mean energy corresponding to A_{3U} is greater than the 1/2 subharmonic steady-state system mean energy at A_{3U} (Section 3.3). In addition, because the system mean energy is directly related to the response amplitude, $p(L|E_{3U})$ may also be approximated by the probability that the transient-state response amplitude R corresponding to A_{3U} is greater than the steady-state 1/2 subharmonic response amplitude $R_{3U}^{(S)}$ at A_{3U}. The response amplitude probability distribution $\tilde{p}(R|(D_3^R)_{3U})$ at the domain upper boundary A_{3U} can be obtained from Eq.(4.29). Therefore,

$$p_{13}(1|3) = p(E_{3U})\,p(R > R_{3U}^{(S)} | A_{3U}) = p(E_{3U}) \sum_{R > R_{3U}^{(S)}} \tilde{p}(R|(D_3^R)_{3U}) \qquad \text{(D.5)}$$

and,

$$p_{23}(2|3) = p(E_{3U})\,p(R \le R_{3U}^{(S)} | A_{3U}) = p(E_{3U}) \sum_{R \le R_{3U}^{(S)}} \tilde{p}(R|(D_3^R)_{3U}) \qquad \text{(D.6)}$$

5. p(1/2|1/3) and p(S|1/3) Based on the response inter-domain transition behavior described in Section 3.3 and the arguments presented above (in 4. p(L|1/2) and p(S|1/2)), the probability of the system response going to the 1/2 subharmonic (D_3) and the small amplitude harmonic (D_2) domains after an exit from the 1/3 subharmonic domain (D_4) can be calculated as,

$$p_{34}(3|4) = p(E_{4U})\,p(R > R_{4U}^{(S)} | A_{4U}) = p(E_{4U}) \sum_{R > R_{4U}^{(S)}} \tilde{p}(R|(D_4^R)_{4U}) \qquad \text{(D.7)}$$

and

$$p_{24}(2|4) = 1 - p_{44}(4|4) - p_{34}(3|4) \tag{D.8}$$

respectively, where, $R_{4U}^{(S)}$ is the steady-state 1/3 subharmonic response amplitude at A_{4U}. The probabilities $p(E_{4U})$ and $\tilde{p}(R|(D_4^R)_{4U})$ are obtained from Eqs.(4.17 and 4.29), respectively.

6. p(1/2|L), p(1/3|L) and p(S|L) During the inter-domain transition following the exit of the system response from the large amplitude harmonic domain, D_1, the response amplitude keeps decreasing while the excitation amplitude varies randomly. Depending on the excitation amplitude variation, the possible destination domains of the transition include the 1/2 subharmonic, D_3, the 1/3 subharmonic, D_4, and the small amplitude harmonic, D_2, attraction domains.

For the system response transition to the 1/2 subharmonic domain, D_3, it is assumed that the excitation amplitude A must be within the domain D_3^A when the response amplitude R decreases to the mean steady-state 1/2 subharmonic response amplitude, $R_3^{(S)}$. Similarly, for the system transition to the 1/3 subharmonic domain, D_4, the excitation amplitude must be within the domain D_4^A when the response amplitude decreases to the mean steady-state 1/3 subharmonic response amplitude, $R_4^{(S)}$.

To estimate the number of excitation cycles required for the harmonic response amplitude decreasing from attraction domain D_1 to D_3 and D_4, the response amplitude decay rate of an unforced linear system is employed (Clough and Penzien, 1993). The damping and stiffness coefficients of the linear system are identical to those of the nonlinear system considered. Thus, the required excitation cycles may be estimated by

$$m(i,j) = \frac{R_i^{(S)} - R_j^{(S)}}{C_S \pi R_j^{(S)}} \sqrt{a_1} \tag{D.9}$$

where, m(i, j) is the excitation cycles of the transition from the attraction domain D_i to the attraction domain D_j. Note that $R_1^{(S)}$ is the steady-state response amplitude corresponding to the excitation amplitude $A = A_{1L}$, in the attraction domain D_1. Let m1 = m(1, 3)+1 and m2 = m(3, 4). Thus, when the response amplitude decreases from $R_1^{(S)}$ to $R_3^{(S)}$, the probability distribution of the excitation amplitude is obtained as

$$p_3(A^{(m1)} | A^{(1)} \in D_1^A) = \int_{A^{(m1-1)}} p(A^{(m1)} | A^{(m1-1)}) \cdots$$

$$\int_{\overline{D}_1^A} p(A^{(3)} | A^{(2)}) \int_{A^{(1)} \in D_1^A} p(A^{(2)} | A^{(1)}) p(A^{(1)} | D_1^A) dA^{(1)} dA^{(2)} \cdots dA^{(m1-1)} \tag{D.10}$$

$$p(A^{(m1)} \in D_3^A) = \int_{D_3^A} p_3(A^{(m1)} | A^{(1)} \in D_1^A) dA^{(m1)} \tag{D.11}$$

where $\overline{D}_1^A$ is the complement domain of D_1^A. A part of the excitation amplitudes $A^{(m1)}$ not within D_3^A will propagate toward D_4^A and the rest are going to D_2^A. Thus,

$$p_4(A^{(m1+m2)} | A^{(1)} \in D_1^A) = \int_{A^{(m1+m2-1)}} p(A^{(m1+m2)} | A^{(m1+m2-1)}) \cdots \int_{A^{(m1+1)}} p(A^{(m1+2)} | A^{(m1+1)})$$

$$\int_{\overline{D}_3^A} p(A^{(m1+1)} | A^{(m1)}) p_3(A^{(m1)} | A^{(1)} \in D_1^A) dA^{(m1)} dA^{(m1+1)} \cdots dA^{(m1+m2-1)} \tag{D.12}$$

$$p(A^{(m1+m2)} \in D_4^A) = \int_{D_4^A} p_4(A^{(m1+m2)} | A^{(1)} \in D_1^A) dA^{(m1+m2)} \tag{D.13}$$

where, $\overline{D}_3^A$ is the complement domain of D_3^A. From Eqs.(D.11 and D.13) and $p_{11}(1|1)$, the probabilities $p_{31}(3|1)$, $p_{41}(4|1)$ and $p_{21}(2|1)$ can be obtained as

$$\begin{aligned}
p_{31}(3|1) &= \left[1 - p_{11}(1|1)\right] p(A^{(m1)} \in D_3^A) \\
p_{41}(4|1) &= \left[1 - p_{11}(1|1)\right]\left[1 - p(A^{(m1)} \in D_3^A)\right] p(A^{(m1+m2)} \in D_4^A) \\
p_{21}(2|1) &= \left[1 - p_{11}(1|1)\right]\left[1 - p(A^{(m1)} \in D_3^A)\right]\left[1 - p(A^{(m1+m2)} \in D_4^A)\right]
\end{aligned} \tag{D.14}$$